ISSN 1980-9743

Soils & Rocks

International Journal of Geotechnical and Geoenvironmental Engineering

Volume 30, N. 1
January-April 2007

Soils & Rocks
Volume 30, N. 1
2007

Soils and Rocks is an International Journal of Geotechnical and Geoenvironmental Engineering published by

ABMS - Brazilian Association for Soil Mechanics and Geotechnical Engineering
Av. Prof. Almeida Prado, 532, IPT/DEC-Prédio 54
05508-901 São Paulo, SP
Brazil

ABGE - Brazilian Association for Engineering Geology and the Environment
Av. Prof. Almeida Prado, 532, IPT/DIGEO- Prédio 59
05508-901 São Paulo, SP
Brazil

SPG – Portuguese Geotechnical Society
LNEC, Avenida do Brasil, 101
1700-066 Lisboa
Portugal

Issue Date: *April 2007*

Issue: *3,200 copies*

Manuscript Submission: *For review criteria and manuscript submission information, see Instructions for Authors at the end.*

SOILS & ROCKS

International Geotechnical and Geoenvironmental Journal

Editor Ennio Marques Palmeira - University of Brasília, Brazil

Co-editor Ricardo Oliveira - COBA, Portugal

Soils and Rocks publishes papers in English in the broad fields of Geotechnical Engineering, Engineering Geology and Environmental Engineering. The Journal is published in April, August and December. Subscription price is US$ 90.00 per year. The journal, with the name "Solos e Rochas", was first published in 1978 by the Graduate School of Engineering-Federal University of Rio de Janeiro (COPPE-UFRJ). In 1980 it became the official magazine of the Brazilian Society for Soil Mechanics (ABMS), acquiring the national character that had been the intention of its founders. In 1986 it also became the official Journal of the Brazilian Society for Engineering Geology (ABGE) and in 1999 became the Latin American Geotechnical Journal, following the support of Latin-American representatives gathered for the Pan-American Conference of Guadalajara (1996). In 2007 the journal acquired the status of an international journal under the name of Soils and Rocks, published by the Brazilian Society of Soil Mechanics and Geotechnical Engineering (ABMS), Brazilian Society of Engineering Geology (ABGE) and Portuguese Society of Geotechnical Engineering (SPG).

Soils and Rocks: International Journal of Geotechnical and Geoenvironmental Engineering (ABMS/ABGE/SPG) - SP, Brasil, 1978

1978,	1 (1, 2)
1979,	1 (3), 2 (1,2)
1980-1983,	3-6 (1, 2, 3)
1984,	7 (single number)
1985-1987,	8-10 (1, 2, 3)
1988-1990,	11-13 (single number)
1991-1992,	14-15 (1, 2)
1993,	16 (1, 2, 3, 4)
1994-2006,	17-29 (1, 2, 3)
2007,	30(1,

ISSN 1980-9743 CDU 624.131.1

ISSN 1980-9743

SOILS & ROCKS

International Geotechnical and Geoenvironmental Journal

Publication of

ABMS - Brazilian Association for Soil Mechanics and Geotechnical Engineering
ABGE - Brazilian Association for Engineering Geology and the Environment
SPG - Portuguese Geotechnical Society

Volume 30, N. 1, January-April 2007

Table of Contents

EDITORIAL

From Solos e Rochas to Soils and Rocks...
Alberto Sayão, Maria Heloísa Frascá, António G. Correia, Ennio Palmeira and Ricardo Oliveira i

Letter from the ISSMGE President
Pedro Sêco e Pinto iii

XXIII MANUEL ROCHA LECTURE

Advances and Remaining Challenges for Geosynthetics in Geoenvironmental Engineering Applications
R. Kerry Rowe 3

ARTICLES

Deflections of Upstream Membrane of Rockfill Dams During Reservoir Filling
Fernando Saboya Jr., Pedricto Rocha Filho, Arthur D.M. Penmam 33

Basic Principles of Eurocode 7 on 'Geotechnical Design'
Roger Frank 39

An Expedite Method to Predict the Shear Strength of Unsaturated Soils
Orencio Monje Vilar 51

Analysis of Piles in Residual Soil from Granite Considering Residual Loads
António Viana da Fonseca, Jaime Alberto dos Santos, Elisabete Costa Esteves, Faiçal Massad 63

BOOK REVIEW

RALPH B. PECK, Educator and Engineer: The Essence of the Man, John Dunnicliff and Nancy Peck Young
By Waldemar Hachich 81

From *Solos e Rochas* to *Soils and Rocks*...

Dear Reader,

This is the first issue of the international journal Soils and Rocks. The publication of this journal was an old dream of the Brazilian geotechnical community that now comes true. An agreement among the Brazilian Association for Soil Mechanics and Geotechnical Engineering (ABMS), the Brazilian Association for Engineering Geology and the Environment (ABGE) and the Portuguese Geotechnical Society (SPG) has made possible the internationalization of the traditional journal *Solos e Rochas*, after about 30 years publishing papers mainly in Portuguese.

One of the main objectives of the journal is to increase the scientific and technical exchange among Brazilian, Portuguese and international researchers and practitioners. From 2007 on, researchers, consultants and practitioners from all geotechnical fields will have a new international journal to publish and discuss their projects and investigations. However, Soils and Rocks aims higher: all efforts will be ensured for the journal to maintain its high standard of quality in all papers and technical notes now to be published by authors from all over the world.

ABMS, ABGE and SPG are confident that Soils and Rocks will soon be one of the leading international journals and will effectively contribute for the development of all fields of Geotechnics.

With our warmest regards,

Alberto Sayão	Maria Heloísa Frascá	António G. Correia	Ennio Palmeira and Ricardo Oliveira
(ABMS)	(ABGE)	(SPG)	(Editors)

Letter from the ISSMGE President

Following the kind invitation, it is for me a great honour and pleasure, on behalf of the International Society of Soil Mechanics and Geotechnical Engineering, to welcome this new number of Soils & Rocks, in English version, edited by ABMS, ABGE and SPG. I would like to stress the very important role played by these Societies for the development of research, education, design and safety evaluation of geotechnical structures in Europe and South America.

The journal *Geotecnia*, published by SPG since 1971, and the journal Soils & Rocks, published in Portuguese by ABMS since 1978, have both contributed as a vehicle of transfer of knowledge.

The cooperation of SPG and ABMS with ISSMGE is impressive and I would like to highlight the roles of TC4 "Earthquake Geotechnical Engineering", hosted by SPG from 1994 to 2000, and TC3 "Geotechnics of Pavements", hosted by SPG since 2001, and TC 41 "Mega Cities" and JTC 1 "Landslides and Engineered Slopes" hosted by ABMS since 2006. Also, I would like to stress the very important role of Prof. Waldemar Hachich, ISSMGE VP for South America and Past President of ABMS. In addition 19 Portuguese experts and 18 Brazilian experts participate in 23 TCs and 4 European TCs of ISSMGE.

On behalf of ISSMGE, I would like to take this opportunity to express my sincere appreciation and deep gratitude to all Past Presidents of ABMS and SPG and particularly to the current Presidents, Prof. Alberto Sayão and Prof. António Correia, for their devotion, time, guidance and efforts since 2004.

It is my hope that the spirit of cooperation fostered by Soils & Rocks will encourage additional projects and will contribute to the advancement of the state-of-art and state-of-practice of geotechnical engineering, following Yeats message *The intellect of man is found to choose perfection of the life or the work.*

As this world is moving in the direction of a global village there is a need of a universal knowledge and a permanent update and renewing. Communication, transfer of experiences and information, discussions of the methodologies and results are the key words.

In this geotechnical world that always changes and progresses, we are facing new challenges that demand great exigency and austerity.

The scientific truth is not definitely achieved and demands from all of us a permanent and continuous effort.

It is important to join the human resources of our geotechnical society, to catalyze our energies to overcome inertias, to feed our dream, to obtain answers to our questions and to open new horizons following the memorable lines of Montaigue *C`est un grand ouvrier de miracles l`esprit humain.*

A brief reflection about our journey shows the great mutations occurred in the geotechnical society that demands tranquillity, clearness, but also opening, dialogue and approach.

We need to humbly recognize that we have not yet achieved our goals related the progress of the knowledge and we have not been capable to communicate with important sectors of our Society. We need to hear the voice of the youth, to renew the old practices and to promote innovation and new findings.

Soils & Rocks will certainly contribute to share new knowledge and for a better interaction between the geotechnicians. To this dream come true, we need to work very hard and to give our hands. I appreciate very much the message of Bernard Shaw: *Some men see things as they are and say "why"? I dream things that never were and say "why not"?* I am confident that, by joining our efforts, we will reach our goals and targets and develop our capacity to transform the projects in actions.

The time demands all arise as we are now on the brink of a new era. Over the past years a number of developments have taken place and we need to mould Soils & Rocks for this momentum to capitalise on the potential benefits.

A special message goes to the journal's co-editors, Prof. Ennio M. Palmeira and Prof. Ricardo Oliveira, and to the Editorial Board to wishing Soils & Rocks a very successful and bright future. Their experience and enthusiasm will certainly contribute for our common goal to move a step forward this prestigious journal.

Last but not least, I would like to address to all ABMS, ABGE and SPG members a word of praise and gratitude for their contributions and a message of hope inspiring in William Hazlitt memorable lines: *A great passion for the object will assure success because the wish for the purpose will show the means*.

Thank you very much for your kind attention.

Pedro Sêco e Pinto
ISSMGE President

XXIII Manuel Rocha Lecture

This lecture has been traditionally promoted by the Portuguese Geotechnical Society to honour the memory of Prof. Manuel Rocha. The XXIII Manuel Rocha Lecture was delivered on October, 16th, 2006, in Lisbon, by Prof. R. Kerry Rowe, from Queen's University, Canada. The introduction speech was presented by Prof. Luís Leal Lemos, who emphasised the great contributions from Prof. Rowe in the field of Geosynthetics. At the end, Dr. António Gomes Coelho highlighted the main topics and was warmly joined by all presents in thanking the speaker, who was given a SPG medal and a photo biography of Manuel Rocha.

Soils & Rocks
v. 30, n. 1

Advances and Remaining Challenges for Geosynthetics in Geoenvironmental Engineering Applications

R. Kerry Rowe

Abstract. Nine issues of importance to the use of geomembranes (GMs) and geosynthetic clay liners (GCLs) as part of composite liners in geoenvironmental applications are examined. These issues include the effect of: GCL-leachate compatibility on hydraulic conductivity; freeze-thaw on GCL performance; internal erosion on GCL hydraulic conductivity; temperature on advection and diffusion as well as desiccation of GCLs and compacted clay liners (CCLs); the choice of protection layer on the strains developed in GMs; wrinkles on strains developed in GMs and the thinning of GCLs; holes in GMs on leakage through composite liners; winkles in GMs on leakage through composite liners; diffusion through GCLs and GMs; and temperature and leachate exposure on the service life of GMs. It is suggested that GCLs and GMs can play a very beneficial role in providing environmental protection. However, like all engineering materials they must be used appropriately and consideration should be given to factors such as those addressed in this paper. There is a need for site specific design, strict adherence to construction specification, and appropriate protection of the geosynthetics after construction. In particular, given the diversity of available GCLs and their different engineering characteristics, GCLs should be selected based on the required engineering properties, not just price.

Key words: geomembranes, geosynthetic clay liners, composite liners, geoenvironmental, hydraulic conductivity, clay-leachate interaction, freeze-thaw, internal erosion, leakage, diffusion, ageing.

1. Introduction

In recent years there have been many advances in the understanding of issues related to the use of geosynthetics such as geosynthetic clay liners (GCLs) and geomembranes (GM) as contaminant barriers. As a consequence there has also been a significant increase in geoenvironmental applications. These applications range from the more traditional use of GCLs and GMs as composite base liners or as part of capping systems for landfills (*e.g.* Rowe *et al.*, 2004b), as liners for contaminated fluids (*e.g.* leachate lagoons, Rowe *et al.*, 2003), as barriers to contain past spills of hydrocarbons (*e.g.* Bathurst *et al.*, 2006), as secondary containment around fuel tanks to prevent possible future contamination in the event of a tank rupture or equipment malfunction, as containment for fluids in heap leach pads (Thiel & Smith, 2004), and as covers and liners for mine waste (*e.g.* Lange *et al.*, 2005).

The objective of this paper is to highlight some of the recent advances in geosynthetic engineering, illustrate some of the important considerations related to design and construction using geosynthetics, and flag some of the remaining challenges related to the use of geosynthetics in geoenvironmental applications. Attention will be primarily focused on data and findings published since 2000. Readers requiring an introduction to the use of geosynthetics in barrier applications are referred to Rowe *et al.* (2004b).

This paper will address nine issues of importance to the use of geosynthetics in geoenvironmental applications: (1) GCL-leachate compatibility; (2) the effect of freeze-thaw on GCL performance; (3) internal erosion of GCLs; (4) temperature; (5) protection of composite liners; (6) wrinkles in GMs; (7) holes in GMs and the consequent leakage through composite liners; (8) diffusion through GCLs and GMs; and (9) service life of GMs. This paper is intended to complement two other extensive examinations of the use of geosynthetics in landfills (Rowe, 1998; Rowe, 2005) and incorporates, but expands on, material presented by Rowe (2006). With respect to issue 1, this paper updates the review reported by Rowe (1998) however there is much valuable information in the 1998 paper which is not repeated here. Issues 2 and 3 are not addressed in either of these earlier papers. Issues 4-9 are discussed in both of these previous papers. This paper will only discuss issues 4 and 9 to the extent necessary to provide context of the overall thrust of designing safe long-term containment and, where appropriate, broadening their applicability to applications beyond landfills or providing new information. The reader is referred to Rowe (2005) for a more in-depth discussion of these issues. In contrast this paper will provide much more detail with respect to issues 3, 5, 6, 7 and 8 than was provided in either previous paper.

2. GCL-Leachate Compatibility

2.1. Municipal solid waste (MSW) leachate

Many researchers (*e.g.* Schubert, 1987; Shan & Daniel, 1991; Daniel *et al.*, 1993; Dobras & Elzea, 1993; Ruhl & Daniel, 1997; Petrov *et al.*, 1997; Petrov & Rowe, 1997;

R. Kerry Rowe, Ph.D., Professor and Vice-President (Research), GeoEngineering Centre at Queen's-RMC, Department of Civil Engineering, Queen's University, Kingston, ON, K7L 3N6, Canada. e-mail: kerry@civil.queensu.ca.
Submitted on ; Final Acceptance on ; Discussion open until August 31, 2007.

Kodikara *et al.*, 2002; Ashmawy *et al.*, 2002; Kolstad *et al.*, 2004; Katsumi & Fukagawa, 2005; Lee & Shackelford, 2005; Guyonnet *et al.*, 2005; Jo *et al.*, 2005, 2006) have discussed the issue of GCL-leachate compatibility and its effect on the hydraulic conductivity of GCLs. The hydraulic conductivity of a GCL has been shown to be highly dependent on: the hydrating conditions, the applied effective stress during permeation, the method of GCL manufacture, and the mass of bentonite in the GCL (Rowe, 1998). For example, Petrov & Rowe (1997) showed that if there is a low applied stress at the time of permeation, there can be an order of magnitude increase in hydraulic conductivity to about 6×10^{-10} m/s as the permeant was changed from water to MSW leachate (Table 1). The effect was far less significant at higher confining stress and the hydraulic conductivity to MSW leachate was still very low at 3×10^{-11} m/s. It has been shown that consolidation during permeation can greatly mitigate the effects of clay-leachate interaction on hydraulic conductivity.

The hydraulic conductivity (k) of a GCL for a given permeant can be directly related to the bulk void ratio of the GCL (e_B) (Petrov *et al.*, 1997). For example, for a particular GCL and MSW leachate it can be shown that there is a relatively straightforward relationship between k and e_B, viz:

$$-11.4 + 0.42e_B < \log_{10} k\,(\text{m/s}) < -11.2 + 0.42e_B \qquad (1)$$

Relationships such as this will be both product and permeant dependent but can be established for any given design situation.

Rowe (1998) demonstrated that when dealing with composite liners, the ability of the GCL to minimize leakage through holes in a GM is not especially sensitive to the hydraulic conductivity of the GCL but, rather, is much more dependent on the interface transmissivity between the GM and the GCL. This helps explain the low leakage reported for composite liners with a GCL as discussed later. Nevertheless consideration should be given to the potential increase in k due to interaction with the leachate and the expected values should be used in the design leakage calculations. Interaction is expected to be greatest for a GCL used in applications where there is low applied stress and high concentrations of salts (especially those with divalent cations). An example of a potentially problematic application would be the use of a GCL as part of a composite liner for a lagoon to contain brines. Applications such as this will require special attention and possibly a GCL with an amended bentonite (rather than the typical sodium bentonite) selected based on clay-permeant compatibility considerations.

2.2. Mine waste waters

The control metal and metalloid contamination derived from waste rock and mine tailings is a major challenge for the mining industry. Past research has focused on covers which reduce acid production by limiting infiltration and oxygen. While there is certainly a need to deal with acid drainage, recent research has suggested that potentially toxic elements (*e.g.* arsenic, selenium and, sometimes, nickel and zinc) can be mobile under neutral-pH conditions. Also reductive dissolution of As-bearing minerals can lead to the release of As (Stichbury *et al.*, 2000). This increases interest in segregating the most hazardous wastes for separate disposal in a fully lined containment facility. GCLs have a potential role to play in containing these contaminants.

The attenuation of single metal and multi-metal permeants by sodium bentonite and similar clay combinations have been examined by a number of investigators (*e.g.* Brain, 2000; Li & Li, 2001; Cooper *et al.*, 2002; Abollino *et al.*, 2003). The primary mechanisms controlling metal mobility in sodium bentonite are (Abollino *et al.*, 2003): (i) cation exchange within the clay lattice structure; and (ii) cation attraction to broken bonds at the edges of the clay mineral. Other mechanisms include (iii) limited anion exchange (30 meq/100 g) where the anions typically attach to the clay structure by substitution of hydroxides at the edges of gibbsite sheets (McKelvey, 1997), and (iv) attenuation of metals by precipitation (Yong, 2001). It is well known that soil pH, redox, and soil porewater composition can have a significant impact on metal mobility (Yong, 2001).

Lange *et al.* (2004, 2005) studied the potential for metal (Al, Fe, Mn, Ni, Pb, Cd, Cu, Zn) migration through GCLs from an acid rock drainage (ARD) solution (pH 3.9). Mn was found to experience the least attenuation and its migration was similarly to Cl. The ARD effluent remained neutral for about 11 pore volumes of permeation during which time Al, Fe and Cu were highly retarded and retained within the clay. Ni, Zn, and Cd were moderately attenuated. The Fe, Zn, Mn, As, Pb and Al were primarily attenuated in the upper portion of the GCL. There was evidence to suggest that Fe and Mn were predominantly attenuated by precipitation of Fe-Mn oxyhydroxides. Ni and Cu were fairly uniformly attenuated throughout the thickness of the GCL.

Table 1 - Effect of applied stress on hydraulic conductivity with respect to water and MSW leachate (after Petrov & Rowe,1997).

Hydration stress (kPa)	Hydrated thickness (mm)	Hydraulic conductivity to water (m/s)	Hydraulic conductivity to MSW Leachate (m/s)
3	12.3	6×10^{-11}	55×10^{-11}
115	6	0.75×10^{-11}	3×10^{-11}

As the buffering capacity of the bentonite was depleted and eventually exhausted, the pH decreased until it eventually reached the influent value of 3.9 after 35 PVs of permeation. The shift in pH resulted in some metals being remobilized from the bentonite back into solution. Thus for ARD solutions there is considerable potential to retard metals but this potential is limited by the buffering capacity of the bentonite. In a design situation, this can be related to the mass per unit area of bentonite in the GCL and the expected flow through the GCL. The hydraulic conductivity of the GCLs permeated with ARD increased from 2.8 x 10^{-12} m/s to 3.7 x 10^{-11} m/s after 35 pore volumes of permeation.

Lange *et al.* (2007) also examined the interaction between a GCL and gold mine leachate (GML). The GML had much higher concentration of Ca^{2+} and Mg^{2+} than the ARD (Table 2) but despite this the concentration of these cations in the effluent from the GCLs permeated with GML was much lower than was observed in the ARD tests. This can be attributed to cation exchange resulting from the high metal loading together with displacement by H^+ ions.

Although both the ARD and GML had high concentrations of sulphate, there was much greater retention of the sulphate by the GCL in the GML tests than in the ARD tests, with much of the sulphate being precipitated in the upper portion of the GCL as gypsum for the GML tests but not for the ARD tests. The significant attenuation of Cd in the GML was presumed to be largely associated with precipitation of gypsum because Huang *et al.* (1999) had demonstrated that Cd can adsorb to gypsum during its crystal growth. There was also more attenuation of arsenic for the ARD samples than the GML samples. The attenuation of arsenate in the GML was also partly attributed to gypsum precipitation with As oxyanions substituting for SO_4^{2-} in the gypsum structure.

Table 2 - Initial concentrations of permeant liquids examined by Lange *et al.* (2005).

Parameter*	Gold mine leachate (GML)	Acid rock drainage (ARD) leachate
Calcium (Ca^{2+})	110.1	0.7
Sodium (Na^{+})	964.0	457.7
Sulphate (SO_4^{2-})	2447.0	2932
Potassium (K^{+})	8.0	779.9
Magnesium (Mg^{2+})	83.5	0.15
Strontium (Sr^{2+})	2.2	n/a
Manganese (Mn^{2+})	2.1	26.59
Aluminium (Al^{3+})	3.56	88.73
Iron (Fe^{2+})	0.41	214.4
Copper (Cu^{2+})	n/a	19.7
Chloride (Cl^{-})	268.0	69
Cadmium (Cd^{2+})	2.1	4.9
Nickel (Ni^{2+})	n/a	20.2
Arsenic (As^{5+})	4.0	4.2
Zinc(Zn^{2+})	n/a	107.2
Lead (Pb^{2+})	n/a	13.9
pH	6.85	3.7

All units in mg/L, with exception of pH; *the valence indicated refers to how the ion was initially introduced.

2.3. Hydrocarbons

Several investigators have examined the effect of organic permeants on the hydraulic conductivity of GCLs. This has included consideration of neat and diluted ethanol (Petrov *et al.*, 1997), gasoline (Shan & Lai, 2002) and Jet A-1 (Rowe *et al.*, 2004a). Because of the hydrophobic nature of many organic contaminants there can be a threshold pressure below which there is no permeation of the hydrocarbon through a water saturated GCL. For example, Shan & Lai (2002) reported no flow of gasoline through a GCL under a hydraulic gradient of 150 over a test period of 3 weeks. Likewise, Rowe *et al.* (2007a) found that there was no flow of Jet A-1 through a hydrated GCL until the pressure difference between the two sides of the GCL exceeded 27 kPa. These tests were conducted with a flexible wall permeameter. Rigid wall permeameters are also commonly used to obtain *k* and Rowe *et al.* (2005a) showed that in these tests, the *k* of GCLs permeated with Jet A-1 increased with increasing hydraulic gradient. This is thought to be because the higher pressures associated with higher gradients overcome interfacial tensions in the smaller pores thereby opening up more flow paths than were available at lower gradients. As a consequence, the values deduced from rigid wall permeameter tests at high gradients may considerably overestimate the *k* that would actually be mobilized in field applications.

It can be concluded from the forgoing that hydrated GCLs can be an excellent hydraulic barrier to hydrophobic hydrocarbons like Jet A-1 in the many practical applications where the hydrocarbon head does not exceed the threshold value.

3. Freeze-Thaw

While there are many applications where a GCL will not be subjected to freezing, there are also many parts of the world where GCLs will be subjected to freeze-thaw cycles. Hewitt & Daniel (1997), Kraus *et al.* (1997), Rowe *et al.* (2007a) and Podgorney & Bennett (2006) performed tests on GCLs subjected to 3, 20, 100 and 150 freeze-thaw cycles respectively and found that there was no significant change in *k* of a GCL with respect to water due to these freeze-thaw cycles. While this is very positive, it should be noted that these tests did not examine the effect of potential interaction of the GCL with the pore water in adjacent soils. If these soils have pore fluid with divalent cations (*e.g.* Ca^{2+} or Mg^{2+}) then cation exchange of these cations for Na^{+} on the

sodium bentonite in the GCL can result in an increase in k of the GCL both in the laboratory (Shackelford *et al.* 2000; Egloffstein 2001; Jo *et al.* 2001, 2004, 2005) and field (James *et al.* 1997; Melchior 1997, 2002; Egloffstein 2001). This, combined with a reduction in swell index due to cation exchange and freeze-thaw, has the potential to give rise to an increase in k of the GCL with time unless the GCL is subjected to sufficient confining stress to prevent shrinkage and crack formation under the combined influence of double layer contraction and ice lensing. Egloffstein (2001, 2002) has suggested that a 0.75-1.0 m thick soil cover is sufficient to protect GCLs from significant increase in hydraulic conductivity. However more research is required to assess the potential effect of relatively low stress and freeze-thaw cycles on the long-term performance of GCLs used in covers and similar near surface applications to confirm when Egloffstein's suggestion is generally applicable.

The effects of freeze-thaw on k of GCLs with respect to hydrocarbons has, until recently, received little attention. This is important for cases like those described by Bathurst *et al.* (2006) where a composite liner was used to contain a hydrocarbon spill at a former DEW-Line site on Brevoort Island in the Canadian Arctic until there can be future remediation. In this case shallow permafrost provides a natural barrier to prevent significant downward migration of hydrocarbons. However an engineered barrier was required to prevent lateral spreading of the hydrocarbon plume. The geosynthetic composite barrier composed of a fluorinated high density polyethylene (f-HDPE) and GCL was installed to cut off flow of hydrocarbons to the sea in the active zone above the permafrost in 2001. Another GM was used to cover the surface area between the source of the plume and the barrier to minimize infiltration of rainwater or runoff into the contaminated zone. The barrier is unfrozen in the summer months but frozen for most of the remainder of the year. Thus the question arises as to how effective the GCL will be as a barrier to hydrocarbons after being subjected to freeze-thaw cycles.

Rowe *et al.* (2004a, 2006, 2007a) performed freeze and thaw tests using flexible wall (FWP) and rigid wall (RWP) permeameters. The GCL samples were hydrated for five days under low confining pressure (15 ± 3 kPa), subjected to up to 100 freeze and thaw cycles, and then first permeated with de-aired water followed by Jet A-1. Tests were also conducted on samples recovered from the field after 1 and 3 years natural exposure to the groundwater and freeze-thaw in the arctic.

Rowe *et al.* (2006) used RWP to permeate GCLs with Jet A-1 until equilibrium was reached. The mean equilibrium k was about 8.0×10^{-11} and 14.5×10^{-11} m/s for 5 and 12 freeze-thaw cycles respectively (*i.e.* about 4.0 and 5.6 times greater than the initial value with respect to water). Thus the combination of high gradients and many pore volumes of permeation increased both the intrinsic permeability and k. This was due to an increase in the pore size with SEM images showing that the bentonite pore size for GCLs subjected to up to 12 freeze-thaw cycles was 2-3 times larger than that of the bentonite in the virgin GCL. Application of Olsen's (1961) cluster model suggested that the double layer contracted by 20-40% after permeating with Jet A-1 while the free-space expanded 1.2-2.5 times that before Jet A-1 permeation.

Tests performed using flexible wall permeameters (Rowe *et al.*, 2007a) found that the threshold pressure of Jet A-1 for hydrated GCLs with no freeze-thaw cycles was between about 27 to 55 kPa. The range of threshold pressure for GCLs exhumed from the field after 3 years and those subjected to up-to 50 freeze-thaw cycles in the laboratory was 13.8-20.7 kPa (*e.g.* see Fig. 1). This reduced to between 0 and 13.8 kPa after 100 freeze-thaw cycles. Thus, freeze-thaw did reduce the threshold pressure and this is attributed to an increase in the size of macro pores in the bentonite following repeated freeze-thaw cycles.

The k (with respect to Jet A-1) of the hydrated GCL recovered from the field after 3 years was less than 3×10^{-12} m/s. The k after up to 50 freeze-thaw cycles in the laboratory was less than 3×10^{-11} m/s at a gradient just above that required to initiate flow. There was some increase in k with 100 freeze-thaw cycles with a maximum value of about 1×10^{-10} m/s. Thus both the laboratory and field evidence suggest that the GCL will provide an effective barrier to hydrocarbons for many years and up to 100 freeze-thaw cycles for the conditions present at Brevoort Island.

4. Internal Erosion

GCLs are commonly used in applications where there may be several to many meters of fluid over the GCL (*e.g.* ponds, lagoons, and landfills when a leachate mound builds up). Since GCLs are relatively thin, these applications can give rise to high gradients and the potential for internal ero-

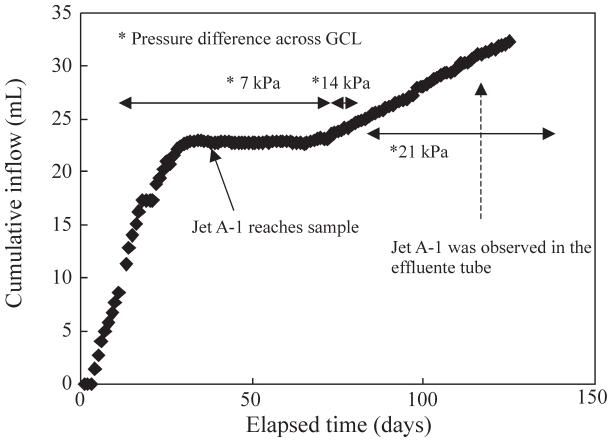

Figure 1 - Variation in cumulative inflow volume through the GCL with time for a GCL subjected to 12 freeze and thaw cycles and permeated with water and Jet A-1 in flexible wall permeameter test (modified from Rowe *et al.*, 2005c).

sion. This is particularly true when the GCL is placed over gravel or a geonet (*e.g.* in a double lined landfill). Giroud & Soderman (2000) conducted an analysis of the implications of bentonite loss from GCLs used above geonet drainage layers and concluded that a bentonite loss in excess of about 100 g/m^2 (*i.e.* about 2.5% of the initial bentonite mass) would impact on the GCL *k* and that for these applications the impact on drainage was more severe than the impact on the permeability of the GCL. Based on this analysis, they concluded that 10 g/m^2 (*i.e.* about 0.25%) could be used as a limit for impact on the drainage layer. Failures have occurred due to internal erosion. For example, Stam (2000) reported a field case where a GCL was used to line a lake. Following observations of excessive leakage, an investigation found "patchy" bentonite piping from the core of the GCL through the lightweight nonwoven geotextile resting on the coarse sand subgrade. While researchers have shown that damaged GCLs can self-heal with only a slight increase in *k* this self-healing process can be compromised and significant bentonite loss can occur if the damaged GCLs are placed on a coarse subgrade with large pore openings (Mazzieri & Pasqualini, 2000).

Rowe & Orsini (2003) studied the performance of five different GCLs (Table 3) resting on a geonet (opening size of 0.8 cm and a diagonal span of 1.2 cm), 6 mm uniform gravel ($d_{85} \approx 7$ mm, $d_{50} \approx 6$ mm, $d_{15} \approx 3.6$ mm and $d_{10} \approx 3$ mm), and a well graded sand ($d_{85} \approx 1.1$ mm, $d_{50} \approx 0.17$ mm, $d_{15} \approx 0.043$ mm and $d_{10} \approx 0.03$ mm). Their findings are summarized in the following paragraphs.

When placed on the geonet, four of the five GCLs tested (BWD, NWD, WD, SNWD; see Table 3) experienced internal erosion (bentonite loss) and an increase in hydraulic conductivity by at least one order of magnitude for heads ranging from 8 m to 45 m. In contrast the BSNWD scrim-reinforced GCL with a total carrier geotextile mass per unit area of 350 g/m^2 did not exhibit any sign of internal erosion (at heads of up to 55 m).

When placed directly over the 6 mm gravel GCLs with a single woven geotextile (BWD, WD, and NWD with the woven down) in contact with the geonet and the NWD (with the light nonwoven geotextile in contact with the geonet) all experienced internal erosion. In these cases the hydraulic conductivity increased by at least one order of magnitude for water heads ranging from ~8 m to ~90 m. In contrast, the scrim-reinforced GCLs (SNWD, BSNWD) did not experience any detrimental effects at hydraulic heads of 40-60 m for the conditions examined.

All of the GCLs tested performed well when placed over the well graded sand subgrade. For these cases even heads in the range 50-80 m did not cause any significant bentonite loss and there was no evidence of internal erosion for GCLs placed over this sand subgrade.

As the loss of bentonite increased, so too did the *k*. However failures, characterized by a significant increase in *k* of the specimen, could initially be quite localized and in some cases failure was associated with relatively little bentonite loss (as little as 1%). This suggests that the limit proposed by Giroud & Soderman (2000) of about 10 g/m^2 (about 0.25%) may be appropriate as a conservative limit for both hydraulic and drainage considerations. Rowe & Orsini (2003) concluded that designs involving GCLs over a gravel or geonet subgrade need to be carefully examined since internal erosion at water heads as low as 8 m caused an increase in the *k* by one to two orders of magnitude. The gravel used in their tests meet the subgrade criteria of ASTM D6102, and thus it appears that GCL installations meeting this standard could experience internal erosion and fail under water heads encountered in reservoirs, lagoons or landfills where leachate mounding occurs.

Rowe & Orsini's work showed that the choice of GCL carrier geotextile could significantly affect GCL performance. A GCL with a woven geotextile down (*i.e.* in

Table 3 - GCLs used in internal erosion tests (after Rowe & Orsini, 2003).

GCL	Product descriptor	Upper geotextile[1]	Core sodium bentonite	Lower geotextile[1]	Total mass/ unit area (g/m^2)	Bentonite moisture content (%)
BWD[2]	BFG5000	Bentonite filled (800 g/m^2) nonwoven 300 g/m^2	Powder 4200 g/m^2	Slit film woven 200 g/m^2	5500	< 15
WD[2]	NS	Staple fibre nonwoven 200 g/m^2	Granular 4340 g/m^2	Slit film woven 105 g/m^2	4645	< 12
NWD[3]	ST	Nonwoven 220 g/m^2	Granular 4800 g/m^2	Slit film woven 100 g/m^2	5100	22
SNWD[2]	NW	Staple fibre nonwoven 200 g/m^2	Granular 4340 g/m^2	Slit film woven, nonwoven composite 305 g/m^2	4845	< 12
BSNWD[2]	B4000	Nonwoven 300 g/m^2	Powder 4700 g/m^2	Slit film woven (100 g/m^2), nonwoven (250 g/m^2) composite	5350	< 15

[1]Polypropylene; [2]Bentofix, thermally-treated and needle-punched; [3]Bentomat, needle-punched.

contact with the 6 mm gravel and geonet) did not perform as well as the other GCLs. GCLs with a nonwoven down performed better for the gravel subgrade, but neither was acceptable for a GCL placed over the geonet. The heavy scrim-reinforced GCLs performed best with BSNWD working well for all cases examined.

For the specific well graded sand subgrade tested, all GCLs performed well. This highlights the need to carefully consider the choice of GCL in the context of the expected gradient and subgrade conditions.

5. Temperature

5.1. Temperature at the base of a landfill

Heat generated by biodegradation of waste or the heat of hydration of incinerated residues (ash) are known to increase the temperature at the base of a landfill. The temperature typically has a maximum value in the main body of the waste and decreases towards the boundaries defined by the surface and the underlying liner (Fig. 2). The rate of increase in temperature with time both in the waste and at the liner may vary depending on the waste management practice that is adopted. For example, Fig. 3 shows temperatures ranging from 24-38 °C below 4-6 year old waste at the Altwarmbüchen Landfill in Germany where waste was placed at a rate of 10-20 m/a but only 14-20 °C after a similar period at the Venneberg Landfill where waste was placed at 2 m/a. The availability of moisture can also have a profound effect on temperature as illustrated by Koerner & Koerner (2006) who monitored the temperature on the GM liner beneath 50 m of waste at two landfill cells north of Philadelphia, USA (mean annual temperature 12.6 °C). The cells had a similar low permeability geosynthetic cover but in one case ("dry cell" in Fig. 4) there was no additional moisture added while in the other case ("wet cell" in Fig. 4) there was moisture augmentation at a rate of approximately 500 m^3 per month. For the dry cell, the average liner temperature has increased to about 32 °C after 10 years. In contrast for the wet cell the temperature increased rapidly to between 41-46 °C.

At the Keele Valley Landfill (KVL) in Canada the temperatures above the liner appear to be leveling off in the 30-40 °C range ("Canada" in Fig. 4). Even higher temperatures have been reported in older landfills without a leachate collection system. For example, at the Tokyo Port Landfill in Japan the temperatures at the base ("Japan" in

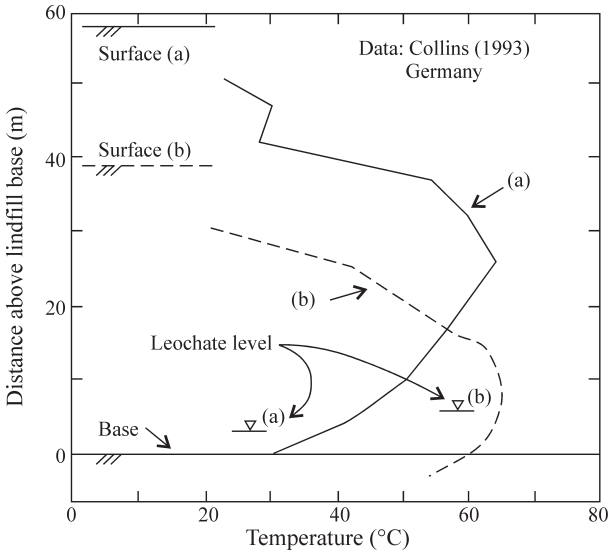

Figure 2 - Temperature variation with depth at two locations, (a) and (b), in an old landfill (1936-1980) in Hannover Germany; waste circa 1938 at bottom (after Rowe, 1998).

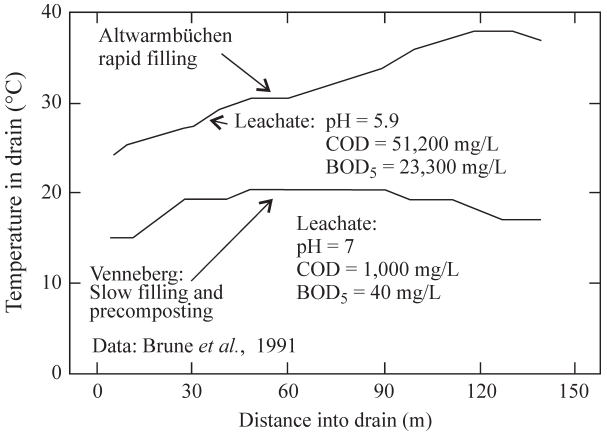

Figure 3 - Temperature in drains at two German landfills approximately 4 years after last waste placed above the drains (modified from Brune *et al.*, 1991).

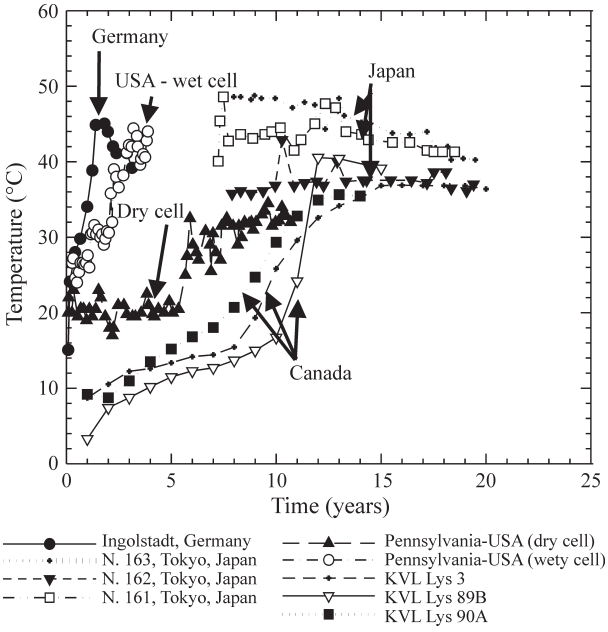

Figure 4 - Some observed temperatures at the base of landfills (US data: Koerner & Koerner, 2006; Canadian data: Rowe, 2005; Japanese data: Yoshida & Rowe, 2003; German data: Klein *et al.* 2001).

Fig. 4) were up to 50 °C 7-10 years after the beginning of landfilling and have reduced to 37-41 °C after 20 years (Yoshida & Rowe, 2003). High temperature is not restricted to MSW landfills. At the Ingolstadt landfill in Germany ("Germany" in Fig. 4), hydration of 9 m of MSW incinerator bottom ash produced a liner temperature of 463 °C 17 months after the start of landfilling.

Temperature influences both k and diffusion coefficient. Table 4 gives the ratio of both the diffusion coefficient and k at different temperatures to that at 10 °C (typical groundwater temperature in many parts of the world). Diffusive and advective transport is, respectively, 100% and 80% higher at 35 °C than at 10 °C (Table 4). Temperature also has a significant impact on service lives of GMs and clay liners as will be discussed later.

The discussion above deals with the temperature at the top of the primary liner. The temperature at the top of the secondary liner will depend on the thermal insulation provided by the material between the primary and secondary GM liner. In the case of double composite liner systems involving just a GM and GCL as the primary liner, unpublished measurements indicate that the temperature of the secondary GM may only be 3 °C or less below that of the primary GM (Legge, pers. comm.). This is consistent with theoretical modelling conducted by Rowe & Hoor (2007) which suggested only about a 1 °C difference assuming no cooling is induced by the leak detection layer. If there is a compacted clay liner (CCL) or foundation layer as part of the primary liner, then the added thermal resistance will lead to a reduction in the increase in temperature on the secondary GM that will depend primarily on the thickness of the clay liner/foundation layer. As shown in Fig. 5, for a steady state 40°C increase in temperature relative to ground water temperature on the primary GM (*i.e.* a primary GM temperature of 50 °C if groundwater temperature is 10 °C), there would be a 30°C increase on the secondary liner for a 0.75 m thick CCL. The calculated increase in temperature in secondary GM for CCL thicknesses of 0.5, 0.75 and 1 m was 33, 30 and 28 °C respectively. For a 20 °C increase at the primary GM (*i.e.* a primary GM temperature of 30 °C if groundwater temperature is 10 °C), the temperature increase at the secondary GM below a 0.75 m thick CCL and 0.3 m leak detection system would be 15 °C. This needs to be considered when assessing the service life of the secondary GM and the potential for desiccation of the secondary clay liner.

Table 4 - Effect of temperature on diffusion coefficient, D_T, and hydraulic conductivity, k_T, in a liner at temperature, T, relative to values at 10 °C (after Rowe, 1998).

Temperature (°C)	D_T/D_{10}	k_T/k_{10}
10	1.0	1.0
20	1.4	1.3
25	1.6	1.5
35	2.0	1.8
50	2.7	2.4
65	3.5	2.9

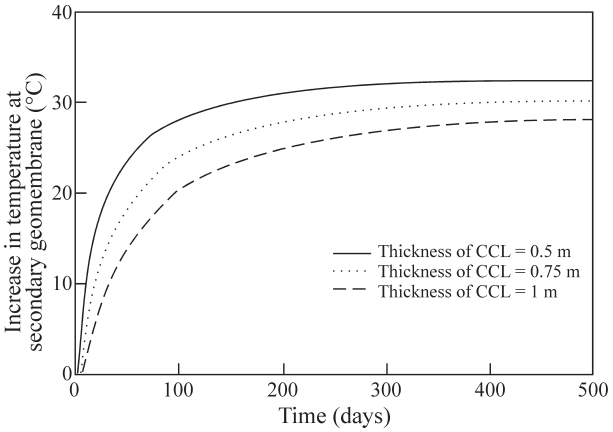

Figure 5 - Effect of primary liner thickness on temperature of secondary geomembrane assuming a 40 °C increase on the primary liner (after Rowe & Hoor, 2007).

5.2. Effect of temperature on GCLs and CCLs

Both GCLs and CCLs are susceptible to shrinkage and desiccation cracking, particularly when below a GM in a composite liner. Geomembrane temperature is very sensitive to solar radiation and can reach 80 °C (Felon *et al.*, 1992). An increase in GM temperature can cause evaporation of water from the underlying GCL into any air space between the GCL and the GM and subsequent movement of this water down-slope upon cooling of the GM. The temperature gradient beneath the GM can also cause migration of moisture from the GCL into the subsoil. Field examples involving desiccation of CCLs and shrinkage of GCLs due to temperature increase induced by solar radiation have been reported by Corser *et al.* (1992), Basnett & Bruner (1993), and Thiel & Richardson (2005). Laboratory studies also suggest that some GCLs are more susceptible to shrinkage than others (Thiel *et al.*, 2006)

Rowe (2005) has provided a recent review of research relating to the desiccation of CCLs and GCLs due to thermal gradients generated by the waste and the reader is referred to that source for details. Based on the numerical studies conducted by Heibrock (1997) and Southen (2005), and the experimental data published by Southen & Rowe (2004, 2005), Rowe (2005) reached a number of tentative conclusions as described below.

The potential desiccation of composite liner systems (both GM/GCL and GM/CCL) is controlled by the temperature gradient (and hence the temperature at the top of the liner). As discussed earlier, this may be a function of landfill operation and the likely temperatures to be experienced at the liner need to be considered in landfill design. For sin-

gle composite liners involving a GCL, it was suggested that:

(a) The unsaturated soil characteristics and initial water content of the foundation layer beneath the GCL greatly influences the potential for desiccation.

(b) The greater the overburden stress at the time of GCL hydration, the lower is the risk of desiccation. Thus both the potential for short term (*e.g.*, solar induced) and long term (waste temperature induced) desiccation can be minimized by placing the waste over the composite liner as quickly as possible after the liner construction. This finding has significant implications for the manner in which many landfills are developed.

(c) Increasing distance to the underlying watertable increased the risk of desiccation for aquifer depths up to about 5 m below the GCL, but relatively little change was predicted for increased depths beyond 5 m due to the offsetting effects of reduced water content and temperature gradient.

For single composite liners involving a CCL, it was suggested that:

(a) The unsaturated soil characteristics of the liner had a significant effect on the distribution of moisture and stress.

(b) The effect of overburden stress was not as significant as for a GCL, although it did still reduce the risk of desiccation.

There is a need for more research into the potential for long-term desiccation of clay liners making up part of a composite liner, especially with respect to the paucity of relevant soil parameters. Current research suggests that there is real potential for desiccation but also suggests that this can be mitigated by appropriate design and construction.

6. Protection of Composite Liners

Geomembrane protection layers most commonly used in North America involve a relatively light needle-punched nonwoven geotextile. This arises, in part, because a geotextile with a mass per unit area as low as 270 g/m^2 has been reported (Reddy *et al.*, 1996) to "completely protect the GM from construction loading". Wilson-Fahmy *et al.* (1996), Narejo *et al.* (1996), and Koerner *et al.* (1996) demonstrated a linear increase in protection resistance with increasing thickness (mass per unit area) of the protection layer and proposed a methodology for selection of geotextile protection layers that will provide short-term protection against puncture under the loads applied by the overlying waste. Badu-Tweneboah *et al.* (1998) proposed a test methodology to assessing the suitability of a protection layer. This approach involves three steps. Firstly, do a full scale test with the actual materials that are being considered for the project (gravel leachate collection layer, protection layer, GM, and subgrade, as appropriate) and subject the system to loads as close as possible to the anticipated loads (construction loads, in-service loads). Secondly, take the GM from the system and conduct a large diameter (0.5 m or more) burst test (hydrostatic test). If inflation is impossible, this means that the GM specimen has a hole (which may not have been visible) and the GM specimen fails the test. If inflation is possible, inflate until the GM fails. If failure occurs at the apex of the dome, the point of maximum stress, then the GM specimen passes the test. If failure of the GM occurs at a location other than the apex of the dome, then the GM has been weakened in the field test and consequently fails the test. Thirdly, if the GM failed, redo the first two steps with different protection layers until a satisfactory design is achieved.

Tognon *et al.* (2000) performed large-scale physical testing of a number of different protection layers and showed that the protection layer between the GM and the overlying drainage material has a critical effect on the tensile strains induced in the GM. The number of indentations and maximum strain induced for the different loadings and protection layers examined by Tognon *et al.* (2000) are summarized in Table 5. The best protection for the underlying GM was provided by a sand filled geocushion or a special rubber geomat, which limited strains induced by coarse (40-50 mm) angular gravel to 0.9% at 900 kPa and 1.2% at 600 kPa respectively. Of the protection layers tested, the

Table 5 - Summary of number of indentations and peak strains observed in large scale tests using 40-50 mm coarse angular leachate collection gravel separated from a 1.5 mm geomembrane over compacted clay by various different protection layers (adapted from Tognon *et al.*, 2000).

Protection layer	Mass/area (kg/m^2)	Vertical pressure (kPa)	N. of indentations (#/m^2)	Maximum indentation (mm)	Peak strain (%)
One layer geotextile 1	435	250	350	5.1	8.0
Two layers geotextile 2	1,200	900	338	7.6	13
Sand filled geocushion	2,130	650	69	3.8	0.8
Sand filled geocushion	2,130	900	78	2.9	0.9
Rubber mat	6,000	600	156	3.3	7.5
Rubber mat with polyester scrim	6,000	600	38	1.7	1.2

worst protection was provided by the lowest mass (435 g/m^2) nonwoven geotextile which allowed 350 indentations/m^2 and a maximum strain of 8% at an applied pressure of 250 kPa, and 1200 g/m^2 of geotextile which allowed about 340 gravel indentations per square metre in the GM and a peak strain (13%) close to the yield strain at 900 kPa. In either case, if only 0.001% of the indentations eventually resulted in a pin hole, this would correspond to over 30 holes/ha.

The two rubber geomats examined were identical except for the presence of a polyester grid reinforcement bonded to the second geomat. The large difference in maximum strains (7.5% and 1.2% respectively at a pressure of 600 kPa) observed for these two geomats suggests that the tensile stiffness provided by the polyester grid played a significant role in reducing lateral deformation of the rubber and hence reducing indentation and strains in the GM. Thus the tensile stiffness of the protection layers may be a critical factor in minimizing strains in GMs.

The tests conducted by Tognon *et al.* (2000) were relatively short-term (200 to 720 min) and at room temperature (24 ± 1 °C). Thus the peak strain may not represent the maximum localized strain that could develop in longer term tests. Additional research is needed to clarify the time dependent effects of strains induced by gravel particles. Nevertheless it is clear that a sand protection layer provides the best potential long-term performance.

7. Wrinkles in Geomembranes

Wrinkles in a GM predominantly arise from thermal expansion when the GM is heated by the sun after placement. Giroud & Morel (1992) performed a theoretical analysis that led to the conclusion that HDPE may be expected to exhibit large wrinkles with heights up to 10 cm and widths up to 30 cm. Rowe *et al.* (2004b) report a case where there were 1200 wrinkles/ha. Some typical wrinkle dimensions observed in the field are summarized in Table 6. Wrinkles are important because of the increased potential for contaminant migration through a hole in the GM at or near the wrinkle. There is also increased potential for development of future holes due to stress cracking at points of high tensile stress in the wrinkle.

Chappel *et al.* (2007) have developed a low altitude air photo system that can be used to quantify the geometry of GM wrinkles at a large scale. The system consists of a Digital Single Lens Reflex (DSLR) camera with remote infrared shutter control mounted on a tethered helium blimp (Fig. 6). This system allows the operator to obtain clear, accurate near-vertical air photos (Fig. 7). The wrinkle geometry is analyzed from the low altitude air photos using the digital image processing capabilities and custom functions in Matlab. This allows the user to geometrically correct images; stitch images of parts of a site together into a single image; and select and quantify wrinkle geometry from the image of the site.

Inspection of Fig. 7 shows: (A) the seams between GM panels at a spacing of about 6.6 m, (B) wrinkles at a spacing of about 3.4 m that run the entire length of the panel along the folds produced during the manufacture of the

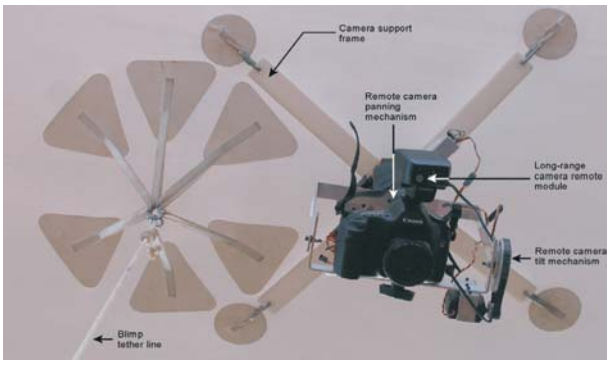

Figure 6 - Photograph showing digital camera mounted to the underside of the blimp (after Chappel *et al.* 2007).

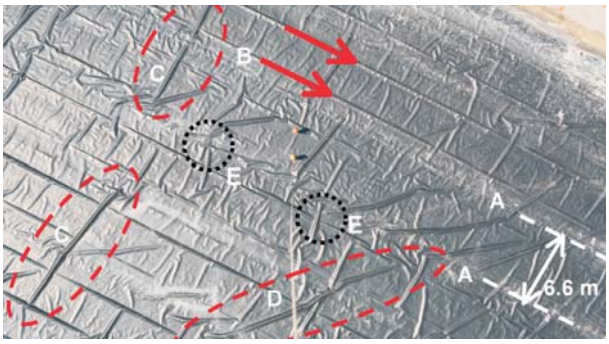

Figure 7 - Air photo of geomembrane installation. 1.5 mm smooth HDPE; Camera elevation 65 m; Latitude 43 °16' N; Air temperature 28 °C; 1:20 pm Aug 18 2006 (modified from Chappel *et al.* 2007).

Table 6 - Reported HDPE geomembrane wrinkle dimensions.

Wrinkle			Comment	Reference
Width (m)	Height (m)	Spacing (m)		
0.2-0.3	0.05-0.1	4-5	Primary wrinkles parallel to seam between rolls; smaller wrinkles perpendicular to main wrinkles	Pelte *et al.* (1994)
0.1-0.8	0.05-0.13	0.3-1.6	Wrinkles < 4 m long	Touze-Foltz *et al.* (2001)
0.3	0.2	-	At the slope to floor transition zone	Davies (pers. comm.)

GM, (C) wrinkles perpendicular to the panel, (D) wrinkles at about 45 ° to the panel, and (E) the interconnectedness of wrinkles. Since fluid entering a hole in a wrinkle can run along the entire interconnected length, the length of a wrinkle should be regarded as the total linear distance fluid can migrate along a wrinkle and its interconnections. For the site shown, there was about 530 m of wrinkle per hectare and about 420 m of connected wrinkle per hectare. As will be discussed in the section on leakage, the presence of wrinkles can significantly increase the leakage through the composite liner.

7.1. Behaviour of geomembrane wrinkles under load

The wrinkles formed during placement of the GM do not necessarily disappear when the GM is covered and the waste is placed (Stone, 1984; Soong & Koerner, 1998; Gudina & Brachman, 2006a,b). Compression of these wrinkles due to loading can be expected to induce tensile strains in the GM and these may contribute to the formation of holes due to stress cracking. Gudina & Brachman (2006a,b) examined the interaction between the granular material and the wrinkle using a specially designed apparatus that allows the simulation of the foundation layer, composite liner with a wrinkle in the GM, the protection layer and the granular drainage layer. The system can then be loaded to simulate pressure due to the waste of 1000 kPa (or more). For example, Fig. 8 shows the initial wrinkle shape and the deformed shape of the wrinkle following application of 1000 kPa for a test with sand above and below the GM (SP). Results are also shown for a test with 50 mm gravel above and a GCL beneath the GM (GP1 and GP2). The gravel resulted in more severe and nonuniform deformation of the GM than the sand due to the discrete nature of the interactions with the coarse gravel. With gravel there was both pinching (GP1) and flattening at the top (GP2) of the GM which give rise to increased tensions in the GM. This indicates the desirability of having a sand protection layer that is of sufficient thickness to cover the wrinkles between the gravel drainage layer and the underlying GM.

Tests performed by Gudina & Brachman (2006a) found that with a compacted clay subgrade beneath the GM, the gap between an initially 200 mm wide and 60 mm high wrinkle and the CCL could be completely filled with clay if sufficient pressure was applied. The pressures required for this ranged from 100 kPa for a CCL with a water content (16%) at the plastic limit for that clay and 500 kPa for the same clay at a water content (13%) 1% wet of standard Proctor optimum.

The strains induced in the GM with a wrinkle are given in Table 7 for four different protection layers and an applied pressure of 250 kPa. Without protection the strains are very large (42%, which is twice the yield strain) but even with a heavy (1200 g/m^2) geotextile protection layer the strains reached 11%. Only the sand protection layer provided low strains (2%) in the GM. Although these tests are

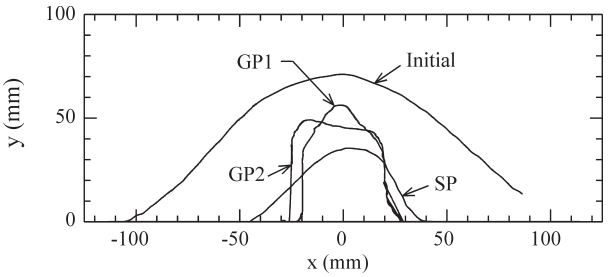

Figure 8 - Wrinkle geometry in a 1.5 mm HDPE geomembrane before and after application of 1000 kPa vertical pressure for 10 h. Results shown for sand above and below the geomembrane (SP) and 50 mm gravel directly above and a GCL beneath the geomembrane at two locations on the wrinkle: GP1 and GP2 (after Rowe *et al.* 2004b).

Table 7 - Strains induced in a geomembrane with a wrinkle at an applied pressure of 250 kPa for different protection layers for a configuration comprised of (from top down) nominal 50 mm gravel, protection layer, geomembrane and CCL compacted at the plastic limit (moisture content of 16%). The initial wrinkle was 60 mm high and 240 mm wide (adapted from Gudina & Brachman, 2006b).

Protection layer	Maximum GM strain (%)
None	42
Needle-punched nonwoven GT (M_A = 390 g/m^2)	15
Needle-punched nonwoven GT (M_A = 1200 g/m^2)	11
150 mm sand layer	2

GT = geotextile; M_A = mass per unit area.

for a limited range of conditions, the message that a sand protection layer is far superior to the use of even a thick geotextile protection layer is consistent with other findings described above.

Gudina & Brachman (2006b) and Dickinson & Brachman (2006) performed tests similar to those discussed above except that instead of a CCL a GCL and sand foundation layer were located below the GM. They found that the GM wrinkle experienced a decrease in height and width when subjected to vertical pressure. However, the gap between the GM and GCL remained for all the tests at applied pressures up to 1000 kPa.

Dickinson & Brachman (2006) focused their attention on the effect of the wrinkle on GCL deformations and the effectiveness of different protection layers to minimize GCL deformations. The thickness of the GCL was found to decrease beside the wrinkle and increase beneath the wrinkle due to lateral extrusion of bentonite into the gap beneath the wrinkle. Without a protection layer the gravel backfill caused bentonite extrusion from beneath gravel contacts to zones in between particles causing large variations in the thickness of the GCL (with a minimum thickness of about

2 mm). More surprising was the finding that the heavy (M_A = 1200 and 2000 g/m^2) nonwoven needle-punched geotextile protection layers tested were not effective at reducing the number and magnitude of these indentations. As shown in Figs. 9 and 10, at an applied pressure of 250 kPa, even with a 2000 g/m^2 protection layer there was thinning of the hydrated GCL to as little as 2.2 mm compared to an average initial thickness of 7.8 mm. In contrast, the 150 mm thick sand protection layer reduced both the number and magnitude of local indentations giving a minimum final GCL thickness at 250 kPa of 4.2 mm with the sand layer. The sand protection layer redistributes the gravel contact stresses such that the majority of the GCL deformation was due to consolidation of the bentonite rather than lateral extrusion. As noted by Dickinson & Brachman (2006), this is preferable because a relatively uniform reduction in void ratio from consolidation would be accompanied by a reduction in hydraulic conductivity.

While more research is needed, it appears that in order to provide the best performance of both the GM and GCL used in composite liners, a 150 mm thick sand protection layer is far preferable to even a thick nonwoven needle-punched geotextile (2000 g/m^2) on the base of a landfill.

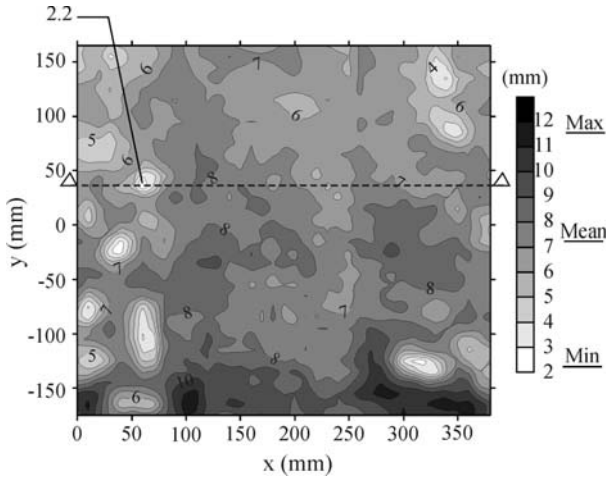

Figure 9 - Contours of the final thickness of a GCL after application of 250 kPa vertical pressure. Configuration comprised (from top down) nominal 50 mm gravel, for a 2000 g/m^2 needle-punched nonwoven protection layer, geomembrane and GCL (w = 115%), sand layer (adapted from Dickinson & Brachman, 2006). Marked cross-section shown in Fig. 10.

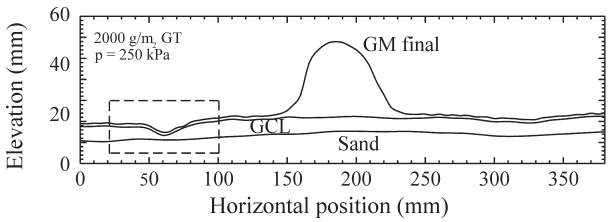

Figure 10 - Cross-section through Fig. 9 at the location of minimum GCL thickness (adapted from Dickinson & Brachman, 2006).

8. Leakage through Composite Liners

8.1. Holes in geomembranes

In the absence of holes, a GM is essentially impermeable to water and hence any leakage (advective transport) through GMs must be through holes in the GM. Based on 205 results from four published leak detection surveys, Rowe *et al.* (2004b) found that: (a) no holes were detected for 30% of the cases; and (b) less than 5 holes/ha were detected for half of the surveys. Nosko & Touze-Foltz (2000) reported 3 holes/ha after installation and 12 holes/ha after placement of drainage layer. Table 8 indicates that 50% of holes in studies reported by Colucci & Lavagnolo (1995) had an area of less than 100 mm^2 (r_o < 5.64 mm). Since the leak detection surveys used to establish the number and size of holes discussed above are conducted shortly after construction of the liner system, it is uncertain how many holes may develop under combined overburden pressures, elevated temperatures and chemical exposure years after construction and placement of the waste. These holes may arise from: (a) indentations at gravel contacts following placement of the waste; (b) stress cracking at points of high tensile strain in wrinkles; and (c) sub-standard seams subjected to tensile stresses.

8.2. Calculation of leakage through holes in the geomembrane

Rowe (2005) has provided an extensive discussion of leakage through composite liners based on both theoretical considerations and observed field behaviour and only a brief summary is provided here - the reader is referred to the prior publication for details. At present, the leakage through composite liners is usually calculated using empirical equations (established by curve fitting families of solutions from analytical equations; *e.g.*, Giroud & Bonaparte, 1989; Giroud, 1997; Giroud & Touze-Foltz, 2005; Touze-Foltz & Giroud, 2005). The results obtained from these equations can be compared with the observed leakage through the primary liner at a large number of landfills with double liner systems as reported by Bonaparte *et al.* (2002).

Table 8 - Reported size of holes in geomembranes (based on data reported by Colucci & Lavagnolo, 1995).

Leak area (mm^2)	Equivalent radius for circular hole, r_o (mm)	Percentage (%)	Cumulative percentage (%)
0-20	0-2.5	23.2	23.2
20-100	2.5-5.64	26.3	49.5
100-500	5.64-12.6	28.2	77.7
500-1000	12.6-17.8	8.8	86.5
10^3-10^4	17.8-56.4	7.8	94.3
10^4-10^5	56.4-178	4.5	98.2
10^5-10^6	178-517	1.2	100

Rowe (2005) made this comparison and concluded that one can not explain the typical observed leakage using the traditional equations and a reasonable number of holes per hectare.

Rowe (1998) presented an analytical solution for the case where a hole coincides with a wrinkle in the GM of length, L, and width, $2b$ (Fig. 11). The transmissivity beneath the wrinkle is much greater than the interface transmissivity, θ, where the GM is in contact with the underlying soil. It is also assumed that $L > b$ such that the effects of leakage at the ends of the wrinkle can be neglected. This solution assumes unobstructed lateral flow along the length, L, and across the width, $2b$, of the wrinkle and then lateral flow between the GM and the soil outside the wrinkle. One dimensional, vertical flow is assumed from the transmissive layer through the underlying soil beneath the wetted distance from the wrinkle (this is an approximation). Rowe's solution allows consideration of interactions between adjacent similar wrinkles assumed to be spaced at a distance $2x$ apart and the leakage, Q, is given by:

$$Q = \frac{2Lk\left[b + \dfrac{1-\exp(-\alpha(x-b))}{\alpha}\right]h_d}{D} \qquad (2)$$

where L is the length of the wrinkle; $2b$ is the width of the wrinkle; k is the hydraulic conductivity of the clay liner; θ is the transmissivity of the GM-clay liner interface; $\alpha = [k/(D\theta)]^{0.5}$; h_d is the head loss across the composite liner; and D is the thickness of the clay liner. Assuming no interaction with an adjacent wrinkle, the leakage, Q, is given by:

$$Q = \frac{2L\left[kb + \sqrt{kD\theta}\right]h_d}{D} \qquad (3)$$

The leakage calculated using this wrinkle analytical solution is compared with that from a $2D$ finite element analysis in Figs. 12 and 13 and again it can be seen that there is excellent agreement between the analytical solution and the 2D numerical analysis with an error of 5% (or less)

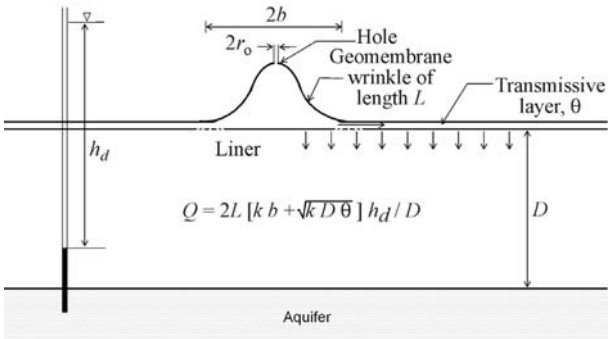

Figure 11 - Schematic defining leakage through a composite liner with a wrinkle. Assumes lateral migration at interface and vertical flow in clay liner.

for both the GM/GCL composite liner (Fig. 12) and GM/CCL composite liner (Fig. 13) for range of cases considered. Figures 12 and 13 also highlight the difference in leakage that would be expected for a hole in direct contact with the clay liner and one in a 15 m long wrinkle.

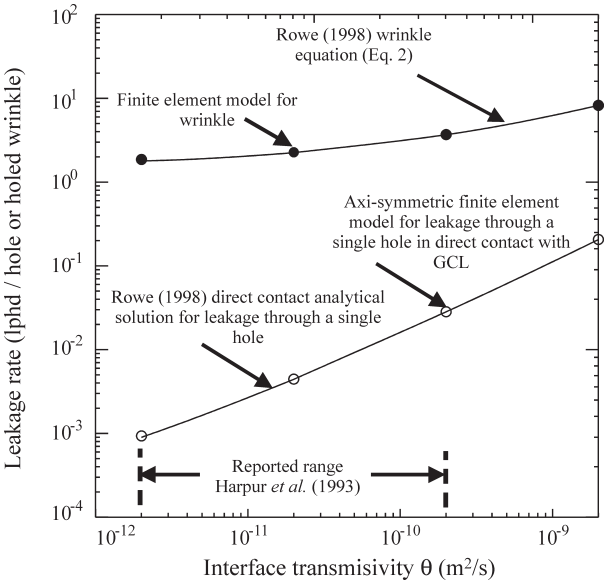

Figure 12 - Comparison of leakage rates for GM/GCL/attenuation layer composite liner and a range of interface transmissivities as calculated from analytical solutions and FEM analysis for (a) a single hole in direct contact with the GCL and (b) a single 15 m long wrinkle with a hole. k_L = 5 x 10^{-11} m/s, H_L = 0.01 m, k_f = 1 x 10^{-6} m/s, H_f = 0.5 m, L = 15 m, B = 30 m and $2b$ = 0.3 m.

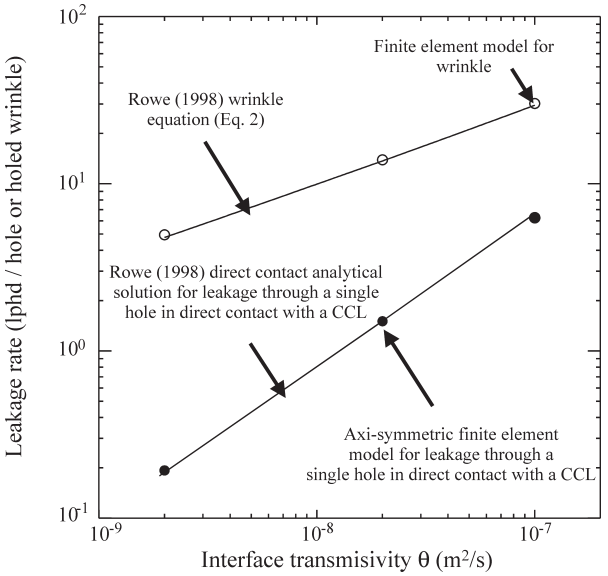

Figure 13 - Comparison of leakage rates for GM/CCL composite liner and a range of interface transmissivities as calculated from analytical solutions and FEM analysis for (a) a single hole in direct contact with the GCL and (b) a single 15 m long wrinkle with a hole. k_L = 5x10^{-9} m/s, H_L = 0.51 m, L = 15 m, B = 30 m and $2b$ = 0.3 m.

Table 9 compares the observed and calculated (using Eq. (2) and accounting for interaction assuming equally spacing of the wrinkles) leakage for a GM over a 0.9 m thick CCL. Three different liner conditions were examined: (a) low hydraulic conductivity liner and good interface conditions; (b) typically specified liner and good interface conditions; and (c) typically specified liner and poor interface conditions. The typical range of observed average leakage could be explained by 12 holed (0.2 m wide) winkles/ha (3 to 30 m long) with a typical liner and good contact (Case (b)). Similarly Table 10 shows that the observed average leakage of 60-160 lphd could be explained by one holed wrinkle that has a 70-180 m long interconnected length per hectare for Case (b) (based on Eq. (3); *i.e.* assuming the wrinkle is linear). The peak leakage of 390 lphd could be explained by about 1 holed 440 m long interconnected wrinkle/ha and good interface conditions (Table 10). Thus the typical observed leakage for composite liners involving CCLs can be readily explained by holes in wrinkles for a reasonable number of holes/ha.

Table 9 also shows observed leakage and the calculated leakage for two GCL cases: (d) low k GCL (assuming no significant clay-leachate interaction) and (e) high k GCL (assuming significant clay-leachate interaction). Both cases assume the highest interface transmissivity measured by Harpur *et al.* (1993). It can be seen that for the best conditions (Case (d)) about 2.5 holed 3-30 m long wrinkles/ha are needed to explain the typical observed range of 0.6-1.5 lphd. Alternatively this range could be explained by one holed 8-20 m long interconnected wrinkle per hectare (Table 10). The peak flow of 54 lphd can be explained by good conditions (Case (d)) and one holed 670 m long interconnected wrinkle per hectare or poorer conditions (Case (e)) and one holed 250 m long interconnected wrinkle per hectare (Table 10). Thus the typical observed leakage for composite liners with GCLs also can be readily explained by holes in wrinkles for the typical number of holes/ha and reasonable combinations of other parameters.

Table 10 - Calculated leakages with one holed wrinkle per hectare for comparison with observed leakages given in Table 9 (after Rowe, 2007).

Case[1, 2]	Liner	k (m/s)	θ (m^2/s)	Wrinkle length (m)	Leakage (lphd)
(b)	0.9 m CCL	1×10^{-9}	1.6×10^{-8}	70	60
(b)	0.9 m CCL	1×10^{-9}	1.6×10^{-8}	180	160
(b)	0.9 m CCL	1×10^{-9}	1.6×10^{-8}	440	390
(d)	GCL[3]	5×10^{-11}	2×10^{-10}	8	0.6
(d)	GCL[3]	5×10^{-11}	2×10^{-10}	20	1.5
(d)	GCL[3]	5×10^{-11}	2×10^{-10}	670	54
(e)	GCL[3]	2×10^{-10}	2×10^{-10}	250	54

[1]Corresponds to same cases as examined in Table 9 but only one holed wrikle and effect of wrinkle length is examined.
[2]$h_w = 0.3$ m, $h_a = 0$, $2b = 0.2$ m.
[3]Calculations assume thickness of 0.01 m.

The monitoring of flows in the leak detection system can provide insights about when there has been damage to the liner. This may be particularly important when the composite liner is comprised of a GM and GCL. It has been shown that this combination generally gives the less leakage and a GM and CCL. However, unless it is protected by an adequate protection layer or operating procedures, this system is the most prone to damage. Even if a landfill is well constructed, subsequent landfill activity such as moving waste can result in holes through the entire GM/GCL primary liner system. This, in turn, can result in the flow in the leak detection system increasing from the normal values (10 lphd or less) to values several orders of magnitude higher. The advantage of a double lined system is that it allows the detection of these accidents and their repair before

Table 9 - Comparison of calculated (with wrinkles) and observed leakage during the active period for 0.9 m thick CCL and GCL. k = hydraulic conductivity, θ = interface transmissivity.

Case	Liner	k (m/s)	θ (m^2/s)	Leakage for stated number of holed wrinkles/ha[1] (lphd)		Observed[2] (lphd)	
				2.5	12	Range	Peak[4]
(a)	0.9 m CCL	1×10^{-10}	1.6×10^{-8}	2-20	10-65	60-160[3]	390[4]
(b)	0.9 m CCL	1×10^{-9}	1.6×10^{-8}	7-70	30-310		
(c)	0.9 m CCL	1×10^{-9}	1×10^{-7}	16-160	80-580		
(d)	GCL[7]	5×10^{-11}	2×10^{-10}	0.6-6	3-30	0.6-1.5[5]	54[6]
(e)	GCL[7]	2×10^{-10}	2×10^{-10}	1.6-16	8-75		

Rounded; [1]Range of calculated values corresponds to $L = 3$ and 30 m (accounting for interaction); Hole $r_o = 5.6$ mm; $h_w = 0.3$ m, $h_a = 0$, $2b = 0.2$ m; [2]based on data from Bonaparte *et al.* (2002) for systems with a GN LDS; [3]Time weighted based on the reported vales for different time periods for 4 landfill cells with 900 mm CCL and GN LDS (from Table 4 of Rowe, 2005); [4]Largest peak value reported for a monitoring period; [5]Mean of average monthly flows in post-closure and active period; [6]Largest peak monthly flow reported; [7]Calculations assume thickness of 0.01 m.

too much waste has been placed over the location. With a single lined system it is unlikely that such a breach would be detected until the waste has all been placed and it is no longer practical to repair. This highlights the need to place an adequate protection layer above the composite liner to minimize the risk of such accidental damage. It also highlights the need to closely monitor not only the construction of the liner but also any waste placement or other work that could potentially cause damage to the liner.

There are a number of other factors that can influence the leakage that is observed in the leak detection system of double lined landfills. For example, the interpretation of data for the initial period may complicated by the contribution of construction water to the measured leakage and interpretation of the data from systems employing CCL layers is complicated by the presence of water that squeezes out of the clay as the load on the clay increases, referred to as consolidation water. However the field cases reported here are all for systems with a geonet leak detection system and there would not be much retained water in these systems. Also Rowe (2005) looked at data for composite liners with CCLs and the was no correlation between leakage and liner thickness as one would expect if consolidation water was representing a significant component of the fluid being collected. Furthermore, the time to for consolidation of typical CCLs is relatively short and the amount of water that would be released more than a few after months loading is quite small and could not explain the leakages reported for CCLs. Thus the most likely explanation for the higher than expected flows based on typical calculations is holes in wrinkles.

Of particular note is the need to design systems involving a geonet leak detection system such that swelling and intrusion (under vertical stress) of any overlying GCL does not compromise the drainage function of the underlying geonet (Shaner & Menoff, 1992; Legge & Davies, 2002).

While the foregoing indicates the necessity of considering holes in wrinkles if one is to reasonably estimate leakage through composite liners (assuming there are wrinkles, as in most cases), it should be emphasized that in the post-closure period the observed leakages (Bonaparte *et al.* 2002) are small. For landfills with composite liners involving a GCL the post closure maximum monthly flow was 10 lphd which corresponds to an advective flux of less than 0.4 mm per year. For landfills with a GM/CCL composite the average peak monthly flow was 60 lphd (*i.e.* an advective flux of about 2 mm per year) and in these circumstances contaminant transport is likely to be controlled by diffusion through the liner system for contaminants that can readily diffuse through a GM.

9. Diffusion through GCL's and Geomembranes

Diffusion is a process wherein contaminants migrate from locations of high concentration (*e.g.* a landfill, lagoon or contaminated groundwater) to a region of lower concentration (*e.g.* clean groundwater). It can occur in air, water, soil or even through solids such as an HDPE GM.

9.1. Basic concepts associated with diffusion in water and saturated porous media

In its simplest form, molecular diffusion in water is a result of the kinetic activity (random movement) of the atoms (*e.g.* H^+, Cl^-, Na^+, Fe^{2+}, Cd^{2+}) or molecules (*e.g.* OH^-, HS^-, HCO_3^-, CH_3COO^-, $Fe(CN)_6^{3-}$,CH_2Cl_2, C_6H_6, $C_6H_5C_2H_5$, H_2O, D_2O). The amount of movement is directly proportional to absolute temperature (*i.e.* there is no movement, and hence no diffusion, only at zero degrees Kelvin). At the location where a contaminant enters a body of water there is a high concentration (*i.e.* large number of atoms and/or molecules of the contaminant per unit volume) and thus a high probability that these molecules will collide with other atoms/molecules. As a result of the collision the atoms/molecules are likely to be propelled out of the region of high concentration into a region of lower concentration.

Imagine, as a very crude analogy, the start of a game of billiards where there is an initial collection of balls at one location on a billiard table. As the cue ball is driven into the collection of balls, the energy imparted by the collision causes the balls to spread out around the table reducing the concentration around the initial location of the clustering of balls. Assuming no balls fall into the pockets in the table, further play is likely to cause further spreading of the balls.

The diffusion coefficient of a given contaminant in water is a complex function of the mass, radius, valence, and concentration/dissociation state of the contaminant, and the viscosity, dielectric constant and temperature of the diffusing medium (water in this case). The presence of soil particles, particularly clay minerals and organic matter, complicates the diffusion process. Diffusion through a network of clay particles (or fibres in a geotextile for the geotextile component of a GCL) involves the diffusive movement of the species of interest in the pore water between the clay particles (or geotextile fibres). There are many complicating factors that affect the diffusion of contaminants through water in the pores of a saturated porous medium (see Chapter 6 of Rowe *et al.* 2004b for a detailed discussion). However for most practical purposes these can be represented in terms of the effective porosity, n, of the medium and an effective diffusion coefficient, D_e. The greater the porosity, the more the pore water (per unit volume) available for diffusion to occur and, hence, the greater the diffusive flux of contaminant (other things being equal). Techniques for establishing the effective diffusion coefficient and their limitations are described by Rowe *et al.* (2004b).

The migration of certain organic contaminants can be retarded by adsorption and/or absorption onto organic matter in the soil or polymer fibres for a needle punched GCL. Another completely different mechanism involves cation

exchange between certain ionic contaminants (*e.g.* NH_4^+, K^+, Mg^{2+}, Fe^{2+} etc) and clay soils (*e.g.* bentonite in a GCL) and this results in a similar reduction in concentration. Since the precise details of the mechanism are not important for most practical purposes, adsorption, absorption and cation exchange are often lumped together and referred to as "sorption". Historically, sorption parameters are obtained from batch tests where a given mass of soil is added to a solution with a known initial concentration of the contaminant of interest. There is then a partitioning of the contaminant between the dissolved phase (*i.e.* in the solution) and the soil. At the point of chemical equilibrium, a partitioning coefficient, K_d, can be deduced. Assuming low concentrations of contaminant, the partitioning coefficient will be a constant for a given contaminant and soil and, as a consequence, the mass of contaminant sorbed onto the soil per unit mass of the soil, C [-], will be a linear function of the concentration, c [ML^{-3}), in the pore fluid:

$$C = K_d\, c \tag{4}$$

where K_d is called the partitioning or distribution coefficient [$M^{-1}L^3$]. More complicated cases (*e.g.* non-linear sorption) are described by Rowe *et al.* (2004b). It should be noted that for organic contaminants the actual mechanism associated with sorption onto organic matter in soil or the geotextile fibres in a GCL involves (a) partitioning of contaminant between the pore fluid and the surface of the solid, and (b) diffusion into the solid organic matter or geotextile fibre. Thus, while it takes some time to reach equilibrium, the time scale is generally short relative to the time scale of the diffusion through the porous medium because the particles are very small (thin, in the case of geotextile fibres) and thus is modelled as instantaneous. The processes involved in sorption of organic contaminants here are similar to those described below for diffusion through GMs. The difference is that in the case of diffusion into organic matter or geotextile fibres in the soil, the contaminant is being removed from solution in a situation where the primary path for diffusion is in the pore fluid and thus it ceases to participate in diffusion from source to receptor (unless the concentration in the pore fluid drops, in which case it can be slowly released back into solution for reversible sorption). In the case of an intact GM discussed below, the only way for the contaminant to diffuse from pore fluid on one side of the GM (*e.g.* source) to that on the other side (*e.g.* receptor) is for the contaminant to diffuse through the GM.

Radioactive contaminants and some organic contaminants will also experience a decrease in concentration due to radioactive decay or biodegradation. This can often be represented in terms of first order decay where the rate of reduction of concentration, *dc/dt*, is proportional to the current concentration, *c*, so that:

$$\frac{dc}{dt} = -\lambda c \tag{5}$$

where λ is the first order decay constant [T^{-1}],

The factors discussed above can be combined and the contaminant transport through the soil component of barrier systems can be modelled by solving the equation for one- dimensional contaminant transport of a single reactive solute through a porous medium (Rowe *et al.*, 2004b):

$$n\frac{\partial c}{\partial t} = nD_e\frac{\partial^2 c}{\partial z^2} - \rho_d K_d\frac{\partial c}{\partial t} - \lambda c \tag{6}$$

subject to appropriate boundary and initial conditions, where c is the concentration at depth z and time t; n is the effective porosity; D_e is the effective diffusion coefficient; ρ_d is the dry density of the medium through which diffusion takes place; K_d is the partitioning coefficient; and λ is the first order decay constant. Typically, diffusion parameters are inferred from laboratory tests conducted using the soil of interest and a leachate similar to that anticipated in the field application. While the diffusion coefficient may vary from soil to soil and case to case, it usually falls within a much narrower range than hydraulic conductivity.

9.2. Diffusion through unsaturated soils

For non-volatile contaminants which will readily diffuse through water but not air, unsaturated soil provides a better diffusion barrier than a saturated soil since they can only diffuse thought the water phase. Equations for estimating the diffusion coefficient for unsaturated soils are given by Rowe *et al.* (2004b). For volatile contaminates the opposite is true. Volatile organic contaminants (VOCs) such as dichloromethane (DCM), 1,2 dichloroethane (DCA), trichloroethene (trichloroethylene, TCE), benzene, toluene, ethylbenzene, m&p-xylene and o-xylene will diffuse orders of magnitude faster in a dry soil than they will through a saturated soil. In an unsaturated soil, they will diffuse in both the gaseous and dissolved phases, but diffusion will be predominantly though the gas filled pores if the water content is low enough to have a significant number of continuous gas filled pores. This issue is addressed in more detail by Rowe *et al.* (2004b), however it is worth noting here that for double liner systems, even if there is no leachate in contact with a primary or secondary GM liner, VOCs in the gaseous phase in the leachate collection system will readily diffuse through typical primary composite liners, an unsaturated leak detection system, and the secondary GM with the secondary liner and attenuation layer providing the most signifiant resistance to their migration.

9.3. Diffusion through hydrated GCLs

There is a direct correlation between the diffusion coefficient and the bulk void ratio of the GCL and Lake & Rowe (2000) showed that the chloride diffusion coefficient ranged between 1 x 10^{-10} m^2/s (0.003 m^2/a) and 4 x 10^{-10} m^2/s

(0.013 m^2/a) for the range of conditions they examined. This may be compared with a typical diffusion coefficient of about 6 x 10^{-10} m^2/s (0.02 m^2/a) through a CCL. Lake & Rowe (2004) reported diffusion coefficients of between about 2 x 10^{-10} m^2/s (0.006 m^2/a) to 3 x 10^{-10} m^2/s (0.009 m^2/a) for several VOCs (DCM, DCA, TCE, benzene and toluene) through a GCL at room temperature and a confining pressure less than 10 kPa. Rowe *et al.* (2005b) extended this work by examining the effect of temperature on the diffusion of benzene, toluene, ethylbenzene, m&p-xylene and o-xylene (BTEX). They showed that the geotextile component of a GCL was the primary contributor to sorption of hydrocarbons by the GCL, and partitioning coefficients (K_d at 22 °C and 7 °C in mL/g) for the entire GCL were: m&p-xylene (42, 25) > ethylbenzene (36, 22) > o-xylene (27, 14) > toluene (15, 8.7) > benzene (4.4, 2.6). The diffusion coefficients (at 22 °C and 7 °C in m^2/s) followed the order benzene (3.7 x 10^{-10}, 2.2 x 10^{-10}) > toluene (3.1 x 10^{-10}, 1.8 x 10^{-10}) > ethylbenzene (2.9 x 10^{-10}, 1.7 x 10^{-10}) > m&p-xylene (2.5 x 10^{-10}, 1.5 x 10^{-10}) ≈ o-xylene (2.6 x 10^{-10}, 1.5 x 10^{-10}). While the change in temperature from 22 °C to 7 °C reduced both the diffusion and sorption coefficients, these reductions had opposite effects on mass transport through the GCL with the decrease in mass transport due to a reduced diffusion coefficient dominating over the increase due to smaller sorption. Thus the net effect was less mass transport at lower temperature.

9.4. Diffusion through geomembranes and composite liners

Although the basic mechanism causing molecular diffusion is the same as for a porous medium (*e.g.* GCL, CCL or underlying subsoil), the details of how diffusion occurs through a "solid" GM are somewhat different. In the case of the saturated porous medium the diffusion occurs in the pore water between the solids (be they soil particles or geotextile fibres) and sorption onto the soil particles or geotextile fibres serves to remove contaminant from the pores and hence from impact on an underlying receptor. In the case of a solid GM, sorption (partitioning) onto the polymer is an essential first step that attaches the contaminant to the plastic and provides an initial concentration for diffusion through the GM (Fig. 14). It needs to be remembered that while a GM is a solid, at the molecular level it is made up of chains of polymers that are vibrating (with the amount of vibration being a function of temperature) and there is space between these polymer chains which, although not visible to us, may be significant with respect to the size of contaminant atoms or molecules. Thus the diffusion of contaminants through an intact GM is a molecule activated process that can be envisioned to occur by steps or jumps over a series of potential barriers, following the path of least resistance. For dilute aqueous solutions, the process involves three key steps (Haxo & Lahey, 1988) as illustrated in Fig. 14: (i) partition of the contaminant between

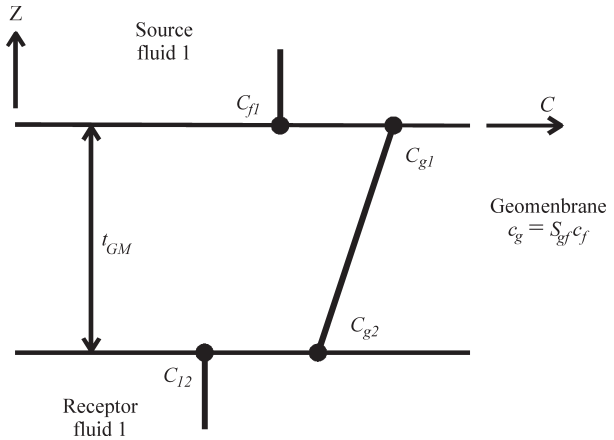

Figure 14 - Concentration profile for diffusion across a geomembrane showing (a) partitioning between the concentration in the source solution, c_{f1}, and the concentration in the adjacent geomembrane, c_{g1}; (b) diffusion profile from the top to bottom of the geomembrane; (c) partitioning between the concentration at the bottom of the geomembrane, c_{g2} and the concentration in the receptor solution, c_{f2}. Note that $c_{g1}/c_{f1} = c_{g2}/c_{f2} = S_{gf}$.

the medium containing the contaminant and the inner (*i.e.* contacting) surface of the GM (sorption); (ii) diffusion of the permeant through the GM; and (iii) partition between the outer surface of the GM and the outer medium (desorption). The diffusive motion depends on the energy availability and the relative mobilities of the penetrant molecules and polymer chains. This will depend on temperature, the size and shape of the penetrant, the nature of the polymer and, potentially, concentration.

The extent to which permeant molecules are sorbed in a polymer depends upon the activity of the permeant within the polymer at equilibrium (Müller *et al.*, 1998). When a GM is in contact with a fluid, there will be a relationship between the final equilibrium concentration in the GM, c_g, and the equilibrium concentration in the fluid, c_f where the concentrations c_f and c_g represent the amount of the substance of interest (contaminant) dissolved per unit volume of the water or GM respectively. The concentration is typically represented in terms of mol per litre (mol L^{-1}) or as a mass concentration in mg/L or µg/L. For the simplest case where the permeant does not chemically interact with the polymer (*e.g.*, as is the case for dilute solutions such as typical landfill leachates and HDPE), the relationship between the concentration in the fluid and the GM is given by (Henry's law):

$$c_g = S_{gf}\, c_f \qquad (7)$$

where S_{gf} is called a partitioning coefficient and in principle is a constant for the given molecule, fluid, GM, and temperature of interest. Note that S_{gf} greater than 1 implies a preference for the GM (*i.e.* the amount of substance per unit volume of the GM is greater that that per unit volume of the fluid). This is typically the case for hydrophobic organic

contaminants (*i.e.* those with low solubility in water) which can readily dissolve in HDPE, with the value of S_{gf} being greater the more hydrophobic the contaminant. Thus S_{gf} for ethylbenzene is greater than for benzene which is greater than for dichloromethane (Table 11). Conversely hydrophilic contaminants (*i.e.* those highly soluble in water, like salts such as NaCl) do not readily dissolve in HDPE and have a value of S_{gf} which is less than unity (see chloride in Table 11) since, at equilibrium, most of the substance will be dissolved in the water rather than the GM.

In the second stage of the migration, diffusion of the sorbed penetrant within the GM can be described by Fick's first law:

$$f = -D_g \frac{dc_g}{dz} \tag{8}$$

where, f is the mass flux, D_g is the diffusion coefficient of the considered contaminant in the GM, c_g is the concentration of diffusing substance in the GM, and z is the direction parallel to the direction of diffusion. In transient state, the governing differential equation is (Fick's second law):

$$\frac{\partial c_g}{\partial t} = D_g \frac{\partial^2 c_g}{\partial z^2} \tag{9}$$

which must be solved for the appropriate boundary and initial conditions.

The last stage in the migration process is permeant desorption from the GM to the outer solution. This stage is similar to the first except that here contaminants will diffuse from the GM into the adjacent fluid so that at equilibrium the contaminant concentration in the adjacent fluid is related to that in the GM by the relationship:

$$c'_g = S'_{gf}\ c'_f \tag{10}$$

where S'_{gf} is the contaminant partitioning coefficient between the outside fluid and the GM. In the simplest case where the solutions on either side of the GM are aqueous, these two partitioning coefficients may be assumed to be the same ($S_{gf} = S'_{gf}$). The two partitioning coefficients described by Eqs. (7) and (10) are conceptually similar to that described for a porous medium by Eq. (4) and can also be obtained in a similar way from batch tests. The parameter differs in detail because of the difference between a porous media and a solid GM and the fact that in the soil, partitioning and the related sorption removes contaminant from the diffusion process through the porous medium while for a solid GM partitioning is associated with the contaminant entering and exiting the GM, with it diffusing through the GM.

Since the primary interest is in the concentrations of contaminant in water (not the GM) it is convenient to express the diffusion equations in terms of the concentration in adjacent solutions c_f. Substituting Eq. (7) into Eq. (8), the flux from an aqueous solution on one side of the GM to an aqueous solution on the other side is given by:

$$f = -D_g \frac{dc_g}{dz} = -S_{gf} D_g \frac{dc_f}{dz} - P_g \frac{dc_f}{dz} \tag{11}$$

where the permeation coefficient (called the permeability in the polymer literature), P_g, is given by:

$$P_g = S_{gf} D_g \tag{12}$$

and where P_g is a mass transfer coefficient that takes into account the partitioning and diffusion processes. There are various methodologies that can be used (Rowe, 1998) to deduce the partitioning, diffusion and permeation coefficients.

The permeation coefficient, P_g, is highly dependent on the similarity of the penetrant and polymer. For example, Eloy-Giorni *et al.* (1996) indicated values of $S_{gf} = 8 \times 10^{-4}$ and $D_g = 2.9 \times 10^{-13}$ m^2/s giving a very low value of $P_g = 2.3 \times 10^{-16}$ m^2/s for water and HDPE. Similarly, August & Tatzky (1984) found that strongly polar penetrant molecules have very low permeation coefficients through polyethylene (with the permeation coefficients being in the following order: alcohols < acids < nitroderivatives < aldehydes < ketones < esters < ethers < hydrocarbons). August *et al.* (1992) found that there was negligible diffusion of heavy metal salts (Zn^{2+}, Ni^{2+}, Mn^{2+}, Cu^{2+}, Cd^{2+}, Pb^{2+}) from a concentrated (0.5 M) acid solution (pH = 1-2) through HDPE over a 4 year test period.

Hydrocarbons can readily diffuse through HDPE GMs, although the permeation coefficient will vary de-

Table 11 - Time to establish steady state diffusion through HDPE geomembrane for three volatile organic compounds.

Contaminant	Diffusion parameters		Time to reach steady state (years)	
	D_g (m^2/a)	S_{gf} (-)	1.5 mm GM	2.5 mm GM
Dichloromethane, CH_2Cl_2	2×10^{-5}	6	0.11	0.3
Benzene, C_6H_6	1.3×10^{-5}	30	0.16	0.4
Ethylbenzene, $C_6H_5C_2H_5$	5.7×10^{-6}	285	0.36	1
Chloride, Cl^-	1.3×10^{-6}	0.0008	1.6	4.4

All numbers have been rounded. Note parameters for chloride represent an upper bound and hence the times shown here are lower bounds (actual time is expected to be longer than shown).

pending on factors such as the crystallinity of the GM, temperature and in some cases, the chemical composition and concentrations in the contaminant source (Sangam & Rowe, 2001). The diffusion of hydrocarbons such as benzene, ethylbenzene, toluene and xylenes can also be reduced by a factor of between about 2 and 5 by using a fluorinated HDPE as an alternative to a conventional GM (Sangam & Rowe, 2005).

Rowe (2005) reported on chloride diffusion tests where a source and receptor are separated by a 2 mm thick HDPE GM. After about 12 years, the receptor concentration remained below about 0.02% of the source concentration and lies within the range of analytical uncertainty for the chemical analysis. This data provides an upper bound of 3×10^{-17} m^2/s on the permeation coefficient of chloride through an HDPE GM ($D_g = 4 \times 10^{-14}$ m^2/s or 1.3×10^{-6} m^2/a, $S_{gf} = 0.0008$).

The time it takes to establish steady stage diffusion through an HDPE GM from a constant source to zero concentration receptor can be obtained by solving Eq. (9) subject to these boundary conditions and only depends on the diffusion coefficient D_g (*i.e.* it does not depend on the partitioning coefficient S_{gf}). The time it takes to reach steady state is given in Table 11 for a number of contaminants and 1.5 and 2.5 mm thick GMs. It can be seen that increasing the thickness of the GM increases the time to reach steady state by about a factor of 2.8 (*i.e.* by the ratio of the square of the thicknesses = $2.5^2/1.5^2$) but even so, for the three hydrocarbons considered, the time is a year or less. Even for chloride it is less than 5 years. However this highlights the fact that the time to reach steady state diffusion only tells a small part of the story since it only depends on D_g and says nothing about the mass flux that is transported from the contaminant source across the GM which also depends on S_{gf} (see Eq. (11)). The impact that this has is illustrated below.

Table 12 summarizes the calculated time required for contaminant to diffuse through an HDPE GM and increase the concentration, c, in a 1 cm thick receptor to the specified levels relative to the constant source concentration c_o for two GM thicknesses and three hydrocarbons (using the diffusion parameters given in Table 11). It can be seen that it takes 3 to 17 days for the concentration in the receptor to reach 0.1% of the source and only 12 to 55 days to reach 10%. In contrast, Table 13 shows that it would take at least 15 years for chloride to reach 0.1% for a 1.5 mm HDPE GM and at least 1500 years to reach 10% of the source concentration. This highlights how effective the GM is as a diffusion barrier to ions like chloride.

To give a sense of the rate of diffusive migration, Table 14 summarizes the calculated distance dichloromethane would diffuse in given time periods. This case considers diffusion from a constant source (c_o) through a 1.5 mm HDPE GM, 8.5 mm thick GCL and underlying subgrade. It assumes no sorption in the GCL or soil and thus represents an upper limit to the extent of migration likely to be observed. The distance at which the concentration reaches a given concentration level ($c/c_o = 0.01$, 0.1 and 0.5) is shown together with an apparent "velocity" of diffusion (the distance divided by the time). It can be seen that within a year DCM could diffuse to the 1% level ($c/c_o = 0.01$) to a depth of up to 0.44 m and in 10 years it would migrate more that 1.5 m. The "velocity" of migration is fastest at low times when the concentration gradient is greatest and decreases with subsequent time. It was found that DCM diffusion was not significantly slower when there was no GM. For example in 1, 2 and 4 years, DCM migrated at the $c/c_o = 0.01$ level to depths of 0.5 m, 0.72 m and 1.03 m with no GM as

Table 13 - Time required for chloride to diffuse through HDPE geomembrane and increase the concentration, c, in a 1 cm thick receptor to the specified level relative to the constant source concentration c_o (in percent)for 1.5 mm HDPE GM ($D_g = 1.3 \times 10^{-6}$ m^2/a; $S_{gf} = 0.0008$).

c/c_o (%)	Time to reach c/c_o in receptor (years)
0.1	15
1	150
10	1500

All numbers have been rounded; Note parameters for chloride represent an upper bound and hence the times shown here are lower bounds (actual time is expected to be longer than shown).

Table 12 - Time required for contaminant to diffuse through HDPE geomembrane and increase the concentration, c, in a 1 cm thick receptor to the specified level relative to the constant source concentration c_o (in percent) for two geomembrane thicknesses.

c/c_o (%)	Time to reach c/c_o in receptor (days)					
	DCM		Benzene		Ethylbenzene	
	1.5 mm	2.5 mm	1.5 mm	2.5 mm	1.5 mm	2.5 mm
0.01	2	5	2	6	5	13
0.1	3	7	3	9	6	17
1	5	12	5	14	10	27
10	12	28	12	30	20	55

All numbers have been rounded.

compared with 0.44 m, 0.66 m and 0.96 m with a GM. The reduction in the distance is a little more significant for contaminants for which S_{gf} is higher.

Similar calculations for chloride show no migration below the GM at the 0.01 level for thousands of years. This is because what does diffuse through the GM diffuses away in the underlying soil because of the very low flux through the GM and the much higher diffusion coefficient in the underlying soil. This again highlights the effectiveness of a GM as a diffusion barrier.

For landfill with double liner systems, the leakage through the primary liner will be mostly collected by the leak detection system. This will minimize the potential for advective movement through the secondary liner. However volatile organic compounds (VOCs) will volatilize in the LDS and can then diffuse through the underlying secondary composite liner, and hence diffusion still needs to be considered for these cases. The time for VOCs to migrate through the primary liner at detectable levels will depend on the thickness of the primary liner (*e.g.* see Table 14). Evidence suggesting the likely diffusion of VOCs through geosynthetic liners arises from field observations reported by Workman (1993), Othman *et al.* (1996), and Shackleford (2005). There are other, as yet unpublished, examples of migration through CCLs.

In summary, HDPE GMs are an excellent diffusion barrier to water and water soluble contaminants such as metal salts. However, they will allow diffusion of VOCs. Control of the migration of these compounds will depend on the clay liner and any attenuation layer between the GM and any receptor aquifer. Additional control can be provided by using a fluorinated HDPE GM.

10. Service Life of Geomembranes

10.1. Geomembranes for MSW landfills

The foregoing sections have demonstrated that even with typical wrinkles and holes in wrinkles, provided there is appropriate construction quality control and construction quality assurance (CQC/CQA), the leakage through composite liners can be controlled to such low values that diffusion becomes the controlling transport mechanism. Geomembranes are also excellent diffusion barriers to ions (like chloride and heavy metals) and the while volatile organic compounds can readily diffuse through the GM they can be controlled by design of the barrier system with an adequate attenuation layer (Rowe *et al.*, 2004b; Rowe, 2005). This all assumes that the GM is performing as designed. However GMs will have a finite service life and their long-term performance will depend on their properties (*e.g.* stress crack resistance, crystallinity, and oxidative induction time), the tensile strains induced by the overlying drainage material and wrinkles (as discussed earlier), the exposure to chemicals in the leachate and temperature. This has been discussed in some detail by Rowe (2005).

It is generally recognized that the chemical ageing of an HDPE GM has three distinct stages (Viebke *et al.*, 1994; Hsuan & Koerner, 1998): (a) depletion time of antioxidants; (b) induction time to the onset of polymer degradation; and (c) degradation of the polymer to decrease some property (or properties) to an arbitrary level (*e.g.* to 50% of the original value). It has been reported that the consump-

Table 14 - Diffusive migration of dichloromethane through composite GM/GCL liner and underlying subgrade. Depth to location where c/c_o = 0.01, 0.1 and 0.5 and corresponding apparent "velocity" of the diffusion front.

Time (years)	c/c_o = 0.01		c/c_o = 0.1		c/c_o = 0.5	
	Depth (m)	"Velocity" (m/a)	Depth (m)	"Velocity" (m/a)	Depth (m)	Velocity" (m/a)
1	0.44	0.44	0.26	0.26	0.06	0.06
2	0.66	0.33	0.39	0.20	0.12	0.06
4	0.96	0.24	0.59	0.15	0.2	0.05
6	1.19	0.20	0.74	0.12	0.26	0.043
8	1.4	0.18	0.84	0.11	0.31	0.039
10	1.55	0.16	0.96	0.096	0.36	0.036
15	1.92	0.13	1.2	0.08	0.45	0.03
20	2.22	0.11	1.4	0.07	0.53	0.027
25	2.5	0.1	1.56	0.062	0.6	0.024
30	2.74	0.091	1.72	0.057	0.66	0.022
40	3.19	0.080	2	0.05	0.78	0.020
50	3.57	0.071	2.25	0.045	0.87	0.017

GM: 1.5 mm $D_g = 1.3 \times 10^{-6}$ m^2/a; $S_{gf} = 6$; GCL: 8.5 mm $D = 0.009$ m^2/a, $n = 0.7$; Attenuation Layer 4 m, $D = 0.02$ m^2/a, $n = 0.3$ no sorption or decay; constant source.

tion of antioxidants and subsequent oxidation reaction in polyethylene can be increased in the presence of transition metals (*e.g.* Co, Mn, Cu, Pd and Fe) present in leachate (Osawa & Saito, 1978; Wisse *et al.*, 1990; Hsuan & Koerner, 1998). Since it is not practical to establish the service life under actual field conditions, accelerated ageing tests are conducted at elevated temperatures and the results are then used to calculate the expected service life at the temperatures expected at the base of a landfill (*e.g.* Hsuan & Koerner, 1998; Sangam & Rowe, 2002; Mueller & Jacob, 2003; Rowe, 2005).

In most cases this testing to assess ageing of GMs has involved immersing samples in a fluid of interest and then, after different periods of immersion, samples are removed and tested to obtain the oxidative induction time (OIT). The ln(OIT) is then the is plotted versus the period of incubation (Fig. 15). The linear plot implies a first order relationship between OIT and time and hence the OIT (an indicator of the total amount of antioxidants) remaining at time t can be given by:

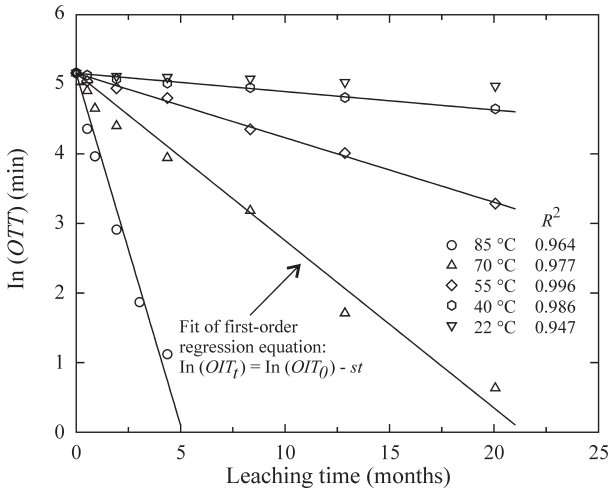

Figure 15 - Variation in ln(*OIT*) with time at different temperatures in leachate. OIT_0 is the initial *OIT* and OIT_t is the *OIT* at time *t* (month), s is the antioxidant depletion rate (month^{-1}) (after Islam & Rowe, 2007).

$$OIT(t) = OIT_o e^{-st} \quad (11)$$

where OIT_o is the initial *OIT* value (typically in minutes) and s the rate of antioxidants depletion (typically in month^{-1}).

Sangam & Rowe (2002) examined the depletion of antioxidants in air, water and simulated MSW leachate while Rowe (2005) and Rowe & Rimal (2007) reported results for simulated liner systems with a collection layer over the geotextile protection layer, the GM and a GCL on a sand subgrade. Based on the laboratory data and Arrhenius modelling, the time required for antioxidant depletion was deduced and is given in Table 15 for the GMs tested. It can be seen that the exposure conditions and temperature have a profound effect on the time to antioxidant depletion. In particular it is noted that there is a significant difference between immersion in water and leachate. Islam & Rowe (2007) have demonstrated that the primary factor affecting this difference is the presence of surfactant in the leachate. Volatile fatty acids and ions typically found in leachate (*e.g.* Na, Cl etc) had no significant effect on the time to antioxidant depletion.

The simulated liner results presented in Table 15 represent only the first stage of the service life. To obtain estimates for Stages 2 and 3, Rowe (2005) used data obtained by Viebke *et al.* (1994) for polyethylene gas pipe with minimal antioxidant and a wall thickness comparable to a GM thickness (2.1 mm). The antioxidant depletion times (Stage 1) for the simulated liner (Table 15) were combined with the service life projections for Stages 2 and 3 based on the activation energies given by Viebke *et al.* (1994) to obtain the "unadjusted" estimates of GM service life given in Table 16. Since Viebke *et al.* (1994) tests were with water on the inside and air on the outside of the pipe wall, the unadjusted values may be expected to overestimate the service life of a GM in a landfill. Thus these values were adjusted to reflect the observed difference between exposure to air, water and a simulated liner exposed to leachate on one side as described by Rowe (2005) to obtain the "adjusted" estimates given in Table 16. It can be seen that for temperatures around 20 °C, service lives are projected to be of the order

Table 15 - Estimated antioxidant depletion time for an HDPE geomembrane (modified from Rowe 2005).

Temperature (°C)	Air[1] t_{air} (years)	Water[1] t_{water} (years)	Leachate[1] $t_{leachate}$ (years)	Simulated liner[2] t_{sl} (years)
10	510	235	50	280
20	235	110	25	115
30	110	55	15	50
35	80	40	10	35
40	55	30	8	25
50	30	15	5	10
60	15	8	3	6

All times greater than 10 have been rounded to nearest 5 years. [1]2 mm HDPE, OIT_o = 133 min (ASTM D3895), crystallinity = 44%; based on data from Sangam & Rowe (2002). [2]1.5 mm HDPE, OIT_o = 135 min (ASTM D3895), crystallinity = 49%.

Table 16 - Estimated service lives for an HDPE geomembrane for a MSW landfill (modified from Rowe 2005).

Temp (°C)	Service life (years) Unadjusted t_{SL}	Service life (years) Adjusted t_{SLa}
20	900	565
30	315	205
35	190	130
40	120	80
50	50	35
60	20	15

All times have been rounded to nearest 5 years.

of 565 to 900 years and hence a service life of 600 years (or more) could be anticipated at a temperature of 20 °C (or less). For liners at a temperature of 35 °C, the service life is of the order of 130-190 years. Finally at temperatures of 50-60 °C, the service lives are very short (15-50 years).

In the context of the earlier discussion of the effect of temperature on primary and secondary liners, it should be noted that for an area where the background temperature is 15 °C and assuming the primary GM temperature increases to 35 °C (*i.e.* by 20 °C), the secondary GM might be expected to be at about 30 °C (assuming a primary composite liner with a GM, 0.75 m compacted clay and an 0.3 m thick gravel leak detection system). Under these circumstances Table 16 suggests that the service life of the primary and secondary GMs would be of the order of 130-190 years and 205-315 years respectively.

The service lives presented in Table 16 provide a general idea of the order of magnitude of the GM service-life and highlight the importance of liner temperature. While these numbers represent the best currently available information they should be used with caution since only the results for Stage 1 are based on actual tests on GMs typically used in landfill applications in a simulated liner configuration.

The calculated antioxidant depletion times (Table 15) and service lives (Table 16) are based on a constant temperature. Rowe (2005) examined the effect of the liner temperature varying with time. This showed that while operational features such as operating a landfill as a bioreactor may shorten the period of high temperatures on the liner, the increase in temperature associated with this mode of operation can actually decrease the overall service life. This highlights the importance of considering the mode of landfill operation when developing a liner design.

10.2. Geomembranes in contact with neat hydrocarbons

As indicated in the previous section, the fluid in contact with the GM can have a profound impact on the depletion of antioxidants and hence the service life of a GM. Since GMs may be used to retain neat hydrocarbons, as discussed earlier, Rowe *et al.* (2007b) immersed both conventional HDPE and fluorinated HDPE (f-HDPE) GM specimens in Jet A-1 and then examined the change in oxidative induction time with the period of immersion. They reported that immersion in Jet A-1 accelerated antioxidant depletion relative to that observed in water or MSW leachate by Sangam & Rowe (2002). Fluorination of the HDPE GM significantly (by a factor of 2.7) reduced antioxidants depletion relative to conventional HDPE. At 23 °C, the total antioxidant depletion time was estimated to be about 2 and 6 years for untreated and fluorinated GMs respectively. This can be compared with projected depletion times of between 20 years and 90 years (at 23 °C) based on Sangam & Rowe's (2002) tests for GM immersed in MSW leachate and water respectively.

11. Conclusions

Over the last decade there have been significant advances in knowledge concerning the factors potentially affecting the performance of GCLs and GMs in a wide range of geoenvironmental applications. This paper has examined nine of these issues and it can be concluded that for the specific materials and conditions discussed:

• GCLs may interact with municipal solid waste (MSW) leachate. The level of interaction is highly dependent upon the vertical effective stress at the time of permeation. At very low stress there may be an order of magnitude increase in GCL hydraulic conductivity (to about 6 x m/s) as the permeant was changed from water to MSW leachate. At stress levels more typical of likely field conditions, the effect is far less significant with a hydraulic conductivity to MSW leachate still very low at 3 x 10^{-11} m/s.

• GCLs have the potential to provide strong attenuation of many metals and metalloids present in acid rock drainage (ARD) leachate and a neutral-pH gold mining leachate (GML). The hydraulic conductivity of the GCLs permeated with ARD increased from 2.8 x 10^{-12} m/s to 3.7 x 10^{-11} m/s after 35 pore volumes of permeation. There was no significant change in hydraulic conductivity for GCLs permeated with GML.

• There is negligible flow of hydrocarbons through a saturated GCL until a critical threshold pressure is exceeded. This threshold pressure is greater than that likely to be experienced in many applications and hence a hydrated GCL is likely to be an excellent barrier to hydrocarbons under these conditions. Above this threshold pressure the effect on intrinsic permeability is largely masked by the effect on density and viscosity such that the hydraulic conductivity of GCLs remains low and it appears that GCLs such as those tested can provide good containment of hydrocarbons for many practical applications.

• Up to 150 freeze-thaw cycles had very little effect on the hydraulic conductivity of GCLs permeated with water under conditions where there was no chemical interac-

tion (cation exchange) with the bentonite prior to permeation. More research is required to assess the potential combined effect of cation exchange and freeze-thaw cycles at relatively low stress on the long-term performance of GCLs used in covers and similar near surface applications.

• 50 to 100 freeze-thaw cycles reduces the breakthrough pressure for permeation by jet fuel through a GCL. This was attributed to an increase in the size of macro pores in the bentonite following repeated freeze-thaw cycles. The hydraulic conductivity after up to 50 freeze-thaw cycles in the laboratory was less than $3x10^{-11}$ m/s at a gradient just above that required to initiate flow. There was some increase in hydraulic conductivity with 100 freeze-thaw cycles with a maximum value of about 1×10^{-10} m/s.

• The hydraulic conductivity (with respect to jet fuel) of GCL recovered from the field in the arctic after 3 years was less than 3×10^{-12} m/s at a pressure just above the breakthrough pressure. Increasing the gradient increases the hydraulic conductivity to 6×10^{-11} m/s. This higher value is at a gradient unlikely to be encountered in a real field situation but is still very low.

• Different GCLs have substantially different susceptibilities to internal erosion that can occur at high hydraulic gradients (*e.g.* in pond and lagoon applications). The choice of GCL carrier geotextile plays a key role in this different performance. GCLs with a woven geotextile in contact with the underlying subgrade did not perform as well as the other GCLs. GCLs with a nonwoven geotextile performed better than the GCLs with a woven over the subgrade but still experienced internal erosion over a geonet at high heads. In contrast, the scrim-reinforced GCL with a carrier geotextile mass of 350 g/m^2 did not exhibit any sign of internal erosion when placed over the geonet, gravel or sand tested at heads of 40-60 m.

• All the GCLs tested performed well with respect to internal erosion when on a suitable sand subgrade.

• The available evidence would suggests that temperatures of 30-40 °C can be expected at the top of the primary liner for MSW landfills. Higher temperatures (40-60 °C) can occur in situations where there is sufficient moisture to accelerate biodegradation of organic waste (*e.g.* in bioreactor landfills or when there is no operating leachate collection system) or due to hydration of incinerator ash.

• Diffusive and advective transport are, respectively, 100% and 80% higher at 35 °C than at a common groundwater temperature of 10 °CC.

• The temperature of the GM in a secondary liner will be highly dependant on the nature of the primary liner. For a geocomposite primary liner comprised of only a GM and GCL, the secondary GM temperature may be expected to be only a few degrees (at most) less than that of the primary GM. As the thickness of the primary liner increases (*e.g.* if there is a foundation layer below the GCL as part of the primary liner or if there is a CCL), the temperature of the secondary GM decreases. The temperature of the primary and secondary GM may have a profound impact on the service life of these GMs.

• Both GCLs and CCLs may be susceptible to shrinkage and desiccation when used as part of a composite liner. This results from exposure to solar radiation prior to placement of adequate cover over the GM or after placement of waste (due to heat generated by the waste as discussed above). The potential for shrinkage and desiccation will depend on the temperature gradient, the characteristics of the GCL or CCL, the unsaturated soil characteristics and initial water content of the foundation layer beneath the clay liner, the overburden stress, and the distance to the underlying watertable. The available information suggests that while there is potential for desiccation and shrinkage, this can be mitigated by appropriate design and construction.

• Typical construction practice will result in GMs developing a significant number of wrinkles (waves) by the time they are covered. Techniques have been developed for quantifying the size and distribution of wrinkles.

• Under typical applied loads, wrinkles tend to remain in the GM. A gap typically remains between the GM wrinkle and a GCL. For a GM with wrinkles initially up to 60 mm high over a CCL, the gap may be filled at stress levels of 100 kPa or more when the CCL is compacted at the plastic limit. The lower the water content of the CCL at the time of compaction (relative to the plastic limit) the higher the pressure needed to extrude sufficient clay to fully close the gap.

• While needle-punched nonwoven geotextiles may provide reasonable protection against short-term holes in an underlying GM (*i.e.* limiting the number of holes to less than about 12 per hectare after placement of the drainage layer), recent research has shown that if gravel is used as the drainage layer (the preferred choice for providing good long-term leachate collection) then typical geotextile protection layers (up to 2000 g/m^2) will not prevent large local strains in the GM and thinning of any underlying GCL (especially near wrinkles). Additional research is needed to clarify the time dependent effects of strains induced in GMs and the GCL by the gravel particles. Nevertheless it is clear that a sand protection layer between the gravel and the GM (perhaps combined with a traditional nonwoven geotextile) provides the best potential long-term performance.

• Field evidence of significant increases in leakage into LDS due to damage to composite liners involving a GM and GCL due to landfill activities after liner construction highlight the need to place an adequate protection layer above the composite liner to minimize the risk of such accidental damage. It also highlights the need to closely monitor not only the construction of the liner but also any waste placement or other work that could potentially cause damage to the liner.

• Field data indicates that the leakage through a GM/CCL composite liner was typically one to two orders

of magnitude higher than that observed for GM/GCL composite liners.

• The calculated leakage obtained assuming direct contact (no major wrinkles) and typical size and number of holes in GMs using commonly used equations significantly underestimated the observed leakage for both GM/CCL and GM/GCL systems.

• The typical observed leakage for composite liners with CCLs and GCLs can be readily explained by holes in wrinkles for the typical number of holes/ha and reasonable combinations of other parameters using the Rowe (1998) equation.

• The design and construction of systems with a geonet leak detection system must ensure that the swelling and intrusion (under vertical stress) of any overlying GCL does not compromise the drainage function of the underlying geonet.

• Available field data suggests that even with typical numbers of wrinkles and holes per hectare, for landfills with good CQC/CQA and where there is no damage to the liner during landfilling activities, the post-closure leakages are very small and contaminant transport is likely to be controlled by diffusion through the liner system for contaminants that can readily diffuse through a GM.

• Volatile organic compounds (VOCs) can diffuse through both GMs and GCLs. Typical diffusion coefficients have been reported for both HDPE GMs as well as GCLs. Diffusion of hydrocarbons is much slower for fluorinated HDPE (f-HDPE) than conventional HDPE GMs. Control of the migration of these compounds will depend on the clay liner and any attenuation layer between the GM and any receptor aquifer.

• Ionic contaminants exhibit negligible diffusion through intact HDPE GMs. The diffusion coefficient for ionic contaminants through GCLs is a function of the bulk void ratio of the GCL.

• For landfills with double liner systems, the leakage through the primary liner will be mostly collected by the LDS. This will minimize the potential for advective movement through the secondary liner. However volatile organic compounds will volatilize in the leak detection system and can then diffuse through the underlying secondary composite liner, and hence diffusion needs to be considered for these cases. The time for VOCs to migrate through the primary liner at detectable levels can range from as little as a year to a decade depending on the thickness of the primary liner and the concentration in the landfill leachate collection system.

• The long-term performance of a GM will depend on the GM properties (*e.g.* its stress crack resistance, crystallinity, and oxidative induction), the tensile strains in the GM (which can be induced by the overlying drainage material and wrinkles in the GM), the exposure to chemicals in the leachate, and temperature.

• The service life of HDPE GMs meeting GRI GM-13 and used in MSW landfills are projected to be of the order of 600 years or more at a temperature less than 20 °C. At a temperature of 35 °C, the service life is projected to be of the order of 130-190 years. At temperatures of 50-60 °C, service lives are very short (15-50 years).

• Immersion of HDPE GMs in Jet A-1 accelerates antioxidant depletion relative to that observed in water or MSW leachate. The antioxidant depletion time was estimated to be about 2 and 6 years for untreated and fluorinated GMs, respectively, at 23 °C. This can be compared with a projected 20 years and 90 years based on GMs immersed in MSW leachate and water respectively (at 23 °C).

The evidence reviewed in this paper suggests that GCLs and GMs can play a very beneficial role in providing environmental protection. Like all engineering materials they must be used appropriately and consideration should be given to factors such as those addressed in this paper. There is a need for site specific design, strict adherence to construction specifications, and appropriate protection of the geosynthetics after construction. In particular, given the diversity of available GCLs and their different engineering characteristics, GCLs should be selected based on the required engineering properties, not just price.

Acknowledgements

The author greatly appreciates the invitation of the Portuguese Geotechnical Society to present the 23rd Manuel Rocha Lecture. He is indebted to the many students and collaborators who have contributed to the research summarized in this paper. The assistance of the following graduate students in preparing figures is gratefully acknowledged: A. Hoor (Figs. 4 and 5), M. Chappel (Figs. 6 and 7), S. Dickinson (Figs 9 and 10), K. Abdel-Atty (Figs. 11-13) and M.Z. Islam (Fig 15). This work was funded by a variety of agencies including the Natural Sciences and Engineering Research Council of Canada (NSERC), the North Warning System Office of the Department of National Defense Canada, EarthTech (an Ontario Centre of Excellence), Terrafix Geosynthetics Inc., and NAUE GmbH & Co. The careful review by Dr. Ennio Palmeira and Dr. J-P Giroud, and the value of discussion with Dr. J-P Giroud, Mr. K. Von Mauberge and Mr. B. Herlin is gratefully acknowledged. The author is also very grateful to Ms. Sera Sheridan for her assistance in the preparation of this paper.

References

Abollino, O.; Aceto, M.; Malandrino, M.; Sarzanini, C. & Mentasti, E. (2003) Adsorption of HMs on Na-montmorillonite. Water Res., v. 37, pp. 1619-1627.

Ashmawy, A.; El-Hajji, D.; Sotelo, N. & Muhammad, N. (2002) Hydraulic performance of untreated and polymer-treated bentonite in inorganic landfill leachates. Clays Clay Miner., v. 50:5, pp. 545-551.

August, H. & Tatzky, R. (1984) Permeability of commercially available polymeric liners for hazardous landfill leachate organic constituents. Proc. Int. Conf. on Geomembranes, IFAI, Denver, v. I, pp. 163-168.

August, H.; Tatzky-Gerth, R.; Preuschmann, R. & Jakob, I. (1992) Permeationsverhalten von Kombinationsdichtungen bei Deponien und Altlasten Gegenueber Wassergefaehrdenden Stoffen. Project 10203412 of the BMBF, published by BAM, D-12200 Berlin, Germany.

Badu-Tweneboah, K.; Giroud, J.P.; Carlson, D.S. & Schmertmann, G.R. (1998) Evaluation of the effectiveness of HDPE geomembrane liner protection. Proc. 6th International Conference on Geosynthetics, IFAI, Atlanta, pp. 279-284.

Basnett, C.R. & Bruner, R.J. (1993) Clay desiccation of a single-composite liner system. Geosynthetics 93, Vancouver, IFAI, pp. 1329-1340.

Bathurst, R.J.; Rowe, R.K.; Zeeb, B. & Reimer, K. (2006) A geocomposite barrier for hydrocarbon containment in the Arctic. International Journal of Geoengineering Case Histories, v. 1:1, pp. 18-34.

Bonaparte, R.; Daniel, D. & Koerner, R.M. (2002) Assessment and recommendations for improving the performance of waste containment systems. EPA Report, Co-operative Agreement Number CR-821448-01-0.

Brain, E.S. (2000) Evaluation of leachate compatibility to clay soil for three geosynthetic clay liner products. Geotechnical Special Publication, 103, GeoDenver 2000 Congress Advances in Transportation and Geoenvironmental Systems Using Geosynthetics, Denver, pp. 117-128.

Brune, M.; Ramke, H.G.; Collins, H. & Hanert, H.H. (1991) Incrustations process in drainage systems of sanitary landfills. Proc. 3rd Int. Landfill Symp., Cagliari, pp. 999-1035.

Chappel, M.J.; Brachman R.W.I.; Take W.A. & Rowe R.K. (2007) Development of a low altitude aerial photogrammetry technique to quantify geomembrane wrinkles. Geosynthetics 2007, Proc. Environmental Conference, Washington, pp. 293-300.

Collins, H.J. (1993) Impact of the temperature inside the landfill on the behaviour of barrier systems. Proc. 4th Int. Landfill Symp., Cagliari, v. 1, pp. 417-432.

Colucci, P. & Lavagnolo, M.C. (1995) Three years field experience in electrical control of synthetic landfill liners. Proc. 5th International Landfill Symposium, S. Margherita di Pula, pp. 437-452.

Cooper, C.; Jiang, J.Q. & Ouki, S. (2002) Preliminary evaluation of polymeric Fe & Al modified clays as adsorbents for heavy metal removal in water treatment. J. Chem. Tech. Biotechnol., v. 77, pp. 546-551.

Corser, P.; Pellicer, J. & Cranston, M. (1992) Observations on long-term performance of composite clay liners and covers. Geotech. Fabrics Report, Nov., pp. 6-16.

Daniel, D.E.; Shan, H.Y. & Anderson, J.D. (1993) Effects of partial wetting on the performance of the bentonite component of a geosynthetic clay liner. Proc. Geosynthetics 93, Industrial Fabrics Association International, St. Paul, Minn., v. 3, pp. 1483-1496.

Dickinson, S. & Brachman R.W.I. (2006) Deformations of a geosynthetic clay liner beneath a geomembrane wrinkle and coarse gravel. Geotextiles and Geomembranes, v. 24:5, pp. 285-298.

Dobras, T.N. & Elzea, J.M. (1993) *In-situ* soda ash treatment for contaminated Geosynthetic Clay Liners, Proc. Geosynthetics 93, Industrial Fabrics Association International, St. Paul, pp. 1145-1160.

Egloffstein, T. (2001) Natural bentonites -influence of the ion exchange and partial desiccation on permeability and self-healing capacity of bentonites used in GCLs. Geotextiles and Geomembranes, v. 19, pp. 427-444.

Egloffstein, T. (2002) Bentonite as sealing material in geosynthetic clay liners - Influence of the electrolytic concentration, the ion exchange and ion exchange with simultaneous partial desiccation on permeability. Zanzinger, H.; Koerner, R. & Gartung, E. (eds) Clay Geosynthetic Barriers. Swets and Zeitlinger, Lesse, pp. 141-153.

Eloy-Giorni, C.; Pelte, T.; Pierson, P. & Margarita, R. (1996) Water diffusion through geomembranes under hydraulic pressure. Geosynthetics Int., v. 3:6, pp. 741-769.

Felon, R.; Wilson, P.E. & Janssens, J. (1992) Résistance mécanique des membranes d'étanchéité. membranes armées en théorie et en pratique. In: Vade Mecum Pour la Réalisation des Systèmes d'Étanchéité Drainage Artificiels Pour les Sites d'Enfouissement Technique en Wallonie. Journées d'Études ULg 92.

Giroud, J.P. (1997) Equations for calculating the rate of liquid migration through composite liners due to geomembrane defects. Geosynthetics Int. v. 4:3-4, p. 335-348.

Giroud, J.P. & Bonaparte, R. (1989) Leakage through liners constructed with geomembranes - Part II. Composite liners. Geotextiles and Geomembranes, v. 8:2, pp. 71-111.

Giroud, J.P. & Morel, N. (1992) Analysis of geomembrane wrinkles. Geotextile and Geomembranes, v. 11:3, pp. 255-276 (Erratum: 1993, v. 12:4, pp. 378).

Giroud, J-P & Soderman, K.L. (2000) Criterion for acceptable bentonite loss from a GCL Incorporated into a liner system. Gesynthetics International, v. 7:4-6, pp. 529-581.

Giroud, J.P. & Touze-Foltz, N. (2005) Equations for calculating the rate of liquid flow through geomembrane defects of uniform width and finite or infinite length. Geosynthetics International, v. 12:4, pp. 191-204.

Gudina, S. & Brachman, R.W.I. (2006a) Physical response of geomembrane wrinkles overlying compacted clay.

Journal of Geotechnical and Geoenvironmental Engineering, v. 132:10, pp. 1346-1353.

Gudina, S. & Brachman, R.W.I. (2006b) Effect of boundary conditions on deflection of GM wrinkles in a GM/GCL composite liner. Proc. 8th International Geosynthetics Conference, Yokohama, pp. 255-258.

Guyonnet, D.; Gaucher, E.; Gaboriau, H.; Pons, C.; Clinard, C.; Norotte, V. & Didier, G. (2005) Geosynthetic clay liner interaction with leachate: Correlation between permeability, microstructure, and surface chemistry. Journal of Geotechnical and Geoenvironmental Engineering, v. 131:6, pp. 740-749.

Harpur, W.A.; Wilson-Fahmy, R.F. & Koerner, R.M. (1993) Evaluation of the contact between geosynthetic clay liners and geomembranes in terms of transmissivity. GRI Seminar on Geosynthetic Liner Systems, Philadelphia, IFAI, pp. 143-154.

Haxo Jr., H.E. & Lahey, T. (1988) Transport of dissolved organics from dilute aqueous solutions through flexible membrane liner. Haz. Waste & Hazardous Materials, v. 5, pp. 275-294.

Heibrock, G. (1997) Desiccation cracking of mineral sealing liners. Proc. 6th Int. Landfill Symp., Cagliari, v. 3, pp. 101-113.

Hewitt, R.D. & Daniel, D. E. (1997) Hydraulic conductivity of geosynthetic clay liners after freeze-thaw. Journal of Geotechnical and Geoenvironmental Engineering, v. 123:4, pp. 305-313.

Hsuan Y.G. & Koerner R.M. (1998) Antioxidant depletion lifetime in high density polyethylene geomembranes. J. Geotech. Geoenv. Eng., v. 124:6, pp. 532-541.

Huang, C.H.; Wu, C.K. & Sun, P.C. (1999) Removal of heavy metals from plating wastewater by crystallization/precipitation of gypsum. J. Chin. Chem. Soc., v. 46:4, pp. 633-638.

Islam, M.Z. & Rowe, R.K (2007) Leachate composition and antioxidant depletion from HDPE geomembranes. Geosynthetics 2007, Proc. Environmental Conference, Washington, pp. 147-159.

James, A.; Fullerton, D. & Drake, R. (1997) Field performance of GCL under ion exchange conditions. J. of Geotechnical and Geoenvironmental Engineering, v. 123, pp. 897-901.

Jo, H.; Katsumi, T.; Benson, C. & Edil, T. (2001) Hydraulic conductivity and swelling of nonprehydrated GCLs permeated with single-species salt solutions. J. of Geotechnical and Geoenvironmental Engineering, v. 127, pp. 557-567.

Jo, H.; Benson, C. & Edil, T. (2004) Hydraulic conductivity and cation exchange in non-prehydrated and prehydrated bentonite permeated with weak inorganic salt solutions. Clays and Clay Minerals, v. 52:6, pp. 661-679.

Jo, H.-Y.; Benson, C.H., Shackelford, C.D.; Lee, J.-M. & Edil, T.B. (2005) Long-term hydraulic conductivity of a geosynthetic clay liner (GCL) permeated with inorganic salt solutions. Journal of Geotechnical and Geoenvironmental Engineering, v. 131:4, pp. 405-417.

Jo, H.; Benson, C. & Edil, T. (2006) Rate-limited cation exchange in thin bentonitic barrier layers. Canadian Geotechnical J., v. 43, pp. 370-391.

Katsumi, T. & Fukagawa, T. (2005) Factors affecting the chemical compatibility and the barrier performance of GCLs. Proc. 16th ICSMGE, Osaka, pp. 2285-2288.

Klein, R.; Baumann T.; Kahapka E. & Niessner R. (2001) Temperature development in a modern municipal solid waste incineration (MSWI) bottom ash landfill with regard to sustainable waste management. Journal of Hazardous Materials, v: B83, pp. 265-280.

Kodikara, J.K.; Rahman, F. & Barbour, S.L. (2002) Towards a more rational approach to chemical compatibility testing of clay. Canadian Geotechnical Journal, v. 39, pp. 597-607.

Koerner, G.R. & Koerner R.M. (2006) Long-term temperature monitoring of geomembranes at dry and wet landfills. Geotextiles and Geomembranes, v. 24:1, pp. 72-77.

Koerner, R.M.; Wilson-Fahmy, R.F. & Narejo, D. (1996) Puncture protection of geomembranes. Part III: Examples. Geosynthetics International, v. 3:5, pp. 655-675.

Kolstad, D.C.; Benson, C.H. & Edil, T.B. (2004) Hydraulic conductivity and swell of nonprehydrated geosynthetic clay liners permeated with multispecies inorganic solutions. Journal of Geotechnical and Geoenvironmental Engineering, v. 130:12, pp. 1236-1249.

Kraus, F.J.; Benson, H.C.; Erickson, E.A. & Chamberlain, J.E. (1997) Freeze - Thaw cycling and hydraulic conductivity of bentonite barriers. Journal of Geotechnical and Geoenvironmental Engineering, v. 123:3, pp. 229-238.

Lake, C.B. & Rowe, R.K. (2000) Diffusion of sodium and chloride through geosynthetic clay liners. Geotextiles and Geomembranes, v. 18:2, pp. 102-132.

Lake, C.B. & Rowe, R.K. (2004) Volatile organic compound (VOC) diffusion and sorption coefficients for a needlepunched GCL. Geosynthetics Int., v. 11:4, pp. 257-272.

Lange, K.; Rowe, R.K. & Jamieson, H. (2004) Metal migration in geosynthetic clay liners. Proc. 57th Canadian Geotechnical Conference, Quebec City, Section 3D, pp. 15-22.

Lange, K.; Rowe, R.K. & Jamieson, H. (2005) Attenuation of heavy metals by geosynthetic clay liners. Proc. GeoFrontiers Conference, Austin, Paper GRI-18, 8 p., CD-ROM.

Lange, K.; Rowe, R.K. & Jamieson, H. (2007) Metal retention in geosynthetic clay liners following permeation by different mining solutions. Geosynthetics International, (in review).

Lee, J.-M. & Shackelford, C.D. (2005) Impact of bentonite quality on hydraulic conductivity of geosynthetic clay

liners. Journal of Geotechnical and Geoenvironmental Engineering, v. 131:1, pp. 64-77.

Legge, K.R. & Davies, P.L. (2002) An appraisal of the performance of geosynthetics material used in waste disposal facilities in South Africa. WasteCon 2002, Durban, 12 p., CD-ROM.

Li, L.Y. & Li, F. (2001) Heavy metal sorption and hydraulic conductivity studies using three types of bentonite admixes. Journal of Environmental Engineering, v. 127, pp. 420-429.

McKelvey, J.A. (1997) Geosynthetic Clay Liners in Alkaline Environments. Testing and Acceptance Criteria for GCLs, ASTM STP 1308. Well, Larry W. (ed), ASTM, West Conshohocken, pp. 139-149.

Melchior, S. (1997) *In-situ* studies on the performance of landfill caps. Proc. International Containment Technology Conference, Florida State University, Tallahassee, pp. 365-373.

Melchior, S. (2002) Field studies and excavations of geosynthetic clay barriers in landfill covers. Zanzinger, H.; Koerner. R. & Gartung, E. (eds) Clay Geosynthetic Barriers. Swets and Zeitlinger, Lesse, pp. 321-330.

Mazzieri, F. & Pasqualini, E. (2000) Permeability of damaged geosynthetic clay liners. Geosynthetics International, v. 7:2, pp. 101-118.

Mueller, W. & Jacob, I. (2003) Oxidative resistance of HDPE. Polymer Degradation and Stability, v. 79, pp. 161-172.

Müller, W.; Jakob, R.; Tatzky-Gerth, R. & August, H. (1998) Solubilities, diffusion and partitioning coefficients of organic pollutants in HDPE geomembranes: Experimental results and calculations. Proc. 6th Int. Conf. on Geosynthetics, Atlanta, IFAI, pp. 239-248.

Narejo, D.; Koerner, R.M. & Wilson-Fahmy, R.F. (1996) Puncture protection of geomembranes Part II: Experimental. Geosynthetics International, v. 3:5, pp. 629-653.

Nosko, V. & Touze-Foltz, N. (2000) Geomembrane liner failure: Modeling of its influence on contaminant transfer. Proc. 2nd European Geosynthetics Conf., Bologna, p. 557-560.

Olsen, H.W. (1961) Hydraulic Flow Through Saturated Clays. D.Sc. Thesis, Massachusetts Institute of Technology, Cambridge.

Osawa, Z. & Saito, T. (1978) The effects of transition metal compounds on the thermal oxidative degradation of polypropylene in solution. In: Stabilisation and Degradation of Polymers, Advances in Chemistry, Series 169. Am. Chem. Soc., Washington, DC, pp. 2897-2907.

Othman M.A.; Bonaparte, R. & Cross, B.A. (1996) Preliminary results of study of composite liner field performance. Proc. 10th GRI Conf.: Field Performance of Geosynthetics and Geosynthetic Related Systems. Drexel University: Philidelphia, pp. 110-137.

Pelte, T.; Pierson, P. & Gourc, J.P.(1994) Thermal analysis of geomembranes exposed to solar radiation. Geosynthetics Int., v. 1:1, pp. 21-44.

Petrov, R.J. & Rowe, R.K. (1997) Geosynthetic clay liner compatibility by hydraulic conductivity testing: Factors impacting performance. Canadian Geotechnical Journal, v. 34:6, pp. 863-885.

Petrov, R.J.; Rowe, R.K. & Quigley, R.M. (1997) Selected factors influencing GCL hydraulic conductivity. Journal of Geotechnical and Geoenvironmental Engineering, v. 123:8, pp. 683-695.

Podgorney R.K. & Bennett J.E. (2006) Evaluating the long-term performance of geosynthetic clay liners exposed to freeze-thaw. J. Geotech. Geoenviron. Eng., v. 132:2, pp. 265-268.

Reddy, K.R.; Bandi, S.R.; Rohr, J.J.; Finy, M. & Siebken, J. (1996) Field evaluation of protective covers for landfill geomembrane liners under construction loading. Geosynthetics International, v. 3:6, pp. 679-700.

Rowe, R.K. (1998) Geosynthetics and the minimization of contaminant migration through barrier systems beneath solid waste. Keynote Lecture, Proc. Sixth International Conference on Geosynthetics, Atlanta, v. 1, pp. 27-103, Industrial Fabrics Association International, St .Paul. (This paper can be downloaded from www.geoeng.ca).

Rowe, R.K. (2005) Long-term performance of contaminant barrier systems. 45th Rankine Lecture. Geotechnique, v. 55:9, pp. 631-678.

Rowe, R.K. (2006) Some factors affecting geosynthetics used for geoenvironmental applications. Keynote Lecture, 5th International Conference on Environmental Geotechnics, Cardiff, v. 1, pp. 43-69.

Rowe, R.K. & Orsini, C. (2003) Effect of GCL and subgrade type on internal erosion in GCLs. Geotextiles and Geomembrane, 21:1, pp. 1-24.

Rowe, R.K & Hoor, A. (2007) Temperature of secondary liners in municipal solid waste landfills. Geosynthetics 2007, Proc. Environmental Conference, Washington, pp. 132-146.

Rowe, R.K. & Rimal, S. (2007) Depletion of antioxidant from HDPE geomembrane in a composite liner. Journal of Geotechnical and Geoenvironmental Engineering (in press).

Rowe, R.K.; Mukunoki, T.; Li, H.M. & Bathurst R.J. (2004a) Effect of freeze-thaw on the permeation of arctic diesel through a GCL. Journal of ASTM International, v: 1:2, pp. 134-146. Available online: www.astm.org; 1 February 2004, 10 p. This was also published by ASTM in hardcopy in Advances in: Geosynthetic Clay Liner Technology R.E. Mackey & von Maubeuge, K. (eds).

Rowe, R.K.; Quigley, R.M.; Brachman, R.W.I. & Booker, J.R. (2004b) Barrier Systems for Waste Disposal Facilities. Taylor & Francis Books Ltd (E & FN Spon), London, 587 p.

Rowe, R.K.; Hurst, P. & Mukunoki, T. (2005a) Permeating partially hydrated GCLs with jet fuel at temperatures from -20 °C and 20 °C. Geosynthetics International, 12:6, pp. 333-343.

Rowe, R.K.; Mukunoki, T. & Sangam, P.H. (2005b) BTEX diffusion and sorption for a geosynthetic clay liner at two temperatures. Journal of Geotechnical and Geoenvironmental Engineering, v. 131:10, pp. 1211-1221.

Rowe, R.K.; Mukunoki, T.; Bathurst, R.J.; Rimal, S.; Hurst, P. & Hansen, S. (2005c) The performance of a composite liner for retaining hydrocarbons under extreme environmental conditions. Geofrontiers 2005, Austin, 17 p, CD-Rom.

Rowe, R.K.; Mukunoki, T. & Bathurst, R.J. (2006) Compatibility with Jet A-1 of a GCL subjected to freeze-thaw cycles. Journal of Geotechnical and Geoenvironmental Engineering, v. 132:12, pp. 1519-1643.

Rowe, R.K.; Mukunoki, T. & Bathurst, R.J. (2007a) Hydraulic conductivity to Jet-A1 of GCLs subjected to up to 100 freeze-thaw cycles. Geoengineering Centre at Queen's-RMC Research report.

Rowe, R.K.; Mukunoki, T.; Bathurst, R.J.; Rimal, S.; Hurst, P. & Hansen, S. (2007b) Performance of a geocomposite liner for containing Jet A-1 spill in an extreme environment. Geotextiles and Geomembranes (in press).

Rowe, R.K.; Sangam, H.P. & Lake, C.B. (2003) Evaluation of an HDPE geomembrane after 14 years as a leachate lagoon liner. Canadian Geotechnical Journal, v. 40:3, pp. 536-550.

Ruhl, J.L. & Daniel, D.E. (1997) Geosynthetic clay liners permeated with chemical solutions and leachates. Journal of Geotechnical and Geoenvironmental Engineering, v. 123:4, pp. 369-380.

Sangam, H.P. & Rowe, R.K (2001) Migration of dilute aqueous organic pollutants through HDPE geomembranes. Geotextiles and Geomembranes, v. 19:6, pp. 329-357.

Sangam, H.P. & Rowe, R.K. (2002) Effects of exposure conditions on the depletion of antioxidants fro high-density polyethylene (HDPE) geomembranes. Canadian Geotechnical Journal, v. 39:6, p. 1221-1230.

Sangam, H.P. & Rowe, R.K (2005) Effect of surface fluorination on diffusion through an HDPE geomembrane. Journal of Geotechnical and Geoenvironmental Engineering, v. 131:6, p. 694-704.

Schubert, W.R. (1987) Bentonite matting in composite lining systems. Geotechnical Practice for Waste Disposal 87, Woods, R.D. (ed), ASCE, New York, p. 784-796.

Shackelford, C.D. (2005) Environmental issues in geotechnical engineering. Proc. 16th International Conference on Soil Mechanics and Geotechnical Engineering, Osaka, p. 12-16, Millpress, Rotterdam, v. 1, p. 95-122.

Shackelford, C.; Benson, C.; Katsumi, T. & Edil, T. (2000) Evaluating the hydraulic conductivity of GCLs permeated with non-standard liquids. Geotextiles and Geomembranes, v: 18:2-3, pp. 133-161.

Shan, H.Y. & Daniel, D.E. (1991) Results of laboratory tests on a geotextile/ bentonite liner material. Proc. Geosynthetics 91, Industrial Fabrics Association International, St. Paul, v. 2, pp. 517-535.

Shan, H. & Lai, Y. (2002) Effect of hydrating liquid on the hydraulic properties of geosynthetic clay liners. Geotextile and Geomembranes, v. 20, pp. 19-38.

Shaner, K.R. & Menoff, S.D. (1992) Impacts of bentonite geocomposites on geonet drainage. Geotextiles and Geomembranes, v: 11:4-6, pp. 503-512.

Soong, T.Y. & Koerner, R.M. (1998) Laboratory study of high density polyethylene geomembrane waves. Proc. 6th Int. Conf. on Geosynthetics, Atlanta, IFAI, pp. 301-306.

Southen, J.M. (2005) Thermally Driven Moisture Movement Within and Beneath Geosynthetic Clay Liner. PhD Thesis, University of Western Ontario, 320 p.

Southen, J.M. & Rowe, R.K. (2004) Investigation of the behavior of geosynthetic clay liners subjected to thermal gradients in basal liner applications. J. of ASTM International, v. 1:2 ID JAI11470, Available online: www.astm.org; 13 p. Also ASTM: Advances in Geosynthetic Clay Liner Technology. Mackey, R.E. & von Maubeuge, K. (eds), p. 121-133.

Southen, J.M. & Rowe, R.K. (2005) Laboratory investigation of GCL desiccation in a composite liner subjected to thermal gradients. J. Geotech. Geoenv. Eng., v. 131:7, pp. 925-935.

Stam, T.G. (2000) Geosynthetic clay liner field performance. Proc. 14th GRI Conference, Las Vegas, pp. 242-254.

Stichbury, M.K.; Bain, J.G.; Blowes, D.W. & Gould, W.D. (2000) Microbially mediated reductive dissolution of arsenic-bearing minerals in a gold mine tailings impoundment. ICARD 2000, Proc. 5th International Conf. on Acid Rock Drainage, v. 1, pp. 97-106.

Stone, J.L. (1984) Leakage monitoring of the geomembrane for proton decay experiment. Int. Conf. on Geomembranes, Denver, v. 2, pp. 475-480.

Thiel, R. & Richardson, G.N. (2005) Concern for GCL Shrinkage when installed on slopes. ASCE GeoFrontiers C, Austin, Paper GRI-18, 7 p., CD-ROM.

Thiel, R. & Smith, M.E. (2004) State of the practice review of heap leach pad design issues. Geotextiles and Geomembranes, v. 22:6, pp. 555-568.

Thiel, R.; Giroud, J.P.; Erickson, R.; Criley, K. & Bryk, J. (2006) Laboratory measurements of GCL shrinkage under cyclic changes in temperature and hydration conditions. Proc. 8th International Geosyntheics Conference, Yokohama, pp. 157-162.

Tognon, A.R.; Rowe, R.K. & Moore, I.D. (2000) Geomembrane strain observed in large-scale testing of protection

layers. J. Geotech. Geoenv. Eng., v. 126:12, pp. 1194-1208.

Touze-Foltz, N. & Giroud, J.P. (2005) Empirical equations for calculating the rate of liquid flow through composite liners due to large circular defects in the geomembrane. Geosynthetics International, v. 12:4, pp. 205-207.

Touze-Foltz, N.; Schmittbuhl, J. & Memier, M. (2001) Geometric and spatial parameters of geomembrane wrinkles on large scale model tests. Geosynthetics 2001, Portland, pp. 715-728.

Viebke, J.; Elble, E.; Ifwarson, M. & Gedde, U.W. (1994) Degradation of unstabilized medium-density polyethylene pipes in hot-water applications. Polymer Eng. and Science, v. 34:17, pp. 1354-1361.

Wilson-Fahmy, R.F.; Narejo, D. & Koerner, R.M. (1996) Puncture protection of geomembranes Part I: Theory. Geosynthetics International, v. 3:5, pp. 605-628.

Workman J.P. (1993) Interpretation of leakage rates in double lined systems. Proc. 7th GRI Conf.: Geosynthetic Liner Systems. Drexel University, Philidelphia, pp. 91-108.

Wisse, J.D.M.; Broos, C.J.M. & Boels, W.H. (1990) Evaluation of the life expectancy of polypropylene geotextiles used in bottom protection structures around the Ooster Schelde storm surge barrier: A case study. Proc. 2nd Int. Conf. on Geotextiles, Las Vegas, v. 1, pp. 283-288.

Yong, R.N. (2001) Geo-environmental Engineering, 1st ed, CRC Press LLC, 320 p.

Yoshida, H. & Rowe, R.K. (2003) Consideration of landfill liner temperature. Proc. 9th. Int. Landfill Sym., Cagliari, Italy, CD-ROM.

Articles

Soils & Rocks
v. 30, n. 1

Deflections of Upstream Membrane of Rockfill Dams During Reservoir Filling

Fernando Saboya Jr., Pedricto Rocha Filho, Arthur D.M. Penmam

Abstract. This paper describes a numerical investigation into the deflection of the upstream membrane of rockfill dams during reservoir impounding. The influence of the angle of the upstream slope on the subsequent deflection suffered by the concrete face slab is investigated. The procedure used for this investigation takes into consideration the gradual change between reloading and primary loading elastic modulus based on stress-state criterion.
Key words: rockfill dam, face deflection, instrumentation.

1. Introduction

De Mello (1982) and others have criticized some of the flatter slopes currently being designed for concrete faced rockfill dams, pointing out that in the past, some rockfill dams were designed with upstream slopes as steep as 60° to the horizontal. Modern compacted rockfill should be able to sustain even steeper slopes, and it was noted that an upstream slope of 65° to the horizontal was used for the Malpasso Dam in Peru. In a potentially highly seismic area of Japan, the Tarumizu Dam was built with an upstream slope of only 15° to the horizontal.

In view of these wide variations, this study was initiated to determine the effect of upstream slope angle on the deflections caused by the pressure from the impounded reservoir water on the upstream membrane. For comparison the actual measured deflections of three CFRD have been included in the study.

In general, it is intended to minimize slope deflections under the imposed hydraulic forces from the impounded reservoir water by good compaction of the rockfill. The stresses imposed on rockfill by the placement and compaction efforts, are usually exceeded by gravity forces by the time the rockfill has reached full height, before the concrete face slab has been placed. The major principal stress is in a generally vertical direction and the minor principal stress in a generally horizontal direction at regions beneath the centerline. The water load imposed normal to the slab by the filling reservoir, increases the minor stress, so reducing the existing stress difference and causing the slab deflections to be minimized. As the reservoir continues to fill, however, the directions of the principal stresses continue to rotate and the direction of the major principal stress may approach that of the direction of the water thrust on the slab. Thus, the existing rockfill stresses are exceeded, causing slab deflections to increase more rapidly. This is particularly the case because the major principal stress is now acting in a general direction along the placed layers, which is a much weaker direction than the vertical direction in which they were compacted.

Research carried out at the Catholic University of Rio de Janeiro, (Saboya Jr *et al.*, 1993), has shown that the angle of the upstream slope plays a very important role in the subsequent deformations suffered by the concrete face slab, and forms an added factor for detailed consideration at the design stage.

2. Stress-Path During Reservoir Filling

Saboya Jr. & Byrne (1993) and Mori & Pinto (1988) have shown that major part of the upstream shell reaches a shear unloading condition at the beginning of the reservoir filling. Despite the fact that the first stress invariant is increasing, the shear stress decreases because the increase in minor principal stress is higher than that of the major principal stress (Fig. 1). When the complete principal stress axis rotation happens, some points will follow the reloading stress path and as the primary loading condition is reached, these points will behave in a much softer manner, as shown by Saboya Jr. (1993).

The interface between reloading and primary loading condition has to be suitably modeled for the understanding of the influence of upstream slope on the slab deflection. Thus, the model proposed by Saboya Jr. & Byrne (op. cit) will be used. This model states that the mechanism that governs the transition between primary loading and unloading is different from that of the reloading and primary loading. The most usual criterion to establish if a localized zone within the body of the dam is under primary loading or unloading-reloading state is called stress level criterion & given by Eq. (1).

Fernando Saboya Jr., Doutor, Laboratório de Engenharia Civil, Universidade Estadual do Norte Fluminense Darcy Ribeiro, Av. Alberto Lamego 2000, 28013-620 Horto, Campos dos Goytacazes, RJ, Brasil. e-mail: saboya@uenf.br.
Pedricto Rocha Filho, PhD, Departamento de Engenharia Civil, Universidade Católica do Rio de Janeiro, Rua Marquês de São Vicente 225/301 Bloco L 22453-900 Rio de Janeiro, RJ, Brazil.
Arthur D.M. Penmam, Doutor, Geotechnical Engineering Consultant, Sladeleye Chamberlaines, AL5 3PW Harpenden, Herts, Reino Unido.
Submitted on July 5, 2005; Final Acceptance on February 10, 2006; Discussion open until August 31, 2007.

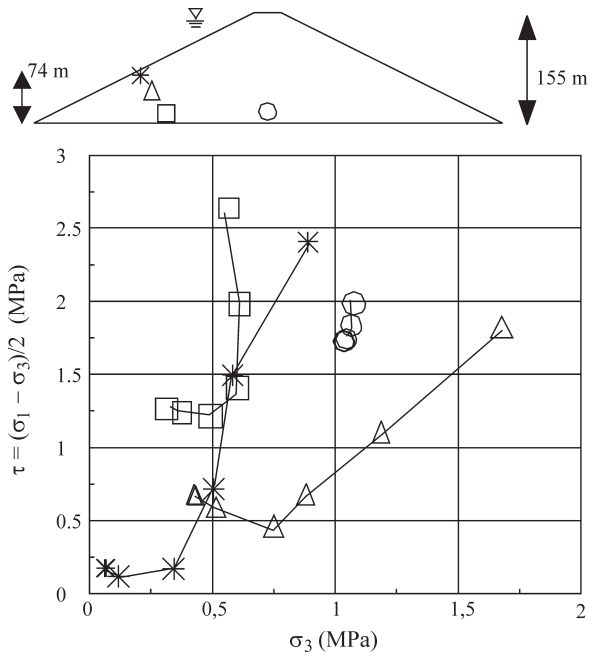

Figura 1 - Stress path during reservoir filling of Foz do Areia Dam (Saboya Jr., 1993).

$$S_L = \frac{(\sigma_1 - \sigma_3)}{(\sigma_1 - \sigma_3)_f} \quad (1)$$

where S_L is the stress level and $(\sigma_1 - \sigma_3)_f$ is the deviator stress at failure.

If the current stress level is equal or higher than the maximum past stress level ever experienced by the element, then it is considered to be in primary loading condition and the loading tangent modulus is used, otherwise the unloading reloading modulus is used.

Duncan *et al.* (1984) show that this criterion should be modified in order to take into account, not only the influence of the stress level, but also the change in confining stress. This criterion, known as the stress-state criterion, is defined as follows:

$$S_S = S_L \left(\frac{\sigma_3}{P_a} \right)^{1/4} \quad (2)$$

where S_s is the stress state and P_a is the atmospheric pressure.

The stress-state criterion considers that the primary loading tangent modulus is used when the current stress state is higher than the maximum past stress state ever experienced by the element. Both criteria are shown in Fig. 2 where the straight and curved lines represent, respectively, the stress level and the stress state criteria.

The main modification proposed by Duncan *et al.* (op. cit) is the gradual transition from primary loading modulus to unloading-reloading modulus. This has been

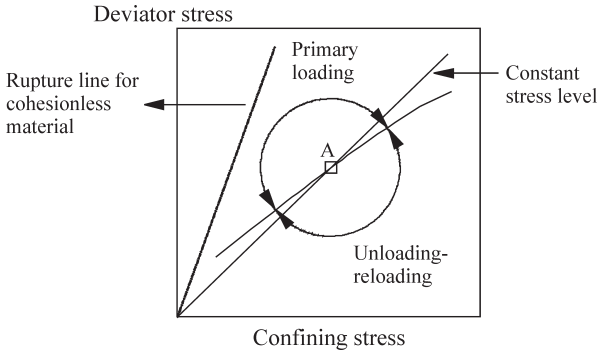

Figura 2 - Stress level and stress state criterion (after Duncan *et al.*, 1984).

proposed aiming to avoid abrupt change in elastic tangent modulus, which could lead to numerical instability in a finite element program. The gradual change in elastic modulus is based on the critical stress level, above which, the primary loading modulus is used and is given by the following expression:

$$S_L^{crit} = \frac{S_S^{max.\,past}}{\left(\frac{\sigma_3}{P_a} \right)^{1/4}} \quad (3)$$

The gradual transition between unloading-reloading and primary loading modulus is given when stress level is situated between $¾ S_L^{crit}$ and S_L^{crit}, as shown in Fig. 3a.

However, Saboya Jr. & Byrne (op. cit), figured out that such a gradual change holds true only for the reloading phase and the modification proposed by Duncan *et al.* (op. cit) strongly overestimates the predicted slab deflection. Thus the model indicated in Fig. 3b has been proposed. It is worth noting that the change from primary loading to the unloading phase is considered to occur in an abrupt way and the change from reloading to the primary loading occurs gradually, using S_L^{crit} as a criterion. This seems to be closer to the actual behavior of rockfill materials.

Figure 4 shows the predicted and observed vertical displacements of Foz do Areia Dam using both criteria. It can be noticed that gradual change for the elastic modulus strongly overestimated the predicted displacement. However, the most important feature is the small influence of the

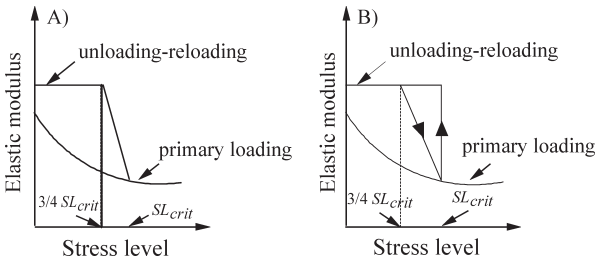

Figura 3 - Loading and unloading criteria: a) Proposed by Duncan *et al.* (1984); b) Proposed by Saboya Jr. & Byrne (1993).

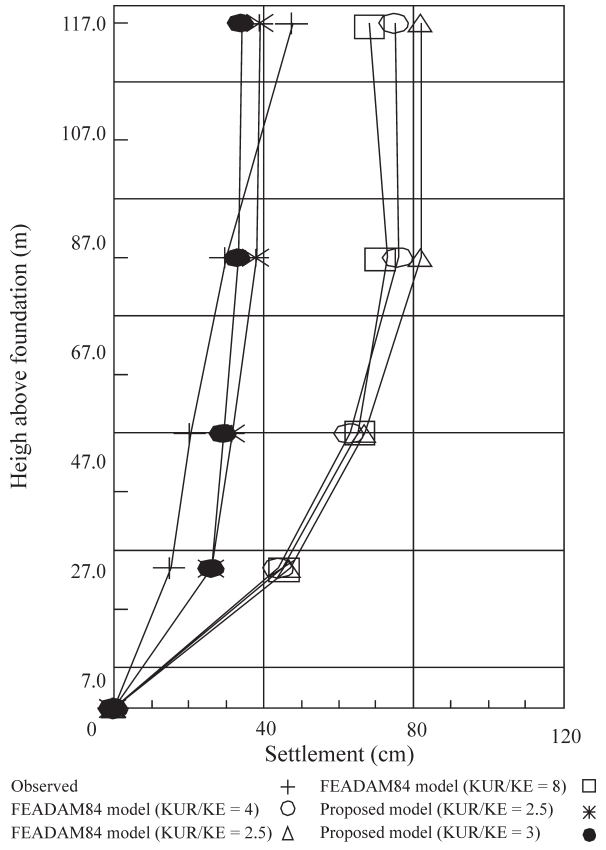

Figura 4 - Predicted and observed vertical displacement under Foz do Areia dam axis (Saboya Jr. & Byrne, 1993).

relationship of unloading-reloading and primary loading hyperbolic parameters, K_{UR} and K_E respectively. This seems to be related to the fact that most parts of the upstream shell might be located at the transition to the unloading zone, during the reservoir filling.

3. Influence of Upstream Slope on the Face Deflection

Hence, it can be said that slab deflection is a function of how the material will respond to different stress paths combined with its initial stress state. As the stress paths, imposed by the reservoir filling, are dependent on the principal stress increment, one can say that the angle of the upstream slope plays a very important role on the final displacements.

To verify such an influence, a hypothetical 100 m high dam with upstream slopes varying from 2V:1H to 1V:3H, was analyzed. These analyses involved both construction and reservoir filling stages. The simulation of the construction stage was necessary, because the determination of the final state of stress is very important. The response of the dam due to water thrust will depend strongly on the initial state of stress that represents the final one obtained from the construction analysis.

A nonlinear elastic hyperbolic model was used and the parameters were derived using the methodology proposed by Saboya Jr. & Byrne for Segredo rockfill material IB. These parameters are presented in Table 1. The analysis were carried out using FEADAM84 computer code (Duncan *et al.*, 1984) and modified by Saboya (1993).

The reservoir filling was simulated in five steps of 20 m each, in order to reveal the stress path followed by the elements during reservoir filling. The most favorable condition will be considered to be that for which the dam shows the highest percentage of elements in the unloading condition at the final load step. In this case, the dam tends to present a stiffer behavior, resulting in smaller slab deflections.

One can say that, for steeper slopes, the increase in minor principal stress is higher than for flatter slopes, leading, therefore, to an earlier unloading situation. However, such a statement might not be true if the face has a certain slope where a most part of the upstream shell comes back earlier to its primary loading conditions. On the other hand, the same reasoning can be applied to flatter slopes, where the percentage of the upstream shell area in the unloading condition, due to smaller increments in minor principal stress, can be very small. Therefore, it can be concluded that there is an "optimum" slope, independent of the height of the dam, in which the combination among the percentage of unloading, reloading and primary loading reaches the most favorable condition.

Figure 5 shows the results obtained for maximum deflection versus face slope. It can be seen that the best slope, considering only a single value of maximum deflection, is about 1V:1H (45 degrees). However, this value alone is not enough to define the most suitable slope. It is very important to emphasize that the best behavior of the face must be related to the smallest deflection gradient. The deflection gradient can be understood as the difference in deflection at different elevations. It can be seen in Fig. 6 that the angle for which the smallest deflection gradient takes place is also 45 degrees.

It is worthwhile also to show the development of the face displacements as a function of principal stress axis rotation. For this reason, two different elevations of the upstream face, were considered: 20% and 40% of the total

Tabela 1 - Hyperbolic parameters used in the analysis (Saboya Jr. 1993).

Material	C_U [1]	K_E	n	R_f	K_B	m	ϕ	$\Delta\phi$
IB	6	350	.37	.60	100	.13	47	8.3

[1]Uniformity coefficient.

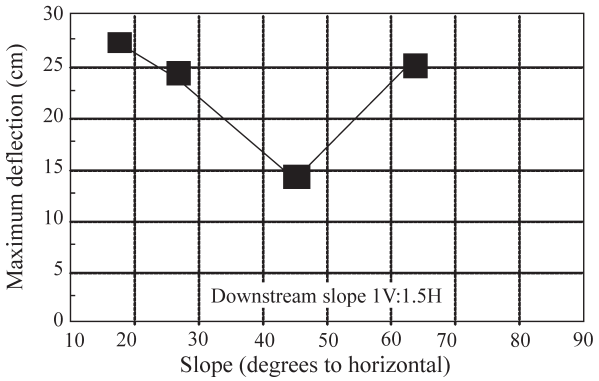

Figura 5 - Maximum deflection *vs.* upstream slope.

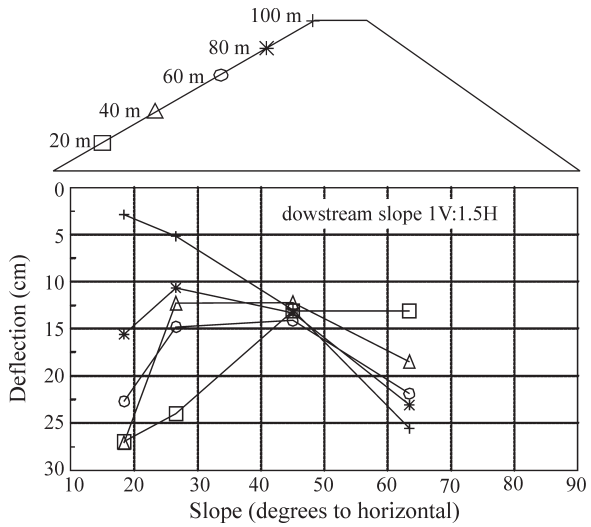

Figura 6 - Differential deflection at different levels.

height of the dam H. Deflections were plotted in a dimensionless way to make them independent of the height of the dam (Figs. 7 and 8).

3.1. Deflection at El. 20% of the total high of the dam

By analyzing the face deflection of a point on the face located at El 20% of H (Fig. 7), it can be noticed that the slopes representing 1V:1H and 2V:1H indicate similar behavior, showing a pronounced increase in the deflection rate when the reservoir level reached 80% of total height of the dam. This seems to be linked to the change between unloading-reloading and the primary loading phase. For slopes of 1V:2H and 1V:3H, it seems that, at that elevation, points never reached the unloading situation, maybe due to small initial stress level (in terms of shear stress) and high load increments in their vicinity. It can be seen that, after reaching the primary loading state, the lines tend to be parallel, indicating similar elastic modulii. In fact, they are not precisely parallel because the confining stresses are different for each curve.

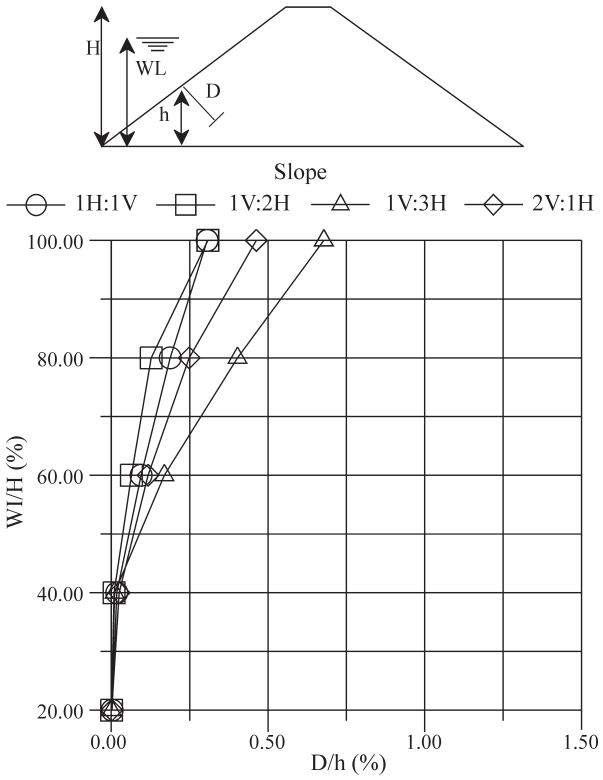

Figura 7 - Non-dimensional deflection at El. 20 m.

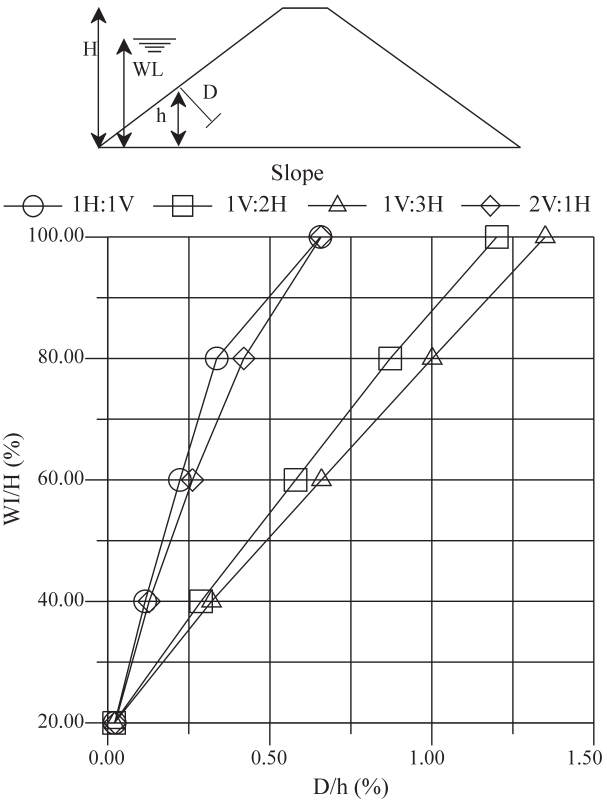

Figura 8 - Non-dimensional deflection at El. 40 m.

3.2. Deflection at El. 40% of the total high of the dam

Figure 8 shows deflections obtained to the point located at El. 40% of H and, as can be seen, the observed behaviour is quite different from that at El. 20% of H, mainly due to the stress state reached during the construction phase. This can explain the good response of the 1V:2H slope where at this elevation the stress level is enough to "hold" the unloading-reloading situation until the reservoir level reaches 80% of the full height of the dam. Similar behaviour is shown by the 2V:1H slope where the deflection rate increases after the reservoir level reaches 80% of the full height of the dam. The 1V:3H slope reaches the primary loading condition at 60% of the dam height, indicating that the stress level at the beginning of the reservoir filling was quite small when compared with the load increments. As noticed for elevation 20% of H, the lines which have reached the primary loading condition, are approximately parallel, and the line representing the 1V:1H slope never reached the primary loading condition. The upstream slope deformed shapes of the hypothetical dams are depicted in Fig. 9. As can be seen, the 1V:1H slope shows smoothest deformed shape due to the fact that most part of the upstream shell is under unloading/reloading condition. The same can be verified for the 2V:1H slope.

3.3. Points of maximum deflection and comparison with Foz do Areia, Segredo and Xingo dams

So far, the evolution of the deflection occurring at fixed elevations for different slopes has been shown. Nevertheless, one might find it of interest to consider only the points of maximum deflection for each slope. This is shown in Fig. 10 and it is quite interesting to notice that the 1V:1H and 2V:1H slopes presented better behavior than the others. The less favorable adopted slope is 1V:3H because of the small value of minor principal stress at the end of the construction period. However, the most interesting feature presented by the plot is that the loci of the maximum deflection are different for each slope studied. In some sense, it cannot be said that the point of the maximum deflection is related to the point of the load resultant, which is always located at

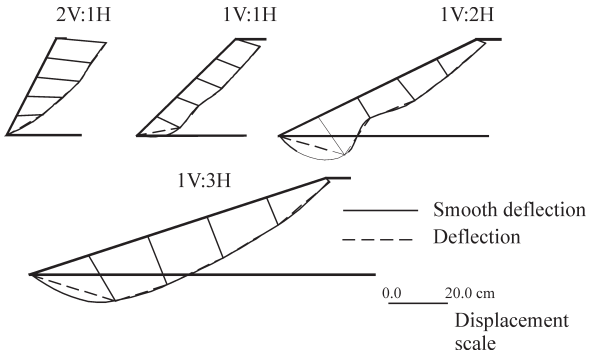

Figura 9 - Deformed shape of the upstream face after the reservoir filling.

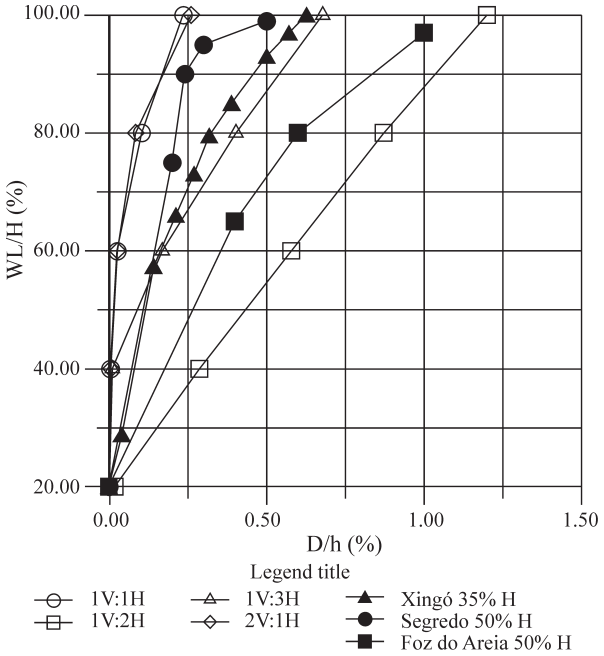

Figura 10 - Comparative evolution of non-dimensional deflections.

one third of water load triangle from the base. The same explanation does not hold true for the direction of the resultant deflection. For instance, the 2V:1H slope had its point of maximum deflection at El. 100% of H, *i.e.*, at the crest. Observed membrane deflections of Foz do Areia, Segredo and Xingo dams were inserted in this plot in order to verify its applicability. It is interesting to notice that for Segredo and Xingo dam, which have upstream slope of 1V:1.3H, their non-dimensional deflections are quite similar to those of the hypothetical dam. As for Foz do Areia dam, despite the fact its upstream slope is 1V:1.4H, the behavior of upstream slope was indeed unexpected. However the main reason for this behavior is that horizontal displacements were not recorded for Foz do Areia Dam and deflections were extrapolated by considering the normal projection of the vertical displacement at the face. This, of course, can lead to overestimated displacements.

The elevation of the points of maximum deflection is supposed to be strongly related to the development of zones under unloading-reloading conditions. To verify such a statement, one can judge it necessary to evaluate the stress state at the end of reservoir filling and try to establish some link between stress-state and deflections. Figure 11 shows the stress state resulting from reservoir filling for these hypothetical dams. As can be seen, embankments with upstream slope varying from 1V:2H to 1V:3H show no elements in the unloading-reloading condition, in the face and, therefore, the non-dimensional deflection curve does not present any point of inflection.

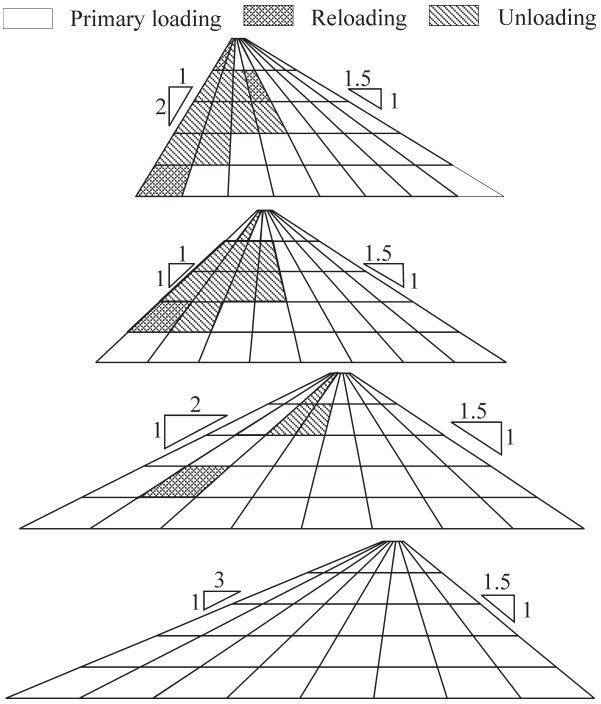

Figura 11 - Stress-state conditions at the end of reservoir filling.

4. Conclusion

The adoption of steeper upstream slopes in concrete face rockfill dams, seeking for the most economic geometry, is a very important task. The importance of this aspect is mainly due to the fact that slope deflections are closely related to the stress-state at the beginning of reservoir filling. Furthermore, the slope angle plays a crucial role on the stress-state reached at the end of construction phase. Thus, the use of elastic analysis for the prediction of face deflection, must incorporate the effects of principal stress axis rotation. Otherwise, the increase on deformation rate, as the reservoir is filling, cannot be modeled, unless more sophisticated elasto-plastic models are used.

Gradual change in elastic modulus during unloading-reloading strongly overestimates such predictions. On the other hand, gradual change in elastic modulus during the reloading curve, seems to be quite suitable in simulating the actual behavior of rockfill dams. These features can be easily incorporated in the hyperbolic model and the predicted responses are quite satisfactory. Results from this research have shown that at slope angles between 1V:1H and 2V:1H, deflections are much smaller than for others angles.

Acknowledgement

The Authors are grateful to the COPEL, Electric Company of Paraná State, for permission the use of the observation data of Segredo and Foz do Areia Rockfill Dams. They are also grateful to Prof. Peter Michael Byrne for his important contributions during the development of numerical analysis. In addition, they wish to thanks the Brazilian Research Scholarship Agency, CAPES, for the financial support of this research. Special thanks are addressed to the reviewers that have contributed to this paper with valuables suggestions.

References

De Mello, V.F.B. (1982) Practice, precedent, principles, problems and prudence in embankment engineering. Proceedings of Symposium on Problems and Practice of Dams Engineering. Bangkok, v. 1, pp. 3-15.

Duncan, J.M.; Seed, R.B.; Wong, K.S. & Ozawa, Y. (1984) FEADAM84: A computer program for finite element analysis of dams. Department of Civil Engineering, Virginia Polytechnic Institute and State University, Blacksburg, p. 1-79.

Mori, R.T. & Pinto, N.L.S. (1988) Analysis of deformations in concrete face rockfill dams to improve face movement prediction. Proceedings of the 6th International Congress on Large Dams, San Francisco, pp. 27-33.

Saboya Jr., F. (1993) Analysis of Concrete Face Rockfill Dams During Construction and Reservoir Filling. Ph.D. Thesis, Universidade Católica do Rio de Janeiro, Brazil (in Protuguese), 216 p.

Saboya Jr., F. & Byrne, P.M. (1993) Parameters for stress and deformation analysis of rockfill dams. Canadian Geotechnical Journal, v. 30:4, pp. 690-701.

Saboya Jr., F.; Rocha Filho, P. & Toniatti, N.B. (1993) Analysis of Segredo dam during construction and reservoir filling. Geotecnia, Journal of the Portuguese Geotechnical Society, v. 70, pp. 1-25.

Notation

C_U = Uniformity coefficient
K_E = Elastic modulus hyperbolic parameter
K_B = Bulk modulus hyperbolic parameter
n, m = Hyperbolic exponent parameters
ϕ = shear strength internal angle
$\Delta\phi$ = Decrease do ϕ for a log cycle of confining stress
R_f = Stress ratio hyperbolic parameter
K_{UR} = Unloading-reloading elastic modulus hyperbolic parameter

Basic Principles of Eurocode 7 on 'Geotechnical Design'

Roger Frank

Abstract: Eurocode 7 on 'Geotechnical design' is now actively being implemented throughout Europe. Part 1 devoted to the 'General rules' has been published in 2004 and National Annexes are presently being prepared (2006) for final implementation in the various European countries. Part 2 on 'Ground investigation and testing' was formally voted positively early 2006 and will be published soon. After describing shortly the history of the development of Eurocode 7, the contents of the two documents are given and the main concepts are described (verifications procedures and geotechnical categories, characteristic values, derived values, ULS verifications, SLS verifications and allowable movements of foundations).

Key words: Eurocode 7, geotechnical design, limit states, foundations, retaining structures, ultimate limit states, serviceability limit states.

1. Introduction: The Eurocode programme

The system of Structural Eurocodes includes the 10 following sets of standards (EN for 'European Norm'):

EN 1990 Eurocode : Basis of structural design;

EN 1991 Eurocode 1: Actions on structures;

EN 1992 Eurocode 2: Design of concrete structures;

EN 1993 Eurocode 3: Design of steel structures;

EN 1994 Eurocode 4: Design of composite steel and concrete structures;

EN 1995 Eurocode 5: Design of timber structures;

EN 1996 Eurocode 6: Design of masonry structures;

EN 1997 Eurocode 7: Geotechnical design;

EN 1998 Eurocode 8: Design of structures for earthquake resistance;

EN1999 Eurocode 9: Design of aluminium structures.

The Structural Eurocodes are design codes for buildings and civil engineering works. They are based on the Limit State Design (LSD) approach used in conjunction with a partial factor method.

Except for EN 1990, all Eurocodes are subdivided into several parts. Eurocodes 2, 3, 4, 5, 6 and 9 are 'material' Eurocodes, *i.e.* relevant to a given material. EN 1990 (Basis of design), Eurocode 1 (Actions), Eurocode 7 (Geotechnical design) and Eurocode 8 (Earthquake resistance) are relevant to all types of construction, whatever the material.

Eurocode 7 should be used for all the problems of interaction of structures with the ground (soils and rocks), through foundations or retaining structures. It addresses not only buildings but also bridges and other civil engineering works. It allows the calculation of the geotechnical actions on the structures, as well the resistances of the ground submitted to the actions from the structures. It also gives all the prescriptions and rules for good practice required for properly conducting the geotechnical aspect of a structural project or, more generally speaking, a purely geotechnical project.

Eurocode 7 consists of two parts:

EN 1997-1 Geotechnical design - Part 1:
General rules (CEN, 2004)

EN 1997-2 Geotechnical design - Part 2:
Ground investigation and testing (CEN, 2006)

The development of Eurocode 7 was strongly linked to the development of EN 1990: 'Eurocode: Basis of structural design', in particular its Section 6 (Verification by the partial factor method) and its Annexes A1 and A2 (Application for buildings and for bridges, respectively), in order to reach a format for verifying ground-structure interaction problems acceptable by all. EN 1990 has been ratified and published in 2002 (CEN, 2002).

After describing shortly the history of the development of Eurocode 7, and giving the main contents of the two parts, the main concepts are described, without recalling all the principles of LSD and of the partial factor method used.

2. History of Eurocode 7 and Implementation

The first Eurocode 7 Group, in charge of drafting a European standard on geotechnical design, was created in 1981. It was composed of representatives of the National Societies for Geotechnical Engineering of the 10 countries forming the European Community at that time. A first model code on general rules for geotechnical design (corresponding to Eurocode 7 - Part 1) was published in 1990 (EC7, 1990).

In 1990, the task of drafting design codes for buildings and civil engineering works was transferred to the Comité Européen de Normalisation (CEN, European Committee for Standardization) and CEN/TC 250 (Technical Committee 250) in charge of all the 'Structural Eurocodes' was created. In particular, SC 7, Sub-Committee 7, is in charge of Eurocode 7 on 'Geotechnical design'. Note that

Roger Frank, Ecole Nationale des Ponts et Chaussées, Paris, France. e-mail: roger.frank@wanadoo.fr.
Submitted on September 9, 2006; Final Acceptance on January 23, 2007; Discussion open until August 31, 2007.

CEN is composed of the national standard bodies of a number of European countries (in February 2006, 29 countries are members, *i.e.* 25 countries of EU, plus 3 countries of EFTA, plus Romania; 5 countries are affiliates). N.Krebs Ovesen (Denmark) was the first Chairman of CEN/TC 250/SC 7, from 1990 until 1998. The author was the Chairman of SC 7 from 1998 to 2004. Since June 2004, Bernd Schuppener (Germany) is the new Chairman.

In 1993, SC 7 adopted the ENV 1997-1 pre-standard: 'Geotechnical design - Part 1: General Rules' (CEN, 1994). It was clear, at that time, that (much) more work still needed to be done before reaching a full European standard (EN) acceptable to all members of CEN. An important fact helped in obtaining, in 1997, a positive vote for the conversion into an EN. It was the recognition by CEN/TC250 that geotechnical design is unique and cannot be considered to be the same as other design practices needed in the construction industry. The models commonly used vary from one country to the other and cannot be harmonised easily, simply because the geologies are different and form the rationale for the so-called 'local traditions' This recognition is confirmed by a resolution taken by TC 250 (Resolution N 87, 1996): '*CEN/TC 250 accepts the principle that ENV 1997-1 might be devoted exclusively to the fundamental rules of geotechnical design and be supplemented by national standards*'.

The work for the conversion of ENV 1997-1 into EN 1997-1 'Geotechnical design - Part 1: General rules' was performed from 1997 to 2003. The formal positive vote by CEN members was obtained early 2004 and CEN finally published Eurocode 7 - Part 1 (EN 1997-1) in November 2004 (CEN, 2004).

Eurocode 7 originally consisted of two other Parts: Part 2, devoted to geotechnical design assisted by laboratory testing and Part 3, devoted to geotechnical design assisted by field (in situ) testing. The corresponding ENVs (ENV 1997-2 and 1997-3) were drafted rather quickly, facing no serious controversy. They were published in 1999 (CEN, 1999a and 1999b) and, in 2001, the members of CEN voted positively for their conversion into a European Norm. During the conversion phase, the two documents were merged into the single document called 'Eurocode 7 Geotechnical design - Part 2: Ground investigation and testing'. The formal positive vote was obtained in May 2006 and the document will now be published soon by CEN (CEN, 2006).

The publication of a Eurocode Part by each national standardisation body with its National Annex (in the official language(s) of the country) has to be completed within two years after publication by CEN. The role of the National Annex is to indicate the decisions corresponding to the so-called "Nationally Determined Parameters (NDPs)". The National Annex can also give a 'normative' status to one or to several of the 'informative' Annexes, *i.e.* it (they) will be mandatory in the corresponding country.

As mentioned above, each country is also free to supplement the general rules of Eurocode 7 by national application standards, in order to specify the calculation models and design rules to be applied in the country. Whatever their contents they will have to respect in all aspects the principles of Eurocode 7.

The 'legal' status of standards/norms is different in each country and the regulatory bodies of the various countries have an important role to play for the implementation of the Eurocodes. A 'Guidance Paper' has been elaborated by the European Commission to co-ordinate the implementation of the Eurocodes into the national regulations (CE, 2003a). The European Commission has also issued a strong recommendation to the Member States inviting them to adopt the Eurocodes in their regulations (CE, 2003b).

3. Contents of Documents

3.1. Part 1: General rules

Eurocode 7 - Part 1 is a rather general document giving only the principles for geotechnical design inside the general framework of LSD. These principles are relevant to the calculation of the geotechnical actions on structures (buildings and civil engineering works) and to the design of the structural elements themselves in contact with the ground (footings, piles, basement walls, etc.). Detailed design rules or calculation models, *i.e.* precise formulae or charts are only given in informative Annexes. As already mentioned, the main reason is that the design models in geotechnical engineering differ from one country to the other, and it was not possible to reach a consensus, especially when many of these models still need to be calibrated and adapted to the LSD approach

Eurocode 7 - Part 1 includes the following sections(CEN, 2004):

Section 1 General

Section 2 Basis of geotechnical design

Section 3 Geotechnical data

Section 4 Supervision of construction, monitoring and maintenance

Section 5 Fill, dewatering, ground improvement and reinforcement

Section 6 Spread foundations

Section 7 Pile foundations

Section 8 Anchorages

Section 9 Retaining structures

Section 10 Hydraulic failure

Section 11 Overall stability

Section 12 Embankments

Sections 8 on anchorages, 10 on hydraulic failure and 11 on site stability are new sections with regard to the pre-standard (ENV 1997-1, CEN, 1994).

A number of Annexes are included. They are all informative, except for Annex A which is 'normative' (*i.e.*

mandatory). The list of the Annexes for EN 1997-1 is the following:

Annex A (normative) Partial factors for ultimate limit states

Annex B Background information on partial factors for Design Approaches 1, 2 3

Annex C Sample procedures to determine limit values of earth pressures on vertical walls

Annex D A sample analytical method for bearing resistance calculation

Annex E A sample semi-empirical method for bearing resistance estimation

Annex F Sample methods for settlement evaluation

Annex G A sample method for deriving presumed bearing resistance for spread foundations on rock

Annex H Limiting foundation movements and structural deformation

Annex J Checklist for construction supervision and performance monitoring

Annex A is important, as it gives the partial factors for ULS in persistent and transient design situations ('fundamental combinations'), as well as correlation factors for the characteristic values of pile bearing capacity. But the numerical values for the partial or correlation factors given in Annex A are only recommended values. The exact values of the factors can be changed by each national standardisation body in the so-called National Annex. All other Annexes are informative (*i.e.* not mandatory in the normative sense). Some of them, though, contain valuable material which can be accepted, in the near future, by most of the countries. The National Annex can give a 'normative(s)' status to one or to several of the 'informative' Annexes, *i.e.* it (they) will be mandatory in the corresponding country.

The national application standards, specifying the calculation models and design rules to be applied in the country, will also depend on the choices made with regard to the application of the informative Annexes of Eurocode 7.

3.2. Part 2: Ground investigation and testing

The role of this part of Eurocode 7 devoted to laboratory and field testing is to give the essential requirements for the equipment and test procedures, for the reporting and the presentation of results, for their interpretation and, finally, for the derivation of values of geotechnical parameters for the design. It complements the requirements of Part 1 in order to ensure a safe and economic geotechnical design.

It makes the link between the design requirements of Part 1, in particular Section 3 'Geotechnical data', and the results of a number of laboratory and field tests.

It does not cover the standardisation of the geotechnical tests themselves. Another Technical Committee (TC) on 'Geotechnical investigation and testing' has precisely been created by CEN to consider this matter (TC 341). In this respect the role of Part 2 of Eurocode 7 is to 'use' and refer to the detailed rules for test standards covered by TC 341.

Eurocode 7 - Part 2 includes the following Sections (CEN, 2006):

Section 1 - General

Section 2 - Planning of ground investigations

Section 3 - Soil and rock sampling and groundwater measurements

Section 4 - Field tests in soils and rocks

Section 5 - Laboratory tests on soils and rocks

Section 6 - Ground investigation report

The Section on field tests in soils and rocks includes:

- cone penetration tests CPT(U)
- pressuremeter tests PMT
- rock dilatometer tests RDT
- standard penetration tests SPT
- dynamic penetration tests DP
- weight sounding tests WST
- field vane tests FVT
- flat dilatometer tests DMT
- plate loading tests PLT

The Section on laboratory testing of soils and rocks deals with:

- preparation of soil specimens for testing
- preparation of rock specimens for testing
- tests for classification, identification and description of soils
- chemical testing of soils and groundwater
- strength index testing of soils
- strength testing of soils
- compressibility and deformation testing of soils
- compaction testing of soils
- permeability testing of soils
- tests for classification of rocks
- swelling testing of rock material
- strength testing of rock material

There are provisions on how to establish and use the so-called 'derived values' from the tests (see paragraph 4.3 below). Some of these provisions are meant to give guidance for using the sample calculation models in the Annexes of Part 1. Part 2 also includes a number of informative Annexes with precise examples of derived values of geotechnical parameters and coefficients used commonly in design.

As is the case in Part 1, most of the derivations or calculation models given are informative, but there is also fairly good agreement about using them in the future throughout Europe. In any case, they are a clear picture of the approaches existing on the continent for the use of *in situ* or laboratory test results in the design of geotechnical structures.

4. Some Aspects pf Eurocode 7

4.1. Verification procedures and geotechnical categories

The discussions about verifications of geotechnical design usually focus on approaches performed through calculations. Nevertheless, it should be stressed that calculations are not the only means for checking that the basic requirements are fulfilled.

Eurocode 7 - Part 1 offers, in fact, various possibilities (clause 2.1 in EN 1997-1):

'*(4) Limit states should be verified by one or a combination of the following:*

- *use of calculations [];*
- *adoption of prescriptive measures, [];*
- *experimental models and load tests, [];*
- *an observational method, [].'*

This paragraph is clear enough. However, it may be useful to add that:

- the adoption of prescriptive measures indicates that, in some circumstances (see the geotechnical categories below), one may avoid calculations which may look long and cumbersome with regard to the problem under consideration;
- the use of experimental models and load tests recalls that the fundamentals of geotechnical design and of its calculation rules are the monitoring of the behaviour of real structures, with recourse, when necessary, to full scale tests;
- finally, mentioning the observational method, shows one of the directions devoted to contemporary geotechnical design (with full consistency with the fundamentals mentioned above).

With regard to the observational method, Eurocode 7 adds that (clause 2.7 in EN 1997-1):

'(2)P The following requirements shall be met before construction is started:

- *acceptable limits of behaviour shall be established;*
- *the range of possible behaviour shall be assessed and it shall be shown that there is an acceptable probability that the actual behaviour will be within the acceptable limits;*
- *a plan of monitoring shall be devised, which will reveal whether the actual behaviour lies within the acceptable limits. The monitoring shall make this clear at a sufficiently early stage, and with sufficiently short intervals to allow contingency actions to be undertaken successfully;*
- *the response time of the instruments and the procedures for analysing the results shall be sufficiently rapid in relation to the possible evolution of the system;*
- *a plan of contingency actions shall be devised, which may be adopted if the monitoring reveals behaviour outside acceptable limits.'*

(note that, in the Eurocodes, when the letter 'P' accompanies the number of a paragraph, it means that it is a principle, *i.e.* a fundamental requirement; paragraphs not marked with 'P' are only 'application rules').

The use of the observational method should grow considerably in the coming years (see Huybrechts *et al.*, 2005).

In order to define the design requirements and the levels needed for the geotechnical investigation, Eurocode 7 introduces three geotechnical categories (clause 2.1 in EN 1997-1). It is a way of introducing, one can say, 'consequences classes' (see Annex B of EN 1990, CEN, 2002).

Geotechnical category 1 corresponds to the simple structures that can be designed and executed, with negligible risk, only on the basis of experience and with a qualitative geotechnical investigation. One can place in this category retaining walls of moderate height or direct foundations for individual houses, in simple geotechnical conditions (no stability nor water problems, etc.).

Geotechnical category 2 covers conventional geotechnical structures, without exceptional risk (*i.e.* without difficult geotechnical conditions or loadings). Eurocode 7 requirements concerning calculations and ground investigations fully apply to category 2 structures (clause 2.1 in EN 1997-1):

'(18) Designs for structures in Geotechnical Category 2 should normally include quantitative geotechnical data and analysis to ensure that the fundamental requirements are satisfied.

(19) Routine procedures for field and laboratory testing and for design and execution may be used for Geotechnical Category 2 designs.

Note: The following are examples of conventional structures or parts of structures complying with Geotechnical Category 2:

- *spread foundations;*
- *raft foundations;*
- *pile foundations;*
- *walls and other structures retaining or supporting soil or water;*
- *excavations;*
- *bridge piers and abutments;*
- *embankments and earthworks;*
- *ground anchors and other tie-back systems;*
- *tunnels in hard, non-fractured rock and not subjected to special water tightness or other requirements.'*

Category 3 includes all geotechnical structures with abnormal risks, for which Eurocode 7 requirements may not be sufficient to ensure an acceptable level of safety. The risks can derive from the ground conditions or from the loading conditions. Examples of structures falling into this

category are large dams, foundations of nuclear power plants, structures on unstable ground, etc. Eurocode 7 clearly indicates that (clause 2.1 in EN 1997-1):

'(21) Geotechnical Category 3 should normally include alternative provisions and rules to those in this standard [EN 1997-1].'

In the Eurocode system, as mentioned earlier, the calculation method prescribed is the LSD approach used in conjunction with a partial factor method. Problems encountered in geotechnical engineering projects are often due to reasons not linked to design calculations. For geotechnical practice, Eurocode 7 - Part 1 also mentions that (clause 2.4.1 in EN 1997-1):

'*(2) It should be considered that knowledge of the ground conditions depends on the extent and quality of the geotechnical investigations. Such knowledge and the control of workmanship are usually more significant to fulfilling the fundamental requirements than is precision in the calculation models and partial factors.*'

4.2. Characteristic values

The present 'philosophy' with regard to the definition of characteristic values of geotechnical parameters is contained in the following clauses of Eurocode 7 - Part 1 (clause 2.4.5.2 in EN 1997-1):

'*(2) P The characteristic value of a geotechnical parameter shall be selected as a cautious estimate of the value affecting the occurrence of the limit state.'*

'(7) [...] the governing parameter is often the mean of a range of values covering a large surface or volume of the ground. The characteristic value should be a cautious estimate of this mean value.'

These paragraphs in Eurocode 7 - Part 1 reflect the concern that one should be able to keep using the values of the geotechnical parameters that were traditionally used (the determination of which is not standardised, *i.e.* they often depend on the individual judgment of the geotechnical engineer, one should confess). However two remarks should be made at this point: on the one hand, the concept of 'derived value' of a geotechnical parameter (preceding the determination of the characteristic value), has been introduced (see paragraph 4.3) and, on the other hand, there is now a clear reference to the limit state involved (which may look evident, but is, in any case, a way of linking traditional geotechnical engineering and the new limit state approach) and to the assessment of the mean value (and not a local value; this might appear to be a specific feature of geotechnical design which, indeed, involves 'large' areas or 'large' ground masses).

Statistical methods are mentioned only as a possibility:

'*(10) If statistical methods are employed [], such methods should differentiate between local and regional sampling [].'*

'(11) If statistical methods are used, the characteristic value should be derived such that the calculated probability of a worse value governing the occurrence of the limit state under consideration is not greater than 5%.
Note: In this respect, a cautious estimate of the mean value is a selection of the mean value of the limited set of geotechnical parameter values, with a confidence level of 95%; where local failure is concerned, a cautious estimate of the low value is a 5% fractile.'

The general feeling is that the characteristic value of a geotechnical parameter cannot be fundamentally different from the value that was traditionally used. Indeed, for the majority of projects, the geotechnical investigation is such that no serious statistical treatment of the data can be performed. Statistical methods are, of course, useful for very large projects where the amount of data justifies them.

4.3. Derived values

Many geotechnical tests, particularly field tests, do not allow basic geotechnical parameters or coefficients, for example for strength and deformation, to be determined directly. Instead, values of these parameters and coefficients must be derived using theoretical or empirical correlations.

The concept of 'derived values' had been introduced in ENV 1997-3 (CEN 1999b), in order to give status to correlations and models commonly used to obtain, from both results of field tests and results of laboratory tests, geotechnical parameters and coefficients which enter directly into the design. Their use is intended, primarily, for the design of pile and shallow foundations as mentioned in the Annexes D, E, F, and G of Eurocode 7 - Part 1.

The definition of derived values is given in Eurocode 7 - Part 2 as:

'*Derived values of geotechnical parameters and/or coefficients, are obtained from test results by theory, correlation or empiricism.*'

From field test results, the geotechnical parameter obtained is either an input for an analytical or indirect model, or a coefficient for use in a semi-empirical or direct model of foundation design.

Derived values of a geotechnical parameter then serve as input for assessing the characteristic value of this parameter in the sense of Eurocode 7 - Part 1 (clause 2.4.5.2 of EN 1997-1) and, further, its design value, by applying the partial factor γ_M ('material factor', clause 2.4.6.2).

The role played by the derived values of geotechnical parameters can be understood with the help of Fig. 1, taken from Eurocode 7 - Part 2. The borderline between Part 1 (EN 1997-1) and Part 2 (EN 1997-2) of Eurocode 7 is also shown on the figure. It can be seen that the requirements concerning the measurements of geotechnical properties, as well as their derived values are covered by Part 2: 'Ground investigation and testing', while those concerning the determination of characteristic values and design values are given, as mentioned above, by Part 1: 'General rules'.

4.4. ULS verifications

The ultimate limit states (ULS) to be checked are defined, in the following manner, by Eurocode 7 - Part 1, consistently with 'Eurocode: Basis of structural design' (CEN 2002) (clause 2.4.7.1 in EN 1997-1):

'*(1)P Where relevant, it shall be verified that the following limit states are not exceeded:*

- *loss of equilibrium of the structure or the ground, considered as a rigid body, in which the strengths of structural materials and the ground are insignificant in providing resistance (EQU);*
- *internal failure or excessive deformation of the structure or structural elements, including footings, piles, basement walls, etc., in which the strength of structural materials is significant in providing resistance (STR);*
- *failure or excessive deformation of the ground, in which the strength of soil or rock is significant in providing resistance (GEO);*
- *loss of equilibrium of the structure or the ground due to uplift by water pressure (buoyancy) or other vertical actions (UPL);*
- *hydraulic heave, internal erosion and piping in the ground caused by hydraulic gradients (HYD).*

Note: Limit state GEO is often critical to the sizing of structural elements involved in foundations or retaining structures and sometimes to the strength of structural elements.'

The ultimate limit states should be verified for the combinations of actions corresponding to the following design situations (see EN 1990, CEN, 2002):

- permanent and transient (the corresponding combinations are called 'fundamental'); in the following these design situations are noted 'p&tds' for convenience;
- accidental;
- seismic (see also Eurocode 8- Part 5, *i.e.* EN 1998-5).

The design values of the actions and the combinations of actions are defined in EN 1990 (partial factors γ for the actions and factors Ψ for the accompanying variable actions).

The debate about the format for checking the GEO and STR ultimate limit states (ULS) was relevant to the persistent and transient design situations ('p&tds'. This debate follows from the ENV 1997-1 (CEN, 1994) formulation which inferred that ULS in persistent and transient design situations had to be checked for two formats of combinations of actions, *i.e.* for Cases B and C, as they were called at that time. B was aimed at checking the uncertainty on the loads coming from the structure, and C the uncertainty on the resistance of the ground. Some geotechnical engineers were in favour of this double check, as others preferred having to use only one single format of combinations of actions

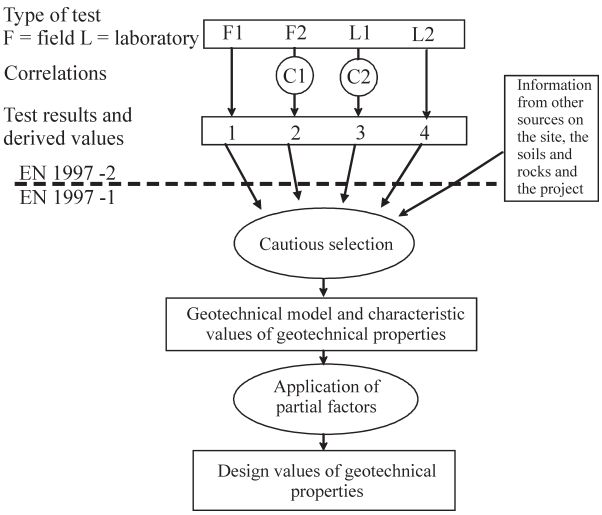

Figure 1 - General framework for the selection of derived values, characteristic values and design values of geotechnical properties (CEN, 2006).

(more details can be found, for instance, in Frank and Magnan, 1999).

The consensus reached between structural and geotechnical engineers opened the way to three different Design Approaches (DA1, DA2 and DA3). The choice is left to national determination, *i.e.* each country will have to state in its National Annex, the Design Approach(es) to be used for each type of geotechnical structure (spread foundations, pile foundations, retaining structures, slope stability).

Generally speaking, for checking ULS - p&tds, three sets of partial factors to be applied to characteristic values of actions are introduced in EN 1990: Sets A, B, and C:

- set A is used for checking the static equilibrium of the structure (EQU);
- set B is relevant to the design of structural members (STR) not involving geotechnical actions;
- sets B and C are relevant to the design of structural members involving geotechnical actions and the resistance of the ground (STR/GEO).

Tables 1, 2 and 3 give, in a simplified manner, the recommended values for buildings for Sets A, B and C, taken from Tables A1.2 (A), A1.2(B) and A1.2(C) of EN 1990 (CEN, 2002). The recommended values given may be modified by National decision.

For STR/GEO ULS in p&tds, the three Design Approaches are the following (clause A1.3.1 in EN 1990):

'*(5) Design of structural members (footings, piles, basement walls, etc.) (STR) involving geotechnical actions and the resistance of the ground (GEO) should be verified using one of the following three approaches supplemented, for geotechnical actions and resistances, by EN 1997:*

Approach 1: Applying in separate calculations design values from Table A1.2(C) and Table A1.2(B) to the

geotechnical actions as well as the other actions on/from the structure. In common cases, the sizing of foundations is governed by Table A1.2(C) and the structural resistance is governed by Table A1.2(B);
Note: In some cases, application of these tables is more complex, see EN 1997.

Approach 2: Applying design values from Table A1.2(B) to the geotechnical actions as well as the other actions on/from the structure;

Approach 3: Applying design values from Table A1.2(C) to the geotechnical actions and, simultaneously, applying partial factors from Table A1.2(B) to the other actions on/from the structure.
Note: The use of approaches 1, 2 or 3 is chosen in the National annex.'

In other words, Design Approach 1 (DA1) is the double check procedure coming from the ENV 1997-1 (B+C verification) and Design Approaches 2 (DA2) and 3 (DA3) are new procedures using a single format of combinations of actions. DA2 is elaborated with 'resistance factors' for the ground (RFA), as DA3 makes uses of 'material factors' for the ground (MFA).

Two important remarks should be made at this point:

- with regard to the choice between expression 6.10 or expressions 6.10a and 6.10b of EN 1990 (see Table 2 for set B), Eurocode 7 only mentions the recommended values of the factors corresponding to expression 6.10 (Table A.3 in the note to paragraph A.3(1)P of AnnexA in EN 1997-1). This derives from the fact that the recommended geotechnical values come from a few calibration studies performed using the values of expression 6.10, while, on the other hand, there is no experience on the use of expressions 6.10a et 6.10b in geotechnical engineering...
- for DA2 and DA3, Eurocode 7 allows to apply the partial factors either on the actions or on the effects of the actions (they are noted γ_F and γ_E, respectively). This is relevant to the factors of set B and of set C (unfavourable variable actions).

Table 4 gives the link between Sets B and C and the corresponding sets of factors for geotechnical actions and resistances: Sets M1 and M2 for material properties (*e.g.* c', ϕ', c_u, etc.) and Sets R1, R2, R3 and R4 for total resistances (*e.g.* bearing capacity, etc.). These sets are defined in Annex A of Eurocode 7 - Part 1. As mentioned above, Annex A also gives recommended values for the partial factors; these values may be set differently by the National Annex. Note that the recommended values for the partial factors γ_M on material properties in Set M1 are always equal to 1.0.

In DA1, the first format (combination 1, former case B) applies safety mainly on actions, while the factors on resistances have recommended values equal to 1.0 (Sets M1 and R1) or near 1.0 (Set R1 in the case of axially loaded piles and anchorages); in the second format imposed by DA1 (combination 2, former case C), the elementary properties of the ground (shear strength parameters) are always factored for the calculation of geotechnical actions and sometimes factored for the calculation of resistances (Set M2); in the case of axially loaded piles and anchorages, the total resistance is directly factored by applying Set R4.

In DA2, safety is applied both on the actions (Set B) and on the total ground resistance (Set R2).

Table 1 - Recommended values for partial factors for actions (Set A) after EN 1990 (CEN, 2002) - ULS in p&tds.

Action	Symbol	Value
Permanent actions		
- unfavourable	$\gamma_{G,sup}$	1.10(1)
- favourable	$\gamma_{G,inf}$	0.90(1)
Variable actions		
- unfavourable	γ_Q	1.50
- favourable		0

(1) As an alternative, the favourable part may be multiplied by $\gamma_{G,inf}$ = 1.15 and the unfavourable part by $\gamma_{G,sup}$ = 1.35.

Table 2 - Recommended values for partial factors for actions (Set B) after EN 1990 (CEN, 2002) - ULS in p&tds.

Action	Symbol	Value		
		Eq. (6.10)	Eq. (6.10a)	Eq. (6.10b)
Permanent				
-unfavourable(1)	γ_{Gsup}	1.35	1.35	1.15(2)
- favourable(1)	γ_{Ginf}	1.00	1.00	1.00
Variable				
- unfavourable	γ_Q	1.50	$1.5\Psi_0$	1.50
- favourable		0	0	0

(1) all permanent actions from one source are multiplied by γ_{Gsup} or by γ_{Ginf}.
(2) value of ξ is 0.85, so that $0.85\gamma_{Gsup} = 0.85 \times 1.35 \cong 1.15$.
Note 1: choice between expression 6.10 or expressions 6.10a and 6.10b used together, is by National decision.
Note 2: γ_G and γ_Q may be subdivided into γ_g and γ_q and the model uncertainty factor γ_{Sd}. γ_{Sd} = 1.15 is recommended.

Table 3 - Recommended values for partial factors for actions (Set C) after EN 1990 (CEN, 2002) - ULS in p&tds.

Action	Symbol	Value
Permanent actions		
- unfavourable	$\gamma_{G,sup}$	1.00
- favourable	$\gamma_{G,inf}$	1.00
Variable actions		
- unfavourable	γ_Q	1.30
- favourable		0

Table 4 - STR/GEO - ULS in p&tds. Partial factors to be used according to EN 1990 and EN 1997-1.

Design approach	Actions on/from the structure	Geotechnical	
		Actions	Resistances
1	B	B and M1	M1 and R1
	C	C and M2	M2 and R1 or M1 and R4*
2	B	B and M1	M1 and R2
3	B	C and M2	M2 and R3

*for piles and anchorages.

In DA3, safety is applied both on the actions (Set B for the actions coming from the structure and Set M2 for the elementary properties of the ground acting on the structure, *i.e.* for the geotechnical actions) and on the geotechnical resistances (Set M2 for the elementary properties; the recommended values for Set R3 for the total geotechnical resistance is always equal to 1.0, except for piles in tension and anchorages for which they are equal to 1.1).

Figures 2, 3 and 4, as well as their captions, illustrate the situation for each of the three Design Approaches (Frank *et al.*, 2004). On these figures, index 'd' indicates a design value different from the characteristic value (application of a partial factor γ different from 1.0) and index 'k' indicates a design value equal to the characteristic value (application of a partial factor γ equal to 1.0).

More details on the use of the three Design Approaches are given, for instance, in Frank *et al.* (2004).

With regard to the design values for accidental situations, Eurocode 7 only states that (clause2.4.7.1 in EN 1997-1):

'(3) All values of partial factors for actions or the effects of actions in accidental situations should normally be taken equal to 1,0. All values of partial factors for resistances should then be selected according to the particular circumstances of the accidental situation.
Note: The values of the partial factors may be set by the National annex.'

4.5. Verification of serviceability limit states (SLS)

The main discussions during the development of Eurocode 7 were about the format for verifying ULS in permanent and transient situations. However, the verification of serviceability limit states (SLS) is an issue equally important in contemporary geotechnical design. This issue is fully recognised by Eurocode 7 which indeed often refers to displacement calculations of foundations and retaining structures, while common geotechnical practice mainly sought so far to master serviceability by limiting the bearing capacity or by limiting the shear strength mobilisation of the ground to relatively low values.

The verification of SLS in the real sense proposed by Eurocode 7 (prediction of displacements of foundations) is certainly going to gain importance in the near future. For the time being, it is an aspect which is too often neglected in common geotechnical practice.

Eurocode 7 - Part 1 repeats the formulation of EN 1990 (clause 2.4.8, EN 1997-1):

'(1)P Verification for serviceability limit states in the ground or in a structural section, element or connection, shall either require that:

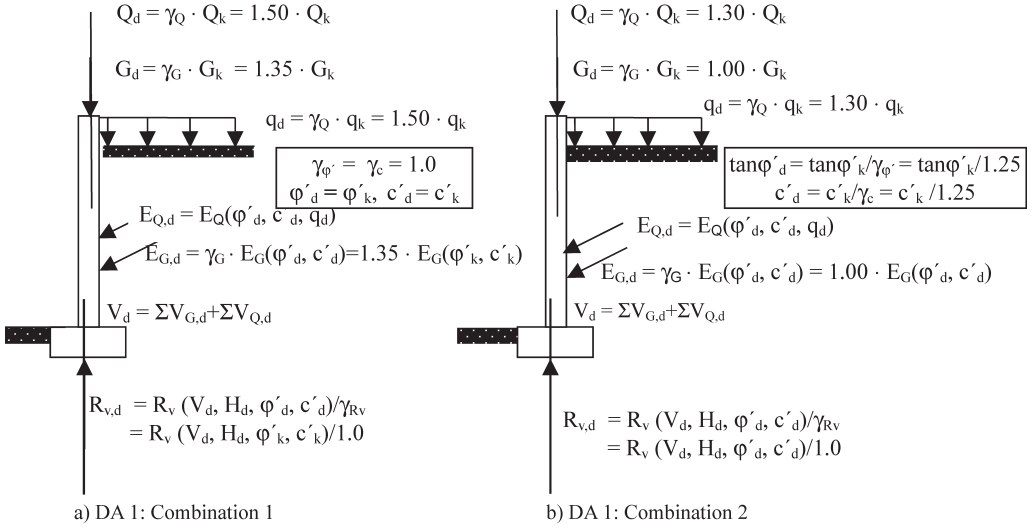

Note: for simplicity, only vertical equilibrium is considered and only unfavourable actions are shown.

Figure 2 - ULS in p&tds. Design Approach 1 - introduction of partial factors (recommended values) in the checking of ground bearing capacity (Frank *et al.* , 2004).

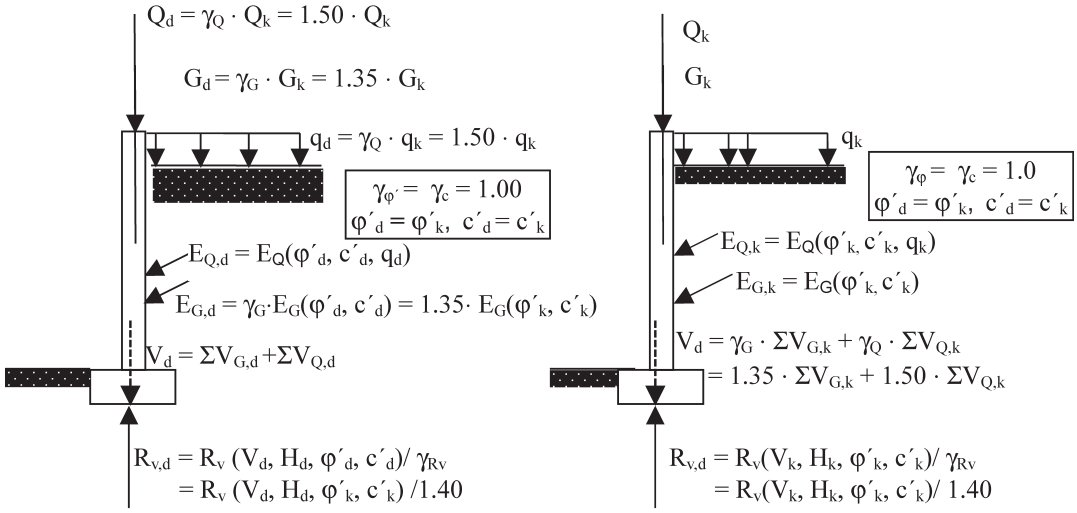

a) Factoring actions at the source (DA 2) b) Factoring effects of actions (DA 2*)

Note: for simplicity, only vertical equilibrium is considered and only unfavourable actions are shown.

Figure 3 - ULS in p&tds. Design Approach 2 - introduction of partial factors (recommended values) in the verification of ground bearing capacity (Frank *et al.* , 2004).

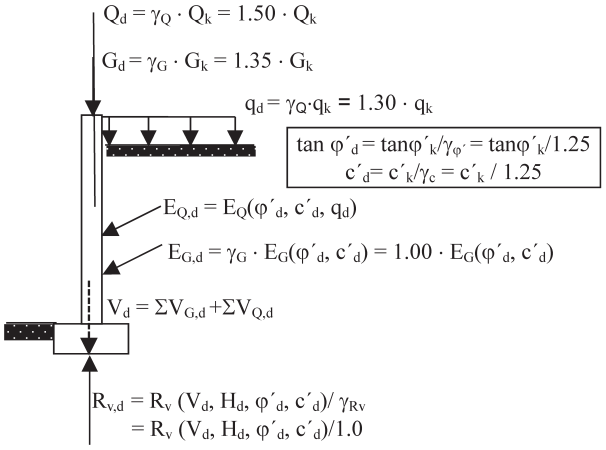

Note: for simplicity, only vertical equilibrium is considered and only unfavourable actions are shown.

Figure 4 - ULS in p&tds. Design Approach 3 - introduction of partial factors (recommended values) in the verification of ground bearing capacity (Frank *et al.* , 2004).

$$E_d \leq C_d, \qquad (2.10)$$

or be done through the method given in 2.4.8(4).

(2) Values of partial factors for serviceability limit states should normally be taken equal to1,0.

Note: The values of the partial factors may be set by the National annex.'

with E_d the design value of the effect of actions and C_d the limiting value (serviceability criterion) of the design value of effect of actions. At the same time, Eurocode 7 introduces immediately the possibility to keep the traditional approach mentioned above (clause 2.4.8 in EN 1997-1):

'(4) It may be verified that a sufficiently low fraction of the ground strength is mobilised to keep deformations within the required serviceability limits, provided this simplified approach is restricted to design situations where:

- *a value of the deformation is not required to check the serviceability limit state;*
- *established comparable experience exists with similar ground, structures and application method.'*

This clause is to be linked to the one dealing with the design methods of spread foundations (paragraph 6.4(5)P in EN 1997-1):

'(5)P One of the following design methods shall be used for spread foundations:

- *a direct method, in which separate analyses are carried out for each limit state. When checking against an ultimate limit state, the calculation shall model as closely as possible the failure mechanism, which is envisaged. When checking against a serviceability limit state, a settlement calculation shall be used;*
- *an indirect method using comparable experience and the results of field or laboratory measurements or observations, and chosen in relation to serviceability limit state loads so as to satisfy the requirements of all relevant limit states;*
- *a prescriptive method in which a presumed bearing resistance is used (see 2.5).'*

Indeed, the indirect method '*chosen in relation to serviceability limit state loads'* comes to applying the traditional method of designing the bearing capacity of spread foundations, *i.e.* a simple calculation comparing the applied

loads for serviceability limit states to a limit load divided by a global factor of safety high enough (usually around 3). Of course, as indicated in Eurocode 7, this can only be valid if there is no need to assess the settlement of the foundation and if conventional structures with well known ground conditions are dealt with.

Paragraph 2.4.8(2) of Eurocode 7 - Part 1, reproduced above, indicating that partial actors for SLS are normally taken equal to 1.0 (in other words that the design values of the various quantities are taken equal to their characteristic values), applies to the actions in the characteristic, frequent or quasi-permanent combinations (see EN 1990), as well as to the geotechnical properties, such as the modulus of deformation. It should be noted that, for determining the differential settlement for instance, sets of lower characteristic values and upper characteristic values can be chosen in order to take account of the ground variability.

With regard to the use of the combinations of actions for SLS, EN 1990 provides (in editorial notes) some guidelines which are summarised in Table 5 (clause 6.5.3 in EN 1990).

When applying equation 2.10 of clause 2.4.8(1)P (see above), it appears that the frequent and quasi-permanent should be recommended; on the contrary, in the case of the alternative method allowed by 2.4.8(4), it seems that the characteristic (or 'rare') combination should be used, because the experience gained in the past was rather for loads near this type of combination.

The last general paragraph in Eurocode 7 - Part 1 about SLS, deals again with the 'displacement approach'. It states that (clause 2.4.8 in EN 1997-1):

'(5)P A limiting value for a particular deformation is the value at which a serviceability limit state, such as unacceptable cracking or jamming of doors, is deemed to occur in the supported structure. This limiting value shall be agreed during the design of the supported structure.'

The application of these general clauses is detailed further down in Eurocode 7 - Part 1 for each geotechnical structure (in the Sections for spread foundations, pile foundations, retaining structures, overall stability and embankments). It is interesting to note that the document insists several times on the difficulty to predict displacements with accuracy (in the present state of geotechnical engineering knowledge, of course!).

4.6. Limiting values of displacements of foundations

The knowledge of limiting allowable displacements of foundations is a subject of prime importance, even though it is not often explicitly addressed. These limiting values depend primarily, of course, on the nature of the supported structure, but it has also been a point of interest for geotechnical engineering for a long time, as well (a summary of data collected for buildings and bridges is given *e.g.* by Frank,1991).

Table 5 - Recommended combinations of actions for checking serviceability limit states SLS.

Combination of actions	Use according to EN 1990
Characteristic	Irreversible limit states
Frequent	Reversible limit states
Quasi permanent	Long term effect and appearance

The limiting values of movements of foundations is the subject, in particular, of clause 2.4.9, as well as of Annex H (informative) of Eurocode 7 - Part 1. It is noted that clause 2.4.9 contains 4 rather strong principles, *i.e.* paragraphs (1)P to (4)P. The first one says:

'(1)P In foundation design, limiting values shall be established for the foundation movements.
Note: Permitted foundation movements may be set by the National annex.'

Furthermore, it seems that not only SLS are concerned (see above) but also ULS (because movements of foundations can trigger an ULS in the supported structure).

Eurocode 7 gives a list of a certain number of factors which should be considered when establishing the limiting values of movements. It is important that these limiting values are established in a realistic manner, by close collaboration between the geotechnical engineer and the structural engineer. If the values are too much severe, they will usually lead to uneconomical designs.

Figure 5 defines the parameters used to quantify movements and deformations of structures. This figure, originally due to Burland and Wroth (1975) is reproduced in Annex H of Eurocode 7 - Part 1.

Annex H (informative) quotes the following limits after Burland *et al.* (1977):

- for open framed structures, infilled frames and load bearing or continuous brick walls: aximum relative rotations between about 1/2000 an about 1/300 to prevent the occurrence of a SLS in the structure;
- for many structures, a maximum relative rotation β = 1/500 is acceptable for SLS and β = 1/150 for ULS; - for normal structures with isolated foundations, total settlements up to 50 mm are often acceptable.

These values can serve as a guide, in the absence of other indications on the limiting values for the deformations of the structures.

5. Liaisons with other CEN and ISO Committees

Inside the Eurocode system itself, there are, of course, many links between the different standards or parts of them. Eurocode 7 on Geotechnical design is more precisely linked to the following ones:

- EN 1990: 'Eurocode: Basis of structural design' which defines the various limit states and design

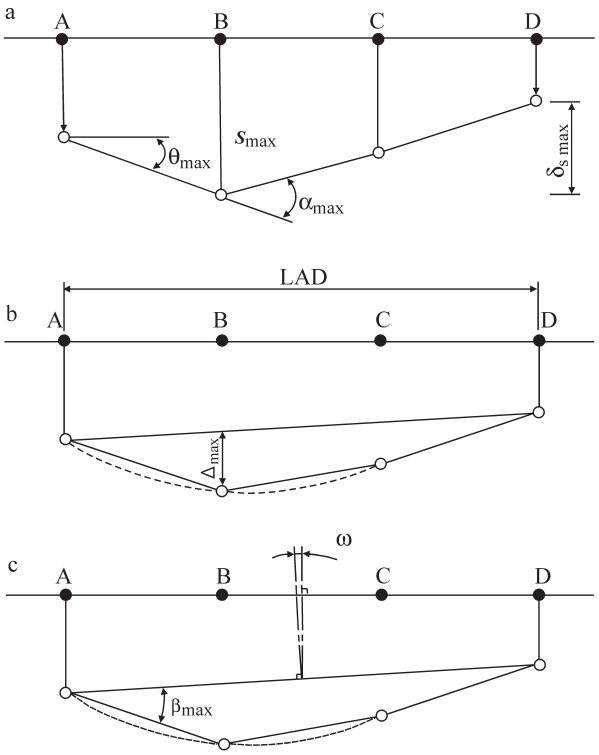

a) definitions of settlement *s*, differential settlement δ*s*, rotation θ and angular strain α.
b) definitions of relative deflection Δ and deflection ratio Δ/*L*.
c) definitions of tilt ω and relative rotation (angular distortion) β.

Figure 5 - Definitions of foundation movements and deformations of structures (CEN, 2004, afterBurland and Wroth, 1975).

situations to be checked, and gives the general rules for taking into account the actions on/from the structures and the geotechnical actions;

- EN1998-5: esign of structures for earthquake resistance. Foundations, retaining structures and geotechnical aspects.

The other Technical Committees of CEN working on standards of interest for Eurocode 7, and for which coordination must be ensured are:

- CEN/TC 341 on 'Geotechnical investigation and testing', as mentioned earlier;
- CEN/TC288 on 'Execution of geotechnical works';
- CEN/TC 189 on 'Geotextiles and geotextile-related products';
- CEN/TC227 on 'Road materials'.

The standards on execution (TC288) and on geotechnical tests (TC341) are particularly important as they complement Eurocode 7, which is devoted only to design.

6. Concluding Remarks

The work for the elaboration of a common framework for geotechnical design throughout Europe, *i.e.* Eurocode 7, started nearly 25 years ago. Given the progress recently achieved, it is now sure that the corresponding standards/codes will be enforced soon.

Whatever the precise legal status of Eurocode 7 in the various countries, it will prove to be very important for the whole construction industry. It is meant to be a tool to help European geotechnical engineers speak the same technical language and also a necessary tool for the dialogue between geotechnical engineers and structural engineers.

Eurocode 7 helps promote research. Obviously, it stimulates questions on present geotechnical practice from ground investigation to design models.

It is our belief that it will also be very useful to many geotechnical and structural engineers all over the world, not only in Europe.

References

Burland, J.B.; Broms, B.B. & De Mello, V.F.B. (1977) Behaviour of foundations and structures. Proc. 9th Int. Conf. Soil Mechs & Fdn Engng, Tokyo, v. 2, pp. 495-546.

Burland, J.B. & Wroth, C.P. (1975) Settlement of buildings and associated damage (Review Paper, Session V). Proc. Conf. Settlement of Structures, Cambridge, pp. 611-654.

CE (2003a) Guidance Paper L. Application and use of the Eurocodes, ref.: CONSTRUCT 03/629 Rev. 1 (27 November 2003), European Commission, Brussels.

CE (2003b) Commission recommendation of 11 December 2003 on the implementation and use of Eurocodes for construction works and structural construction products (2003/887/EC). Official Journal of the European Union, 19.12.2003, EN, L 332/62&63.

CEN (1994) Eurocode 7 Geotechnical design - Part 1: General Rules. Pre-standard ENV 1997-1. European Committee for Standardization (CEN): Brussels.

CEN (1999a) Eurocode 7 Geotechnical design - Part 2: Geotechnical design assisted by Laboratory Testing. Pre-standard ENV 1997-2. European Committee for Standardization: Brussels.

CEN (1999b) Eurocode 7 Geotechnical design - Part 3: Geotechnical design assisted by Field Testing. Pre-standard ENV 1997-3. European Committee for Standardization: Brussels.

CEN (2002) Eurocode: Basis of structural design. European standard, EN 1990: 002. European Committee for Standardization: Brussels.

CEN (2004) Eurocode 7: Geotechnical design - Part 1: General rules, EN 1997-1: 2004 (E), (F) and (G), November 2004, European Committee for Standardization: Brussels.

CEN (2006) Eurocode 7: Geotechnical design - Part 2: Ground investigation and testing. Final draft, prEN 1997-2, February 2006, European Committee for Standardization: Brussels.

EC7 (1990) Eurocode 7: Geotechnics. Preliminary draft for the European Communities, Geotechnik, 1990/1.

Frank R (1991) Quelques développements récents sur le comportement des fondations superficielles (Rapport général, Session 3), Comptes rendus 10ème Cong. Européen Méca. Sols et Tr. Fond., Florence, v. 3, pp. 1003-1030 (English version: Some recent developments on the behaviour of shallow foundations. General report, Proc. 10th European Conf. Soil Mechs & Fdn Engng, Florence, v. 4, pp. 1115-1141, 1994).

Frank, R.; Bauduin, C.; Driscoll, R.; Kavvadas, M.; Krebs Ovesen, N., Orr, T. & Schuppener B. (2004) Designer's Guide to EN 1997 Eurocode 7 - Geotechnical Design. Thomas Telford, London, 216 p.

Frank, R. & Magnan, J.P. (1999) Quelques réflexions sur la vérification des états limites ultimes suivant l'Eurocode 7 (in French - A few thoughts about ultimate limit states verifications following Eurocode 7). Workshop on the Eurocodes, Proc. 12th European Conf. Soil Mechs. & Geot. Engng, Amsterdam, v. 3, pp. 2179-2183.

Huybrechts, N.; Patel, D. & De Vos, M. (2005) The use of the observational method. Final Report WP3 on Innovative design methods in geotechnical engineering European network 'GeoTechNet'.

An Expedite Method to Predict the Shear Strength of Unsaturated Soils

Orencio Monje Vilar

Abstract. An expedite method to predict the shear strength of unsaturated soils is proposed and tested against many soils of different origins and subjected to different test types. The method uses an empirical hyperbolic function that has been successfully used to fit experimental data. The parameters of this function are obtained considering effective shear strength parameters from saturated soil and from test results of air dried samples tested without the need of suction control. Air dried samples can be, alternatively, replaced by test results of samples tested at suction larger than the maximum suction expected in the problem under analysis. The good agreement between the estimate functions and the experimental data shown by both alternatives makes them promising and reliable to estimate unsaturated shear strength parameters for preliminary purposes.

Key words: unsaturated soil, suction, shear strength, prediction, laboratory tests.

1. Introduction

The interest in unsaturated soil behavior has increased in recent years. Many advances in methods of testing and analyses have been proposed, however the major drawback when trying to characterize unsaturated soils in the laboratory still arises from the need to control or measure soil suction. Soil suction is usually imposed through the axis translating technique (Hilf, 1956), the osmotic technique (Kassif & Bem Shalon, 1971) and using saline solutions to control relative humidity (Soto, 2004). Measurement of suction is undertaken most commonly using mini tensiometers, psycrometers (Edil *et al.*, 1981) or high capacity tensiometers (Ridley & Burland, 1995).

A common feature of all the experimental techniques devised to test unsaturated soils are that they are time consuming or complex or both, requiring specialized expertise. Thus, it is not surprising that there has been a significant research effort directed towards the development of methods to predict the basic soil properties, such as the unsaturated hydraulic conductivity (van Genutchen, 1980, among others) and the shear strength. A common approach of the methods of estimating the shear strength of unsaturated soils is to use the soil water retention curve (SWRC) and effective shear strength parameters for saturated soil (Oberg & Salfors, 1997; Vanapalli *et al.*, 1996; Fredlund *et al.*, 1996). Khalili & Khabbaz (1998) used a traditional effective stress approach that is also based on effective strength parameters, c' and ϕ', and a single stress variable, χ, proposed by Bishop (1959) and defined as

$$\sigma' = (\sigma - u_a) + \chi (u_a - u_w) \quad (1)$$

where σ is the total stress, u_a is the pore air pressure, u_w is the pore water pressure, c' is the effective cohesion intercept and ϕ', the effective angle of internal friction of the saturated soil. These authors proposed a unique relationship between the effective stress parameter χ and the ratio between suction $(u_a - u_w)$ and air entry value $(u_a - u_w)_b$, the suction ratio.

Rassam & Cook (2002) have proposed a method where the shear strength envelope can be obtained using effective shear strength parameters for saturated soil, the SWRC and the test results from one unsaturated specimen at the residual water content. The method uses a power additive function and the predicted envelopes were in close agreement with experimental measurements for a variety of soil types.

In this paper an expedite method to predict the shear strength of unsaturated soils is proposed. The method uses data from saturated samples (effective stress parameters) and from air dried samples or, alternatively, from samples tested at a known suction that is larger than the maximum expected suction in the problem.

2. Fundamentals

Many authors, such as Bishop *et al.* (1960), Fredlund *et al.* (1978), Ho & Fredlund (1982), Escario & Saez (1986) have dealt with the shear strength of unsaturated soils. Most of the proposed experimental techniques use the axis translating technique to impose or to control soil suction. Triaxial compression tests and direct shear tests are commonly used and the usual drainage control include the drained test (CD), in which the pore air and pore water pressures are kept constant during all the test and the constant moisture test (CW) in which the pore air pressure is controlled and the pore water pressure is measured, as the flow of water is impeded.

Test results have been analyzed using an effective stress approach (Bishop, 1959) or independent stress state variables (Fredlund *et al.*, 1978). The former is based on

Orencio Monje Vilar, Doutor., Professor Titular, Escola de Engenharia de São Carlos, Universidade de São Paulo, Av. Dr. Carlos Botelho 1465, São Carlos, SP, Brasil. e-mail: orencio@sc.usp.br.
Submitted on November 23, 2005; Final Acceptance on May 11, 2006; Discussion open until August 31, 2007.

Eq. (1), while the later uses independent stress state variables, the net normal stress (σ - u_a) and the matric suction (u_a - u_w). The Fredlund *et al.* (1978) approach can be expressed as

$$\tau = c' + (u_a - u_w)\tan\phi^b + (\sigma - u_a)\tan\phi' \quad (2)$$

where τ = the shear strength of the unsaturated soil and ϕ^b = the angle of internal friction with respect to matric suction.

Equation (2) can be expressed as

$$\tau = c + (\sigma - u_a)\tan\phi' \quad (3)$$

where the total intercept of cohesion, c, is equivalent to

$$c = c' + (u_a - u_w)\tan\phi^b \quad (4)$$

Thus, the model relates an increase in matric suction to a linear increase in shear strength, more specifically by increasing cohesion. However many test results have shown that the influence of suction on shear strength is not linear (Escario & Saez, 1986; Rohm & Vilar, 1995; Satija, 1978). In fact, in spite of the different assumptions in the derivation of effective stress approach and independent stress state variables, it is easy to show that they are related since

$$\chi = \frac{\tan\phi^b}{\tan\phi'} \quad (5)$$

As it is known that χ is non linear with the degree of saturation, it is not surprising that ϕ^b should not be constant with suction.

Some empirical functions have been proposed to deal with the non linearity of the shear strength envelope of unsaturated soils. For instance, Abramento & Carvalho (1989) have proposed a potential function and de Campos & Carrillo (1995) a fourth order polynomial function.

The following hyperbolic equation is being used by the author to represent the influence of matric suction on the unsaturated shear strength of some Brazilian soils (Rohm & Vilar, 1995; Teixeira & Vilar, 1997 and Machado & Vilar, 1998).

$$c = c' + \frac{\psi}{a + b\psi} \quad (6)$$

where a and b are fitting parameters and $\psi = u_a - u_w$.

The use of Eq. (6) can be illustrated by applying it to test data of some soils available in the literature. The characteristics and properties of these soils are presented in Table 1. This table also summarizes data from other soils that will be used later. Figure 1 shows the experimental data and fitting curves for some of the listed soils. The chosen soils comprise a wide range of soil types and test conditions that include undisturbed and compacted samples tested in direct shear tests, triaxial compression tests and unconfined compression tests performed with suction control. The equation matches the experimental data with little scatter, illustrating its usefulness in representing the effect of suction on shear strength of unsaturated soils. The fitting parameters and coefficient of determination (R^2) are presented in Table 2.

3. The Proposed Procedure

The good agreement between the fitting equation and the experimental data suggests that it can be used to predict the unsaturated shear strength if the fitting parameters could be obtained from other sources of data, such as the effective stress envelope.

Figure 2 shows a sketch of the hyperbolic function to represent the shear strength variation with suction and its link with SWRC. The qualitative features of the relationship between both curves are discussed and used to establish the assumptions used to derive the *a* and *b* hyperbolic parameters.

It is known that below the air entry value the soil remains saturated and the effective stress principle still remains valid. If the Fredlund *et al.* (1978) equation is considered, it is easy to show that in the saturated state $\phi^b = \phi'$. The air entry value depends on many aspects such as the void ratio and confining stress. To keep the proposed procedure as simple as possible and to avoid the introduction of additional parameters in the proposed model, it is considered that the slope of the relationship between c and ψ (Eq. (7)), as ψ approaches zero, is tanϕ', that is

$$\left.\frac{dc}{d\psi}\right|_{\psi \to 0} = \frac{1}{a} = \tan\phi' \quad (7)$$

As suction increases the soil begins to desaturate and most of the results published so far shows an increase in shear strength with suction up to a maximum. After that, shear strength remains almost constant (Escario, 1988, de Campos & Carrillo, 1995, Machado & Vilar, 1998) and some particular soils have shown that shear strength drops off to a lower value as suction is increased (Escario, 1988; Gan & Fredlund, 1996). Considering the experimental errors inevitably present and for the sake of simplicity it will be assumed that shear strength reaches an ultimate value in any case. So, as ψ approaches infinity, shear strength approaches an ultimate or unsaturated residual value, c_{ult} or τ_{ult}, depending on how shear strength is represented, value that is probably related to the residual water content of the soil.

Assuming that shear strength will reach an ultimate value at the residual water content, the following statement can be written:

$$\lim_{\psi \to \infty} c = c_{ult} = c' + \frac{1}{b} \quad (8)$$

or that

Table 1 - Properties and characteristics of some unsaturated soils.

Soil	Soil type	ϕ' (°)	c' (kPa)	Remarks
1	Sandy clay (compacted)	30	30	LL = 33%; PI = 10%; γ = 16 kN/m^3; w = 15.5%; triaxial CD tests [Teixeira & Vilar, 1997]
2	Copper tailing dam (compacted)	38.7 to 40.1	9.2	Sand (SM); γ_d = 18.4 kN/m^3; NP; w = 13%; CD and CW tests [Drumright & Nelson, 1995]
3	Clayey silt (statically compacted)	29	7.8	PI = 23%; γ = 14.8 kN/m^3; w = 22.2% (Dhanauri clay) ; $\psi_b \approx$ 40 kPa [Satija,1978 apud Fredlund *et al.*, 1987)]
4	Glacial till (compacted clayey sandy silt)	25.5	44.4	LL = 36%; PI = 19%; γ_{dmax} = 18 kN/m^3; w_{opt} = 16%; e = 0.51 to 0.77; multistage direct shear tests; $\psi_b \approx$ 70 kPa [Gan *et al.*, 1988]
5	Clayey sand (undisturbed colluvium)	29	0	γ = 16 kN/m^3; w = 15.8%; e = 0.99; LL = 28%, PI = 12%; triaxial CD tests [Machado & Vilar, 1998]
6	Clayey sand (undisturbed colluvium)	31.2	10.5	γ = 17.1kN/m^3; w = 16.4%; e = 0.88; LL = 31%, PI = 11%; triaxial CD tests [Machado & Vilar, 1998]
7	Clayey sand (undisturbed residual soil from sand-stone)	26.4	28.3	γ = 18.8kN/m^3; w = 16.7%; e = 0.68; LL = 28%, PI = 11%; triaxial CD tests [Machado & Vilar, 1998]
8	Yellow clayey sand (undisturbed colluvium)	26.4	0	LL = 46%, PI = 23%; γ = 14.9 to 15.7 kN/m^3; w = 23.2 to 24.8%; e = 1.1 to 1.3. CD direct shear [de Campos & Carrillo, 1995]
9	Clayey sand (undisturbed mature residual soil)	28.7	13.7	LL = 51%, PI = 18%; γ = 15.6 to 17.1 kN/m^3; w = 16.4 to 17.7%; e = 0.9 to 1.1. CD direct shear [de Campos & Carrillo, 1995]
10	Expansive clayey silt (statically compacted)	21.2	35	LL = 48%; PI = 25%; γ_d = 15 kN/m^3; w = 17% [Miao *et al.* 2001]
11	Glacial till (compacted)			LL = 35.5%; PI = 18.7%; Standard Proctor δ_{max} = 18.8 kN/m^3; w_{opt} = 16.3%
	$\sigma - u_a$ = 25 kPa	23	4 to 15	Specimens with δ = 17.3 kN/m^3; w = 13%; CD direct shear [Vanapalli et al., 1996]
	$\sigma - u_a$ = 100 kPa			
	$\sigma - u_a$ = 200 kPa			
12	Decomposed fine ash tuff (silty coarse sand)	40	0	Multistage CD direct shear; samples US-5 and US-3 [Gan & Fredlund, 1996]
13	Clayey sand (undisturbed colluvium)	40	0	LL = 39%, PI = 14%; γ_d = 13.3kN/m^3 Triaxial Tests, $\sigma_3 - u_a$ = 10 kPa [Abramento & Carvalho, 1989]
14	Madrid gray clay (statically compacted)			LL = 71%, PI = 35%; Standard Proctor γ_{dmax} = 13.3kN/m^3; w_{opt} = 33.7%
	$\sigma - u_a$ = 120 kPa		74.1	
	$\sigma - u_a$ = 300 kPa		163	Specimens with γ = 13.3kN/m^3; w = 29%; CD direct shear [Escario & Saez, 1986]
	$\sigma - u_a$ = 450 kPa	25.2	229.6	
	$\sigma - u_a$ = 600 kPa		311.1	
	$\sigma - u_a$ = 750 kPa		377.8	
15	Clayey sand (colluvium, undisturbed)	25.2	5.4	γ = 16.5kN/m^3; w = 20.0%; e = 1.00; LL = 38%, PI = 14%; triaxial CD tests [Rhom & Vilar, 1995]
16	Residual soil from gneiss (Silty clayey sand, compacted)	32	10.3 (w_{opt}) 6.4 (dry)	LL = 47%, PI = 13%; Standard Proctor γ_{dmax} = 15 kN/m^3; w_{opt} = 25 % Unconfined compression tests with suction measurements (high capacity tensiometer); Specimens with γ = 15 kN/m^3; w = 25% (w_{opt}) and γ = 14.5 kN/m^3; w = 17% (dry) [Oliveira & Marinho, 2004]
17	Sandy clay (colluvium, undisturbed)	24.5	10.2	γ = 17 kN/m^3; e = 0.90-0.95; LL = 54%, PI = 26%; Direct shear tests [Soares & de Campos, 2005]

LL - liquid limit; PI - plasticity index; γ - unit weight; γ_d - dry unit weight; w-moisture content; w_{opt} - optimum moisture content; e - void ratio; CD - consolidated-drained triaxial compression test.

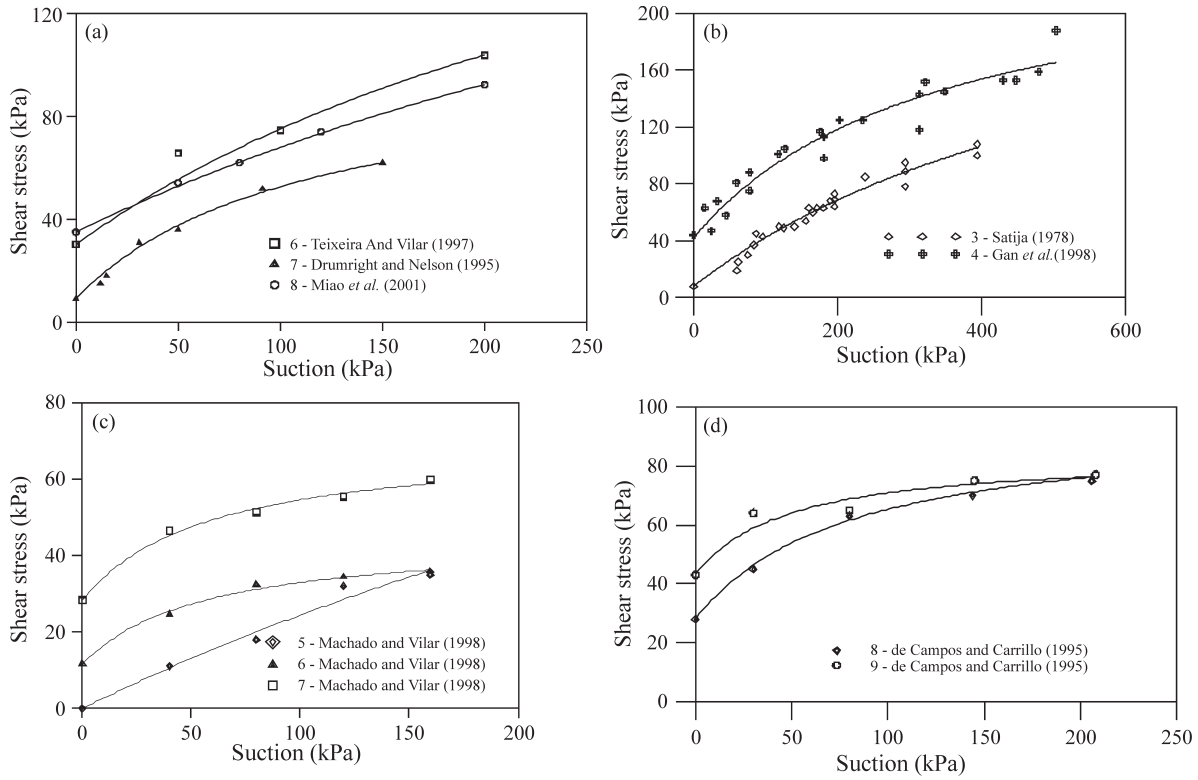

Figure 1 - Unsaturated shear strength data fitted with hyperbolic function, Eq. (6).

Table 2 - Fitting parameters of hyperbolic function applied to soils plotted in Fig. 1 and coefficient of determination (R^2).

Soil	1	2	3	4	5	6	7	8	9	10
a	1.166	1.35	2.59	1.81	3.57	1.686	1.398	1.18	1.15	2.417
b	0.0082	0.0095	0.0038	0.0047	0.0053	0.0298	0.024	0.015	0.0244	0.0055
R^2	0.98	0.99	0.96	0.94	0.99	0.98	0.99	0.99	0.93	0.99

$$b = \frac{1}{c_{ult} - c'} \tag{9}$$

Thus, if the effective shear strength parameters at saturation and the ultimate shear strength at the residual moisture content are measured, both parameters *a* and *b* can be obtained and the unsaturated shear strength can then be predicted based on the assumption that the relationship between suction and shear strength follows the general form of Eq. (6). Two alternatives of practical interest have been devised to deal with such question.

3.1. Alternative 1

As the residual water content is approached it is very difficult for liquid water to migrate. Water movement is primarily commanded by vapor flow at low flow rates and is reasonable to assume that in a specimen under these conditions the matric suction variation during shearing will not produce any significant change in mechanical properties, such as the shear strength. Since the procedure can be implemented considering only the unsaturated residual cohesion (through Eq. (9)) without reference to associated matric suction, it is proposed that testing of air dried specimens could be used to establish the residual cohesion. So a simplified testing procedure could be followed, performing, for instance, constant moisture tests drained to the air in order to approach the usual condition of drained tests and to avoid the complex procedures of suction controlled tests.

This proposition will be checked using data from Futai (2002), Reis (2004) and Escario (1988). Futai (2002) and Reis (2004) followed the previous condition of tests and performed suction controlled drained (CD) tests and constant moisture (CW) tests with air dried samples from two horizons of residual soils. Escario (1988) performed suction controlled direct shear tests up to large values of suction, probably beyond the residual suction of the soils studied, the Madrid gray clay and the Guadalix red clay.

The characteristics of these soils are presented in Table 3, together with parameters for the proposed model.

Futai (2002) tested a mature and a young residual soil from gneiss. These two materials showed angles of internal friction varying with the suction and to predict the shear strength envelope, the cohesion intercepts were directly taken from the envelopes without any arrangement regarding the variation of internal friction. The air dried samples presented a cohesion intercept of 125 kPa for the mature soil and of 77.5 kPa for the young residual soil. These values, together with the cohesion of the saturated sample allow to calculate *b* using Eq. (9) and to predict the envelope, which matches fairly well the experimental results, as shown in Figs. 3(a) and 3(b).

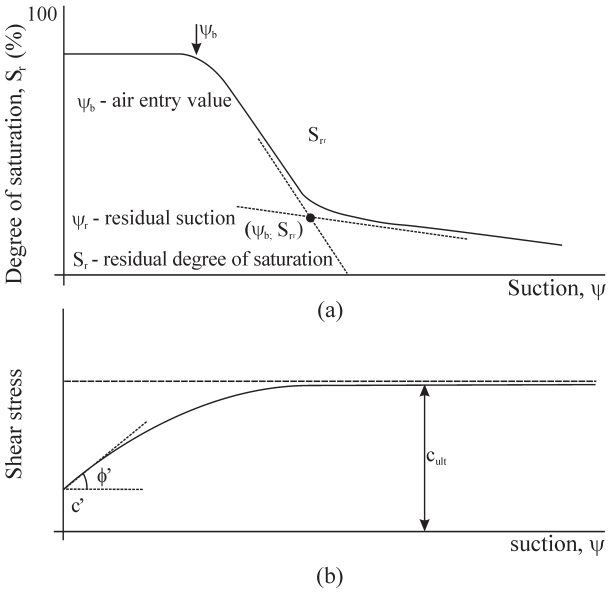

Figure 2 - (a) Soil water retention curve and typical elements; (b) Hyperbolic function and assumed conditions to derive *a* and *b* parameters.

The prevision considering the ultimate or residual strength applied to the data of Reis (2004) is shown in Fig. 4(b). In this case, the air dried samples of young residual soil presented a cohesion intercept of 115 kPa, while the mature soil showed cohesion of 215 kPa, considering an adjusted envelope with friction angle of 31°. It can be seen a good agreement between experimental and predicted data for the lower suction, but the predicted data become lower than the experimental ones for the larger suction. The deviation reaches a maximum, of about 20%, for the young soil, with calculated values lower than the measured ones. For this soil, the method was not so precise to predict the shear strength for the entire range of suction. However, it is worth to say that the method is still interesting as it is preferable a conservative than an optimistic prediction for preliminary studies.

As far as the data of Escario (1988) is concerned, Fig. 5 shows that the predicting equation nicely fits the experimental data and also confirms the good performance of the procedure. In this case, the value corresponding to the largest suction used in the tests was assumed as the value at the residual condition.

Table 3 - Characteristics of the soils tested by Futai (2002), Reis (2004) and Escario (1988).

Soil	Soil types	ϕ' (°)	*c*' (kPa)	c_{ult} (kPa)	*a*	*b*	R^2	Remarks
18	Sandy clay (undisturbed) 1 m depth	27.3°	17	125	1.94	0.0093	0.99	w_L = 57%; PI = 29%; γ = 15 kN/m^3; w = 30%; e = 1.1-1.2; triaxial CD tests [Futai, 2002]
19	Young residual soil from gneiss (undisturbed sandy silt)	26.4°	33.5	77.5	2.016	0.0227	0.99	w_L = 42%; PI = 19%; γ = 17 kN/m^3; w = 25%; e = 0.8-0.9; triaxial CD tests [Futai, 2002]
20	Young residual soil from gneiss (silty sand, undisturbed)	28°	24.0	115	1.88	0.011	0.98	w_L = 38%; PI = 15%; γ = 18 kN/m^3; w = 17.5%; e = 0.75; triaxial CD tests [Reis, 2004]
21	Mature residual soil fron gneiss (sandy silt clay, undisturbed)	31	19.2	215	1.665	0.0051	0.98	w_L = 48%; PI = 17%; γ = 17 kN/m^3; w = 26%; e = 0.9; triaxial CD tests [Reis, 2004]
22	Madrid gray clay (statically compacted)	25.2°	170	580	2.126	0.0024	0.98	LL = 71%, PI = 35%; Standard Proctor γ_{dmax} = 13.3kN/m^3; w_{ot} = 33.7% Specimens molded γ = 13.3kN/m^3; w = 29%; CD direct shear Escario (1988)
23	Guadalix de la Sierra red clay (statically compacted)	32.5°	93	650	1.570	0.018	0.98	LL = 33%, PI = 14%; Standard Proctor λ_{dmax} = 18kN/m^3; w_{ot} = 17% Specimens molded λ = 18kN/m^3; w = 13.6%; CD direct shear Escario (1988)

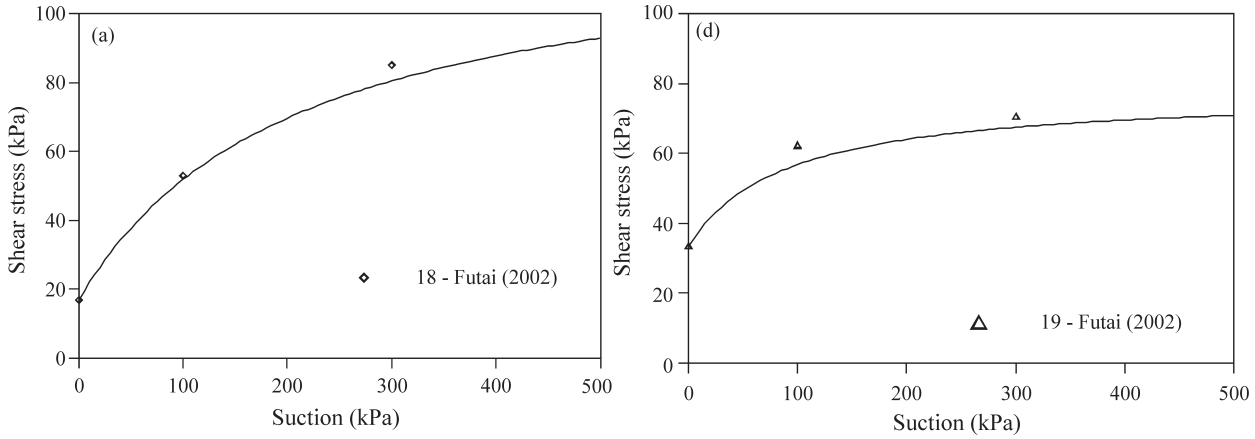

Figure 3 - Shear strength envelopes of residual soil and experimental and predicted shear strength considering results of tests with air dried samples: (a) mature soil; (b) young soil (data from Futai, 2002).

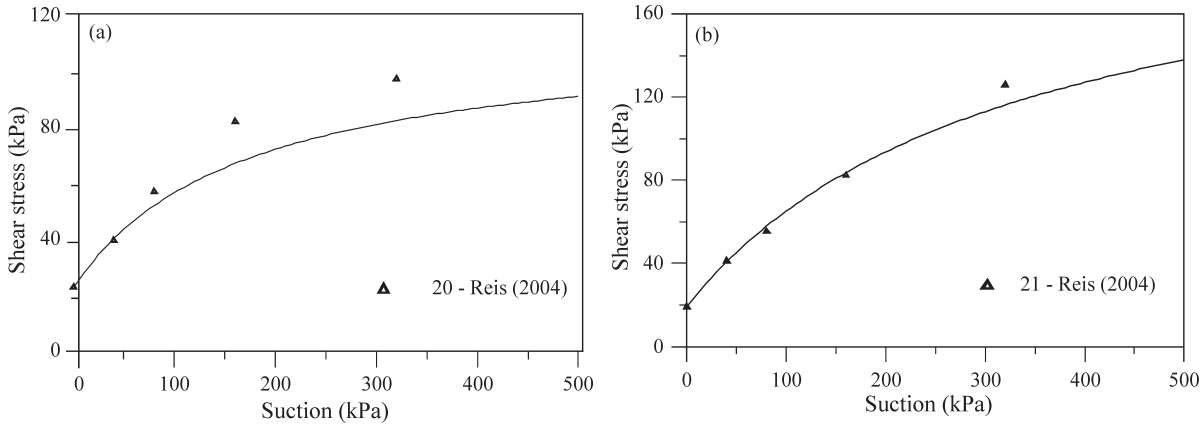

Figure 4 - Shear strength envelopes of residual soil from gneiss and experimental and predicted variation of shear strength considering results of tests with air dried samples: (a) young soil; (b) mature soil (data from Reis, 2004).

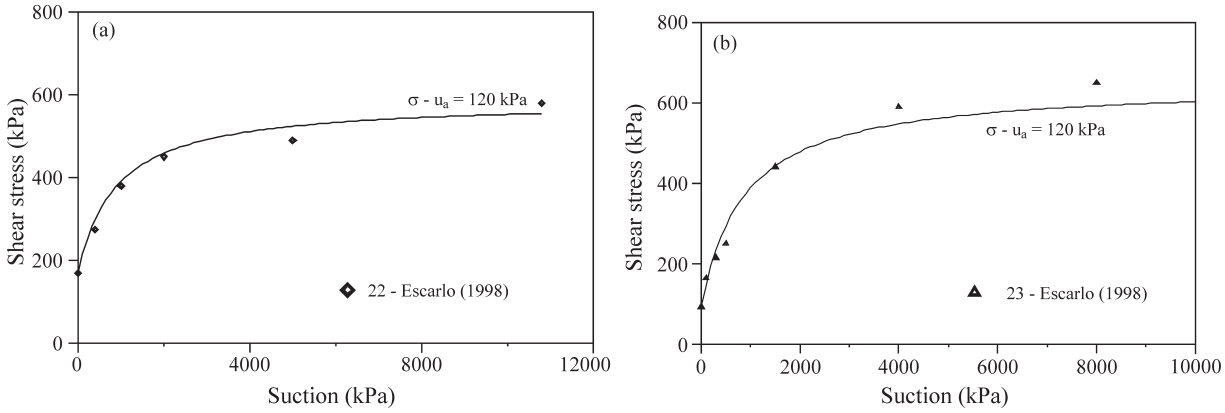

Figure 5 - Experimental and predicted shear strength envelopes considering one set of tests with dry samples. (a) Madrid gray clay. (b) Guadalix red clay (data from Escario, 1988).

3.2. Alternative 2

Most test results presented in the literature are from soils that were tested under some limited value of soil suction and still show a tendency of increase shear strength. Consequently, it is probable that the residual shear strength was not reached. This feature can be accommodated by changing the way parameter *b* is obtained. The point corresponding to the maximum test suction belongs to the curve

that represents shear strength envelope. So, calling c_m the maximum measured cohesion (or τ_m the maximum shear strength) at the maximum value of matric suction, ψ_m, it can be easily shown that

$$b = \frac{1}{c_m - c} - \frac{a}{\psi_m} \quad (10)$$

substituting for a

$$b = \frac{1}{c_m - c} - \frac{1}{\psi_m \tan\phi'} \quad (11)$$

The use of Eqs. (6), (7) and (11) will be illustrated considering the data shown in Table 1. Table 4 shows some additional data for soils listed in Table 1 along with the derived soil parameters obtained and the coefficient of determination for the experimental and predicted data.

Figure 6 shows a comparison between the predicted function and experimental results. As it can be seen, there is a good agreement between them with coefficients of determination (R^2) being larger than 0.95 for most of the data tested.

The performance of both alternatives of the proposed method was very good. Results from many types of soils and different test conditions were reproduced quite well, making the method a practical and reliable tool to calculate the shear strength of unsaturated soils. The method was kept as simple as possible and demands the use of saturated effective shear strength parameters and only one set of tests on air dried samples or at a known suction. The option of testing air dried samples can speed up the preliminary eval-

Table 4 - Parameters used to validate the alternative procedure of predicting unsaturated shear strength.

	Input parameters				Output parameters		
Soil	ϕ' (°)	c' (kPa)	c_m (kPa)	ψ_m (kPa)	a	b	R^2
1	30	30	103.8	200	1.733	0.0049	0.97
2	38.7 to 40.1	9.2	62	150	1.218	0.0108	0.99
3	29	7.8	104*	394	1.805	0.0058	0.96
4	25.5	44.4	173*	498	2.098	0.0035	0.94
5	29	0	35	160	1.805	0.0173	0.94
6	31.2	10.5	36	160	1.652	0.031	0.98
7	26.4	28.3	60	160	2.016	0.0019	0.98
8**	26.4	28	47	206	2.016	0.0115	0.96
9**	28.7	43	47	208	1.827	0.021	0.91
10	21.2	35	92.3	200	2.579	0.0045	0.99
11**							
$\sigma - u_a$ = 25 kPa		10	73			0.0112	0.97
$\sigma - u_a$ = 100 kPa	23	38	113	500	2.356	0.0086	0.99
$\sigma - u_a$ = 200 kPa		84	164			0.0078	0.90
12**							
$\sigma - u_a$ = 100 kPa	40	150	183.7	307	1.193	0.0258	0.94
$\sigma - u_a$ = 20 kPa		53	68	330		0.063	0.83
13	40	0	17.5	60	1.193	0.0373	0.89
14**							
$\sigma - u_a$ = 120 kPa		74.1	238.5			0.00396	0.99
$\sigma - u_a$ = 300 kPa		163	363			0.0029	0.99
$\sigma - u_a$ = 450 kPa	25.2	229.6	459.3	1000	2.126	0.00223	0.99
$\sigma - u_a$ = 600 kPa		311.1	555.6			0.00197	0.98
$\sigma - u_a$ = 750 kPa		377.8	651.9			0.00152	0.99
16							
wot	30.6	10.3	115	285	1.692	0.0038	0.98
dry	29.2	6.4	67.1	275	1.790	0.0094	0.98

* average value near the maximum suction.
**c' and c_m are the whole shear strength (cohesion intercept plus friction component).

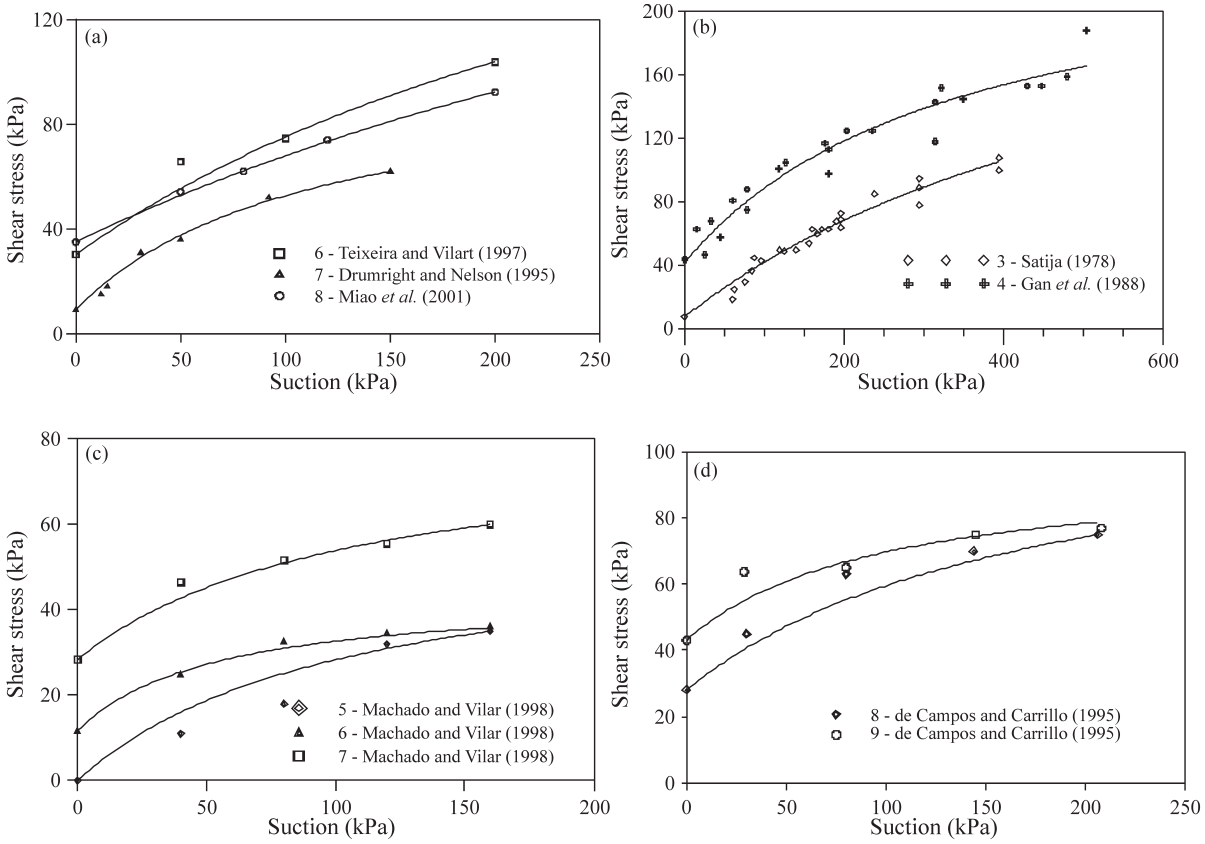

Figure 6a-d - Experimental and predicted shear strength of soils from Table 1, considering the effective shear strength parameters of saturated soil and the shear strength at the largest suction used in the tests.

uation of soil parameters and avoid the use of complex test arrangements usually demanded by tests on unsaturated soil.

3.3. Limitations of the proposed procedure

Figure 7 shows a typical set of data which shows a decrease in shear strength after a maximum. The soil is a coarse silty sand and the decrease is more noticeable for the lower net normal stress used in the tests, when the soil showed a dilating behavior. In predominantly granular soils it is expected that the main contribution to soil suction is that from capillarity as the effect of adsorptive forces will be less pronounced in these soils. So it is reasonable to admit that the effect of suction on shear strength will reach a maximum and will reduce as strain and dilation induce a perturbation on capillary meniscus, thus causing a reduction on shear strength and other mechanical properties that depend on suction.

In this case, depending on the largest value of suction used in the tests, predicted values can be lower than the measured ones. This will take place when this suction is larger than the suction related to peak value of shear strength. As the model considers that shear strength associated to the largest suction used in the tests is the maximum, the difference between measured and predicted values will increase the larger is the decrease of shear strength past a maximum. In the case of the test results of Fig. 7, the coefficient of determination is still high but one must be aware that in granular soils the model can yield conservative values.

Equation (12) can be formulated as an alternative to fit test results of soils whose shear strength rise and then fall with increasing suction.

$$c = c' + \frac{\psi}{a + b_1 \psi^{\lambda}} \qquad (12)$$

This equation needs three parameters, a, b_1 and λ. The parameter a is the same in both Eqs. (6) and (12) and can be obtained following Eq. (7). However, parameters b_1 and λ will need two additional tests at different suctions to be determined. In addition it can not be assigned to them a physical meaning as done with the a and b parameters of Eq. (6).

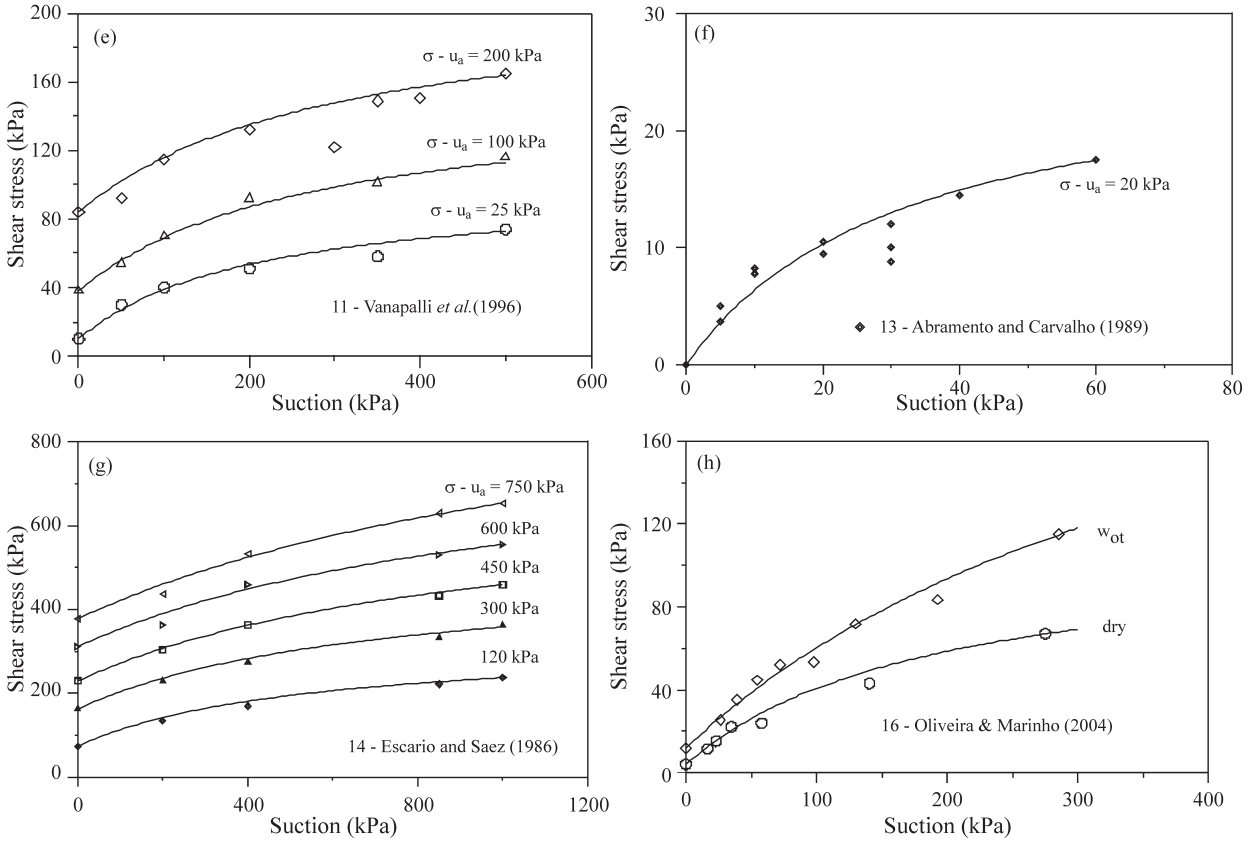

Figure 6e-h - Experimental and predicted shear strength of soils from Table 1, considering the effective shear strength parameters of saturated soil and the shear strength at the largest suction used in the tests.

Figure 7 shows the data of Gan & Fredlund (1996) fitted with Eq. (12), together with the curve yielded by Eq. (6). The adjustment of Eq. (11) to the experimental data was obtained from best fitting analysis, for parameters b_1 and λ, since parameter a is 1.913 from Eq. (7). For the test US3, the R^2 obtained was 0.96, b_1 = 0.00043 and λ = 1.83, while for the test US5, the correspondent values were 0.98; 0.002 and 1.456. It can be seen that, in these cases, Eq. (12) is able to fit experimental data fairly well, yielding best results than Eq. (4). However, it must be emphasized that the example of use of Eq. (12) rests on best fit analysis as the parameters cannot be determined following an easily and straightforward procedure as is the case of the method here proposed. So the major interest in using Eq. (12) is as a mathematical function that can be useful to fit test results from soils with a behavior similar as the one shown in Fig. 7, but not as an equation easily used in a prevision procedure.

Contrary to the available theory of unsaturated soil, some soils have shown a large increase in shear strength for low values of suction. In this range of suction, especially beneath the air entry value of the soil, it should be expected that the angle ϕ^b would reach as much as the value of ϕ', however values of ϕ^b larger than ϕ' have been reported by many authors (Rohm & Vilar, 1995; Abramento & Carvalho, 1989; Soares & de Campos, 2005). In these cases the proposed procedure will reproduce the experimental data in a conservative way or even fail. Figure 8(a) illustrates the use of the proposed method to the data of Rhom & Vilar (1995). It can be seen that for the lower net normal stress that the shear strength is underestimated as ϕ^b is larger than ϕ'. In extreme cases, such as in the soil tested by Soares &

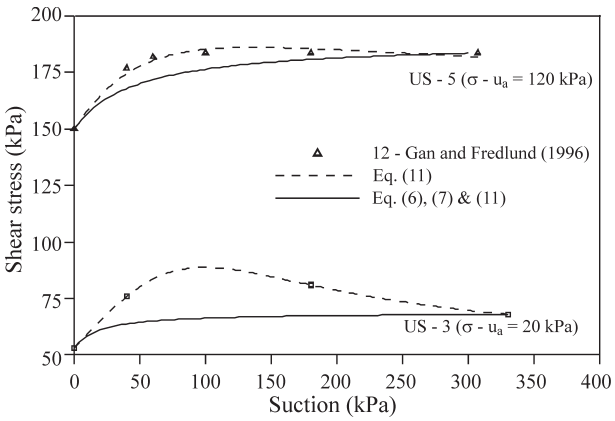

Figure 7 - Ash tuff tested by Gan & Fredlund (1996) fitted with Eq. (12) and values predicted by Eqs. (6), (7) and (11).

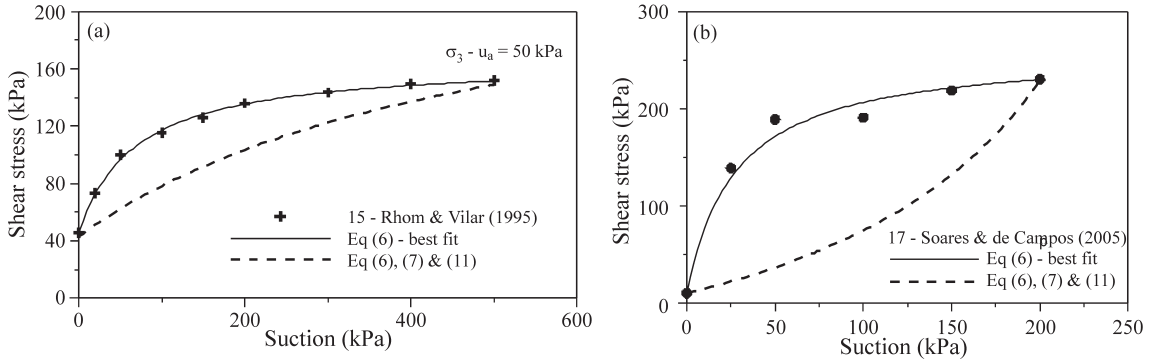

Figure 8 - Some limitations of the proposed procedure for soils that show a large increase in shear strength with suction. (a) underestimated values; (b) failure of the procedure.

de Campos (2005), the procedure will fail, as can be seen in Fig. 8(b). It is not known the mechanism that leads these soils to this behavior. In common they are of lateritic nature, their air entry value is almost zero and they reach the residual condition at relatively low values of suction. Laterites are known to harden after wetting and drying. Cut slopes in lateritic soils begin to develop a hard crust on its surface after few days of exposure in a process commanded by evaporation and silica deposition (Vilar *et al.*, 1986). Thus the development of any kind of incipient cementation during the process of suction installation (especially when the specimen is wetted and then drained) should not be excluded as one of the possible reasons that justify the behavior shown for these lateritic soils.

When applying the procedure, caution should be exercised when the product of the parameter *b* and matric suction is negligible when compared to *a* as the relationship between shear strength and suction will be almost linear and represented by

$$c = c' + \psi \tan\phi' \qquad (13)$$

Thus the prevision will yield values corresponding to the effective shear strength and in this situation the effect of matric suction will be similar to the confining effective stress.

The prevision will fail and should not be used when the value of *b* parameter, as calculated through Eq. (11), is negative as is the case of the soil of Fig. 8(b).

The adopted mathematical expression and the test results used to check the proposed method suggest that the predicted values are always underestimated. No reasons for overestimated values have been devised up to now.

The limitations noted so far and others that may arise as more data become available should be seen as a common feature of all the empirical methods.

4. Conclusion

An expedite procedure to predict the shear strength envelope of unsaturated soils was developed and tested against many soils of different origins, showing a good agreement between experimental and calculated values. The method requires effective stress parameters from saturated samples and results of only one set of tests performed on air dried specimens or, alternatively, on specimens tested under a controlled suction, larger than the maximum suction expected in the problem under analysis. The use of air dried samples may be a promising option and could replace the more sophisticated suction controlled tests, considering the good agreement between the limited test data available and the values predicted by the procedure here presented. The procedure has some limitations, as any empirical method, and is intended to be a tool to estimate the shear strength parameters of unsaturated soils for preliminary purposes, not to replace a more complete characterization of soil properties.

References

Abramento, M. & Carvalho, C.S. (1989) Geotechnical parameters for the study of natural slopes instabilization at Serra do Mar, Brazil. Proceedings of the 12th International Conference on Soil Mechanics and Foundation Engineering, Rio de Janeiro, v. 1, pp. 1599-1602 .

Bishop, A.W. (1959) The principle of effective stress. Tecknish Ukeblad, v. 106, pp. 859-863.

Bishop, A.W.; Alpan, I.; Blight, G.E. & Donald, I.B. (1960) Factors controlling the shear strength of partly saturated soils. ASCE Research Conference on Shear Strength of Cohesive Soils, Boulder, Colorado, pp. 503-532.

de Campos, T.M.P & Carrillo, C.W. (1995) Direct shear testing on an unsaturated soil from Rio de Janeiro. Proceedings of the First International Conference on Unsaturated Soils, v. 1, pp. 31-38, Balkema, Paris.

Drumright, E.E. & Nelson, J.D. (1995) The shear strength of unsaturated tailings sand. Proceedings of the First International Conference on Unsaturated Soils, Balkema, Paris, v. 1, pp. 45-50.

Edil, T.B.; Motan, S.E. & Toha, F.X. (1981) Mechanical Behavior and Testing Methods of Unsaturated Soils. Yong, R.N. & Townsend, F.C. (eds), Laboratory Shear Strength of Soil, ASTM, STP 740, pp. 114-129.

Escario, V. & Saez, J. (1986) The shear strength of partly saturated soils. Géotechnique, v. 36:3, pp. 453-456.

Escario, V. (1988) Formulae for the shear strength envelope of partially saturated soils. Ingenieria Civil - CEDEX, Report n. 68. (in Spanish).

Fredlund, D.G.; Morgenstern, N.R. & Widger, R.A. (1978) The shear strength of unsaturated soils. Canadian Geotechnical Journal, v. 15:3, pp. 313-321.

Fredlund, D.G.; Rahardjo, H. & Gan, J.K.M. (1987) Nonlinearity of strength envelope for unsaturated soils. Proceedings of the 6th International Conference on Expansive Soils, New Delhi, v. 1, pp. 49-54.

Fredlund, D.G.; Xing, A.; Fredlund, M.D. & Barbour, S.L. (1996) The relationship of the unsaturated soil shear strength to the soil-water characteristic curve. Canadian Geotechnical Journal, v. 32, pp. 440-448.

Futai, M.M. (2002) Theoretical - Experimental Study of the Behavior of Non-Saturated Tropical Soils Applied to a Gully Erosion. Doctor Thesis, COPPE, Universidade Federal do Rio de Janeiro, 559 p.

Gan, J.K.M.; Fredlund, D.G. & Rahardjo, H. (1988) Determination of the shear strength parameters of an unsaturated soil using the direct shear testing. Canadian Geotechnical Journal, v. 25, pp. 500-510.

Gan, J.K.M. & Fredlund, D.G. (1996) Shear Strength characteristics of two saprolitic soils. Canadian Geotechnical Journal, v. 33, pp. 595-609.

Hilf, J.W. (1956) An Investigation of Pore Water Pressure in Compacted Cohesive Soils. Technical Memo 654. U.S. Bureau of Reclamation, Denver.

Ho, D.Y.F. & Fredlund, D.G. (1982) A multistage triaxial test for unsaturated soils. Geotechnical Testing Journal, v. 5: pp. 18-25.

Kassif, G. & Ben Shalon, A. (1971) Experimental relationship between swell pressure and suction. Géotechnique, v. 21:3, pp. 245-255.

Khalili, N & Khabbaz, M.H. (1998) A unique relationship for c for the determination of the shear strength of unsaturated soils. Géotechnique, v. 48:5, pp. 681-687.

Machado, S.L. & Vilar, O.M. (1998) Shear strength of unsaturated soil: Lab tests and predicting equations. Solos e Rochas, v.21:2, pp. 65-78 (in Portuguese).

Miao, L.; Yin, Z. & Liu, S. (2001) Empirical function representing the shear strength of unsaturated soils. Geotechnical Testing Journal, v. 24:2, pp. 220-223.

Oberg, A. & Salfors, G. (1997) Determination of shear strength parameters of unsaturated silts and sands based on the water retention curve. Geotechnical Testing Journal, v. 20:1, pp. 40-48

Oliveira, O.M. & Marinho, F.A.M. (2004) Unsaturated shear strength behavior of a compacted residual soil. Proc. 2nd Asian Conf. on Unsaturated Soils, Osaka, Japan, pp. 237-242.

Rassam. D.W. & Cook, F. (2002) Predicting the shear strength envelope of unsaturated soils. Geotechnical Testing Journal, v. 25:2, pp. 215-220.

Reis, R.M. (2004) Stress-Strain Behaviour of Two Horizons of a Residual Sol from Gneiss. Doctor Thesis. Universidade de São Paulo, São Carlos, 190 p. (in Portuguese).

Rhom, S.A. & Vilar, O.M. (1995) Shear strength of an unsaturated sandy soil. Proceedings of the First International Conference on Unsaturated Soils, Balkema, Paris, v. 1, pp. 31-38.

Ridley, A.M. & Burland, J.B. (1995) A new instrument for the measurement of soil moisture suction. Géotechnique, v. 44:2, pp. 321-324.

Satija, B.S. (1978) Shear Behavior of Partly Saturated Soils. PhD Thesis, Indian Institute of Technology, Delhi, (apud Fredlund *et al.*, 1987).

Soares, R.M. & de Campos, T.M.P. (2005) Shear strength of a non saturated colluvial soil from Rio de Janeiro. Proc. IV Brazilian Conf. on Slope Stability, Salvador, Bahia, v. 1, pp. 165-172 (in Portuguese).

Soto, M.A. (2004) Comparison Between Methods of Imposing and Controlling Suction in Tests with Unsaturated Soils. Doctor Thesis. Escola de Engenharia de São Carlos, USP, São Carlos (in Portuguese).

Teixeira, R.S. & Vilar, O.M. (1997) Shear strength of na unsaturated compacted soil. Proceedings of the 3rd Brazilian Symposium on Unsaturated Soils, Rio de Janeiro, v. 1, pp. 161-169 (in Portuguese).

van Genutchen, M. Th. (1980) A closed-form equation for predicting the hydraulic conductivity of unsaturated soils. Soil Science Society of America Journal, v. 44, pp. 892-898.

Vanapalli, S.K.; Fredlund, D.G.; Pufahl, D.E. & Clifton, A.W. (1996) Model for the prediction of shear strength with respect to soil suction. Canadian Geotechnical Journal, v. 33, pp. 379-392.

Vilar, O.M.; Rodrigues J.E.; Bjornberg, A.J.S. & Paraguassu, A.B. (1986) The phenomenon of silicification in slopes. Proc. V Int. Congress IAEG, Buenos Aires, v. 3, pp. 931-932.

Analysis of Piles in Residual Soil from Granite Considering Residual Loads

António Viana da Fonseca, Jaime Alberto dos Santos, Elisabete Costa Esteves, Faiçal Massad

Abstract. The paper deals with the analysis of static loading tests carried out in 3 different types of piles: bored piles with temporary casing, continuous flight auger, CFA, piles (bored and CFA piles with circular section - nominal diameter Ø600 mm) and driven piles (with square section - width 350 mm). These piles were installed in the CEFEUP/ISC'2 experimental site, located in the Campus of the Faculty of Engineering of the University of Porto (Portugal), in a contact zone between the gneissic rocks and the granite mass. After a brief geological and geotechnical site characterization, the paper presents a detailed description of the piles and the instrumentation installed in two of them. Previous analyses of the test data are summed up, emphasising the difficulties in determining the residual loads resulting from the installation processes and the unloading and the reloading cycles applied to the static loading tests. This paper aims to quantify these locked-in toe residual loads, using a mathematical model - the Modified Two Straight Lines Method (MDRM) - that allows the interpretation of the pile head load-settlement curve and the determination of the shaft and toe resistances, apart from the toe residual loads. For the shaft and toe resistances, the MDRM led to consistent results with those inferred from both, the previous analysis and the extensometer measurements; the ultimate unit shaft resistance was estimated in 60 kPa. As far as the toe's residual loads are concerned, the estimated values of about 150 kN for the bored piles were also consistent with those measured but very different from that guessed in previous analysis, about 300 kN. For the driven pile, this paper arrived at an upper bound of 500 kN for the residual load and a lower bound of 60 kPa for the ultimate unit shaft resistance.

Keywords: piles, capacity, residual loads, mathematical model, saprolitic soils.

1. Introduction

In the north-western region of Portugal residual soils from granite are dominant. The thickness of these regional saprolitic soils may some times attain more than 20 m, with more common values of 5 to 10 m. The current design practice of bored and driven piles in residual weathered formations is merely semi-empirical and based on bearing capacity analysis (in general, without deformation analysis). Fully instrumented pile load tests are very much informative for the elaboration of specific correlations between load-deformation behaviour and in situ tests results, for establishing well-based design criteria.

In the Fall of 2003, the Faculty of Engineering of the University of Porto (FEUP) and the High Technical Institute of the Technical University of Lisbon (ISTUTL) invited the international geotechnical community to participate in a prediction event on pile capacity and pile load-movement response to an applied loading sequence. The event was organized by FEUP and ISTUTL in collaboration with the Portuguese Geotechnical Society, TC16 and TC18 of the ISSMGE and the organizers of the ISC'2 Conference in Porto in September 2004. A very extensive site characterization had been held, including a large variety of in situ tests in order to develop an International Prediction Event (Class A) of Bored, CFA and Driven Piles. Researchers and designers were invited to deal with this investigation results in order to predict the real response of the pile foundations. Several in-situ testing techniques were used - SPT, CPT and CPTU, PMT and DMT; Seismic: Cross-Hole (CH) and Down-Hole (DH). Undisturbed samples were recovered and an extensive laboratory-testing program was carried out: oedometric consolidation tests, CK_0D triaxial tests using local strain measuring devices and bender-extender elements, as well as resonant column tests. In December 2003, a total of 33 persons from 17 countries submitted predictions. Static loading tests were then performed. A summary of the capacity predictions and the static loading tests has been published by Santos *et al.* (2005, 2006) and a more detailed report in Viana da Fonseca & Santos (2006). This paper presents the steps involved in preparing the international pile prediction event, the analysis of the relevant test data, and the results of the predictors' efforts.

Three different kinds of piles were executed: bored piles with temporary casing, continuous flight auger, CFA, piles (bored and CFA piles with circular section - nominal diameter Ø600 mm) and driven piles (square section with 350 mm width). For the former types, a hydraulic rotary rig

António Viana da Fonseca, Associate Professor, Faculty of Engineering, University of Porto, Rua Dr. Roberto Frias, 4200-465 Porto, Portugal. e-mail: viana@fe.up.pt.
Jaime Alberto dos Santos, Assistant Professor, High Technical Institute, Technical University of Lisbon, Av. Rovisco Pais, 1049-001 Lisboa, Portugal. e-mail: jaime@civil.ist.utl.pt.
Elisabete Costa Esteves, MSc Assistant School of Engineering, Polytechnic Institute of Porto, Rua de S. Tomé, Porto. e-mail: efm@isep.ipp.pt.
Faiçal Massad, Professor, Polytechnic School, University of São Paulo, Av. Prof. Almeida Prado 271, Trav. 2, Cidade Universitária, 05508-900 São Paulo, SP, Brasil. e-mail: faical.massad@poli.usp.br.
Submitted on August 8, 2006; Final Acceptance on January 26, 2007; Discussion open until August 31, 2007.

on a base machine, allowed a temporary casing, installed by jacked and rotary crowd system, followed by a dry concretion, while, in CFA, an injection of concrete (slump of 190 mm) with a pressure of 6 MPa at the beginning, was made while pulling out the auger. The equipment used for driving the precast piles was a 40 + 10 kN hydraulic hammer, falling from about 23 cm, mounted on a base machine.

Although the results of these tests have already been analysed elsewhere (Viana da Fonseca *et al.*, 2004, 2006, Santos *et al.*, 2005, 2006, Costa Esteves, 2005; Fellenius *et al.*, 2007), in this paper a different approach is described taking into account the residual loads resulting from the installation process and loading cycles.

This work aims to quantify these toe residual loads, using a mathematical model developed from the Cambefort's Laws, and considering piles compressibility (Baguelin & Venon, 1972) and the residual loads and the inversion of the balanced negative shaft load (Massad, 1992, 1995). Based on this model, methods of analysis of the pile head load-settlement curve were developed allowing the identification of the shaft and base resistances, apart from the toe residual loads.

2. Site Characterization

As described elsewhere (Viana da Fonseca *et al.*, 2004, 2005, 2006, detail diverse aspects of this rich and specific profile), the CEFEUP/ISC'2 experimental site is located in a contact zone between the gneissic rocks and the granite mass. The type of regional transition between the two bodies is not a single discontinuity surface but a gradual one, consisting of an eastward "probabilistic" decreasing of feldspar bands maintaining the geological planar anisotropy, with constant strike and dip, but with frequent zones of abrupt lithologic changes. The weathering process tends to transform the feldspar into kaolin mainly in the geological contact zones where namely later fluid weathering action was more intense. Typical Porto granite is a leucocratic alkaline rock, medium to coarse grained, with mega-crystals of feldspars and two micas.

A detailed experimental work was carried out in order to characterize the extent of the weathered profile. The tests layout is presented in Fig. 1 (Viana da Fonseca *et al.* 2004).

Apart from the natural spatial variability of the structure and fabric of these residual soils due to some preserved relic heritage, there is evidence of a fairly homogeneous pattern of ground profile in geotechnical terms, as demonstrated by the results obtained with continuous sampling taken from drilling, with the SPT sampler and from high quality samplers. The former are shown in Fig. 2. Their description is presented schematically in this figure, including photos of samples obtained from borehole S3.

The first stage of the site characterization included 4 SPT, 5 CPTU, 5 DMT, 3 PMT and several CH, DH, SASW and CSWS, while in the second stage 4 CPTU and 4 DMT were performed. The technical data of the first stage of in

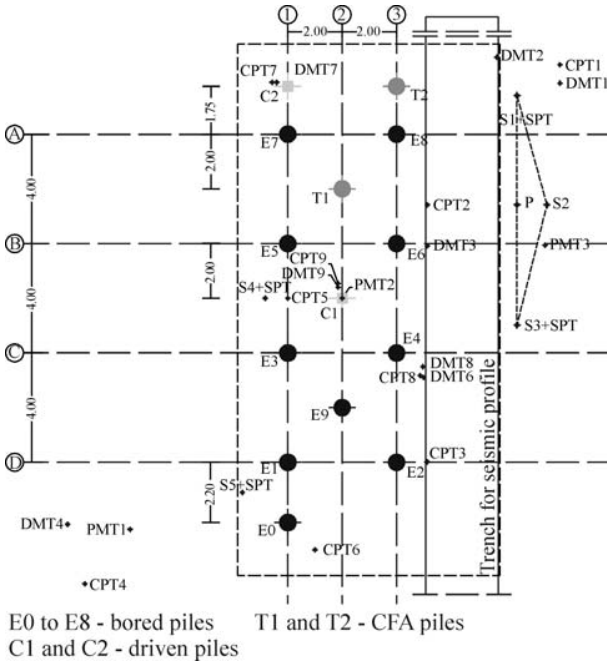

Figure 1 - Layout of the site characterization activities (including location of the piles).

situ tests is summarized in Fig. 2 (above) as well as in the forecoming Fig. 3. Other results can be found in Viana da Fonseca *et al.* (2006).

The results of grain size analyses show that both clay and silt particles decrease with increasing depth, whereas sand particles increases with depth. Kaolinite is the main mineral in the clay fraction (details in Viana da Fonseca *et al.*, 2006).

Undisturbed samples were carefully taken from the experimental site, in boreholes at specific depths, using high quality piston samplers - Shelby, Mazier and T6S-Triplex (Viana da Fonseca & Ferreira, 2002). The laboratory tests conducted in the first phase of the programme, comprised 6 CK0D triaxial - 4 in compression with bender element (BE) readings and 2 in extension - with local strain measurements, 2 resonant column tests (RC), and 1 oedometer test. A general overview of the obtained results is presented in Viana da Fonseca *et al.* (2006).

A first insight to these tests results, pointed out the following strength parameters: $\phi' = 45.8°$; $c' = 4.5$ kPa. At rest coefficient K_0 was taken as 0.50. Regional experience indicates even lower values (Viana da Fonseca & Almeida and Sousa, 2001, Viana da Fonseca, 2003).

3. Piles Description

3.1. Types of installed piles

In the experimental site, 3 different kinds of piles were executed: 600 mm O.D. diameter bored piles ("E"-piles) installed using a temporary casing, 600 mm O.D. diameter augered (CFA) piles ("T"-piles) and 350 mm diam-

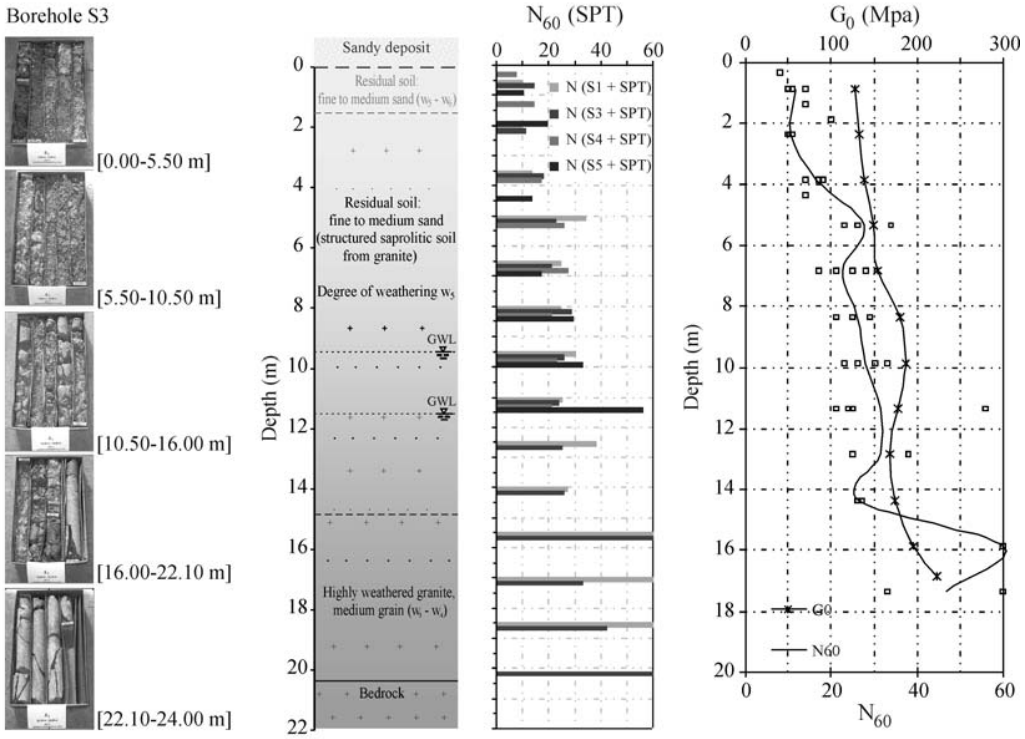

Figure 2 - Geotechnical profile with photos taken from samples obtained in borehole S3; N_{60} results in depth with average shear modulus G_0 from CH shear waves, across two different sections: S2-S1 & S3-S2.

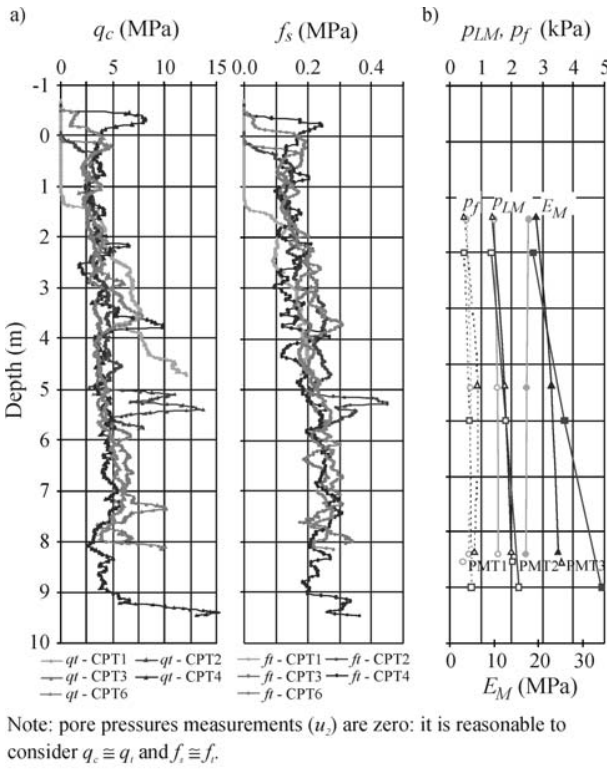

Note: pore pressures measurements (u_2) are zero: it is reasonable to consider $q_c \cong q_t$ and $f_s \cong f_t$.

Figure 3 - *In-situ* tests profile: a) CPTU: q_c and f_s; b) PMT: p_f, p_{LM} and E_M.

eter square, driven, precast concrete piles ("C"-piles). For the former types, a hydraulic rotary rig on a base machine, allowed a temporary casing, installed by jacked and rotary crowd system, followed by a dry concretion, while, in CFA, an injection of concrete (slump of 190 mm) with a pressure of 6 MPa at the beginning was made while pulling out the auger. The equipment used for driving the precast piles was a 40 + 10 kN hydraulic hammer, falling from about 23 cm, mounted on a base machine. These 3 different types of piles were loaded axially side by side up to failure (piles E9-bored, T1-CFA and C1-driven). The location of the piles is represented in the layout map (Fig. 1).

The C-piles, were driven on September 17, 2003 with a 40 kN drop hammer. In January 2004, Pile C1 was subjected to a static loading test (Fig. 4).

The E-piles, namely the one denoted by E9, were constructed in August 2003 by first using a rotary drilling rig to install a temporary casing that was cleaned out using a 500 mm cleaning bucket (Fig. 5). The external diameter of the cutting teeth at bottom of the temporary casing was 620 mm. The concrete was placed by using a drop chute in the water-filled casing. Concrete slump was 180 mm and concrete "over-consumption" was below 10%. The casing was withdrawn on completion of the concreting. In January 2004, Pile E9 was subjected to a static loading test.

The T-piles, namely the one denoted by T1, were constructed in August 2003 using a rotary drilling rig and a 600 mm continuous flight auger with a 125 mm I.D. stem.

Figure 4 - Sequence of the execution tasks for the precast concrete driven piles.

Figure 5 - Sequence of the execution tasks for the bored piles with temporary casing.

The maximum torque of the rotary head was 120 kNm and the pull-down force was 45 kN. The auger penetration rate was approximately 25 mm/s. The concrete grout was ejected with a 6 MPa pressure at the beginning of the grout line and a steady concrete flow of 700 L/min (Fig. 6). Concrete slump was 190 mm and concrete "over-consumption" was 6%. In January 2004, Pile T1 was subjected to a static loading test.

3.2. The static pile load tests (SPLT) - Instrumentation

The 3 different kinds of piles were loaded axially by static test in utmost similar ground conditions since they were conducted in close proximity. The location of the piles was shown in Fig. 1 and the layout of the testing area is disposed in Fig. 7, together with photos of the testing assembling. Information about the piles were provided to the predictors as:

- 10 bored piles (E0 to E9, with a circular section of 600 mm in diameter). The drilling equipment was a Soilmec R-620 hydraulic rotary rig mounted on a Caterpillar 3.30C base machine; temporary casing installed by jacking and rotating crowd system;
- 2 CFA piles (T1 and T2, with a circular section, 600 mm in diameter). The drilling equipment: was a Soilmec R412 HD rotary drilling rig;
- 2 driven piles (C1 and C2, square section with 350 mm width). The drilling equipment was a Banut 40 + 10 kN hydraulic hammer mounted on an Akerman H14B base machine.

The bored piles E1 to E8 piles with 22 m of embedded length were built for reaction purposes. All the others are short piles with 6 m of embedded length.

The static pile load tests (SPLT) were performed following the recommendations of ERTC3-ISSMGE (De Cock *et al.*, 2003) and ASTM Dl 143-81. For each loading

Figure 6 - Sequence of the execution tasks for the CFA piles.

Figure 7 - a) Layout of the experimental site; pile tests: b) driven pile (C1); c) bored pile (E9); d) CFA pile (T1).

stage the load was maintained until the displacement rate became less than 0.3 mm/h, with a minimum of 0.5 h and a maximum of 2 h.

Each of Piles E9 and T1 was instrumented with six retrievable Geokon extensometer Model A9 anchors, placed in a PVC pipe centrically cast in the pile at 1,020 mm spacing with the first anchor 150 mm below the pile head. The lowest anchor was 750 mm above the pile toe. The positions of the extensometer anchors in Piles E9 and T1 are shown in Fig. 8. In pile T1 there is similar pattern.

The instrumentation provides the change of length (shortening) between each anchor and the lowest anchor (Anchor #6) as induced by the load applied in the static loading test. A shortening between anchor points divided by the length between the points corresponds to the average strain over that distance. The use of retrievable extensometer instrumentation does not allow residual loads to be measured; these may assume substantial values in driven piles, but also non-negligible levels in cast-in-situ piles (Fellenius 2002a, 2002b).

In addition to the anchors, a 350 mm diameter flat-jack load cell was placed between two 25 mm thick, 450 mm diameter steel plates in Pile E9. The load cell was connected to the bottom of the rebar cage and lowered with the cage into the pile before grouting. The operating pressure range of the load cell ranged from zero through 20 MPa (Fellenius *et al.*, 2007). The cell pressure measured in the static loading test multiplied with the pile cross sectional area was assumed to correspond to the portion of applied load reaching the pile toe. However, after the loading tests had been completed, the piles were extracted and inspected and the following was detected: while the pile surfaces were smooth and measurements of the actual diameter of Pile E9 showed it to range from 611 mm through 605 mm, *i.e.*, only marginally larger than the nominal 600 mm diameter, the measurement of the diameter at the pile toe show that, starting at about 0.5 m above the pile toe, the diameter had reduced conically toward the toe to a value of about 525 mm. Figure 9 shows a photo of the extracted pile and load cell.

The validity of the assumed conversion from cell pressure to load is questionable. It is likely that the stress in the donut-shaped concrete zone outside the load-cell will experience a stress that is different to that of the pressure inside the load cell, and, therefore, the pile toe load determined from the load-cell pressure would be under- or over-estimating the load at the pile toe to variable and unknown degree in the test. Confirming the mentioned uncertainty with the toe loads determined from the toe-cell pressure, the loads in Pile E9 determined from the strain measurements in the pile are not in perfect agreement with the toe-cell values by any assumed pile diameter. This is debated in the analyses presented in what follows.

3.3. Structural materials (reinforced concrete) properties

The prediction of the behaviour of the piles subjected to compression loads is conditioned by the pile structural

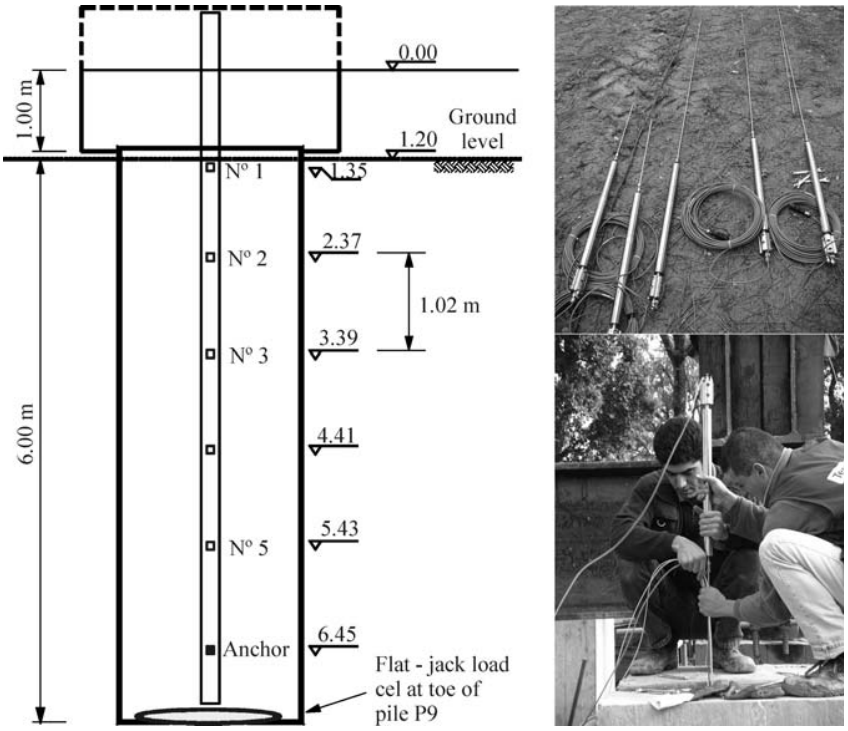

Figure 8 - Positions and illustration of extensometers anchors in Pile E9 and load cell (Fellenius *et al.* 2007).

Figure 9 - Photo of Pile E9 after extraction with detail of the pile toe and load cell after it was removed from pile (Costa Esteves, 2005).

material - reinforced concrete. This has leaded to a careful evaluation of the mechanical properties (with emphasis to the Young's modulus) of the reinforced concrete, differently manufactured and disposed in the three classes of piles. While the reinforcing steel is - for its industrial reproducibility - very much stable in its properties, the concrete is not. This is obviously associated to its variable composition in manufacturing and the moulding process and the ambient conditions during the execution of piles.

For this reason, while the properties of the precast concrete (for the driven piles) were faithfully accepted (see Table 1 in paragraph 6.1), in the bored and augered piles this has demanded some steps and constitutive evaluations, as described in what follows.

Several cubic specimens, taken for the occasion of the placement of the concrete, were tested by standard processes and the "characteristic" compression strength was calculated by usual processes, taking into account the necessary statistic coefficients. The values obtained for each group of piles for this average resistance (deduced from the characteristic) were 35,7 MPa, for the bored, and 49 MPa, for the augered. This has allowed for a first determination of the Young modulus, by applying correlative equations proposed by the European codes. Values obtained for the three classes were 30.8, 36.1 and 36.3 GPa, for the bored, augered and driven piles, respectively.

In doubt with this indirect evaluation of the modulus, taken from the correlation with the compression strength, compression tests with local and precise instrumentation were executed with rotary cored specimens, taken from the tested piles, and different values were attained, especially for the bored and augered piles: 20.0 GPa and 39.2 GPa, respectively.

This was at first time surprising, mostly because of the very much lower value obtained from these thorough and rigorous tests in the bored piles. It should, however, be denoted that there is a singular pattern of the stress-strain response, which reveals a lower stiffness in the low levels of induced stress that is attributed to the poorer quality of the "concrete was placed by using a drop chute in the water-filled casing", in the "E-piles". This is not observed in the "grout concrete that was ejected with high pressure" in the "T-Piles". This concrete is, by being prepared with better aggregates and a chemical additive for decreasing its viscosity, composed with a smaller percentage of water, which endows a smaller void ratio, resulting in a more stable and dense micro-structure. On the other side, the less controlled concrete and the eventual air-inducting deposition method on the bored piles, has created a softer material, which may be also more sensible to the less effective curing conditions in the most superficial layers, in a warm climate.

Weaker concretes are also more sensible to the time factors (creep) than the high quality ones. Being the static pile test loading steps sustained for a relevant period (between 1/2 to 2 h), they are very different of the transient condition of the coring specimens tested in laboratory, tested in very rapid cycles. This has been proved in creeping tests over different classes of concretes.

For all what has been said, the surprising differences in the Young modulus between the bored and augered piles can be justified. In the back-analysis made with the extensometer measurements this may - and will - be expressed.

4. Results of the Static Pile Load Tests (SPLT)

Pile C1 was loaded in increments of 130 kN with two early unloading cycles. When a total load of 1,300 kN had been reached at a pile head movement of 4.9 mm, the pile movement increased progressively (Fig. 10). A maximum

load of 1,500 kN was reached at a total movement of 50 mm, beyond which the movement continued for a slightly decreasing load.

Piles E9 and T1 were loaded in increments of 150 kN. The loading sequence was in cycles to 300 kN followed by unloading, to 600 kN followed by unloading, and to 900 kN followed by unloading, whereafter the piles were loaded to maximum loads of 1,350 kN and 1,200 kN, respectively (Fig. 10). For both Piles E9 and T1, the movement at 1,200 kN applied load was 100 mm, *i.e.*, 17% of the pile head diameter.

This driven pile C1, although having a smaller cross-section (43.3% of the others) has shown a stiffer response than piles E9 and T1. This is a clear indication that the installation effects play a crucial role in pile behaviour. In this case, the pile driving process may have induced a significant increase of the horizontal stresses in the surrounding soil, as well as some densification. For piles E9 and T1, the ultimate resistance cannot be clearly defined - Fig. 10.

The ultimate pile capacity for the driven pile C1 was reached for a relative settlement of about 10%. This value seems to be in good agreement with recent studies in centrifuge tests with displacement piles in sands (Fioravante *et al.*, 1995).

On the other hand, for the "non-displacement" piles E9 and T1, even for a relative settlement of about 25%, the ultimate resistance was not reached.

The five extensometers measuring shortenings over the 1,020 mm distance allowed the determination of the pile stiffness ES (Fellenius *et al.*, 2007). This was performed by means of the tangent modulus approach (Fellenius 1989, 2001). Values of 20 GPa and 40 GPa - almost equal to those deferred from the compression tests on rotary cored specimens (see above) - were obtained under the assumption that the pile diameter is equal to the nominal 600 mm value. These figures are in close agreement with the results obtained in the tests over the concrete samples, as described above.

Figures 11 and 12 shows the evolution of the load distribution for shaft and base components obtained from the extensometers during the 5th cycle of the static loading tests on piles E9 and T1. The measurements were extrapolated (dashed lines) to estimate the base load. It is clear from this

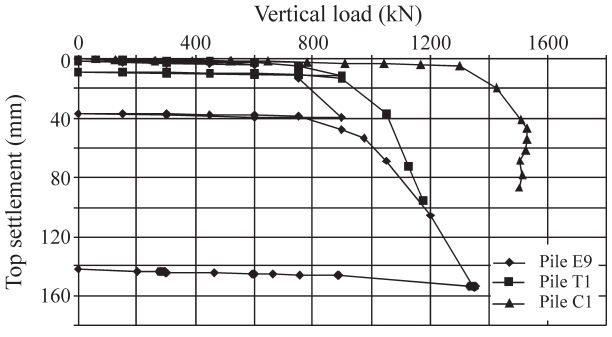

Figure 10 - Load-settlement curves from static load test.

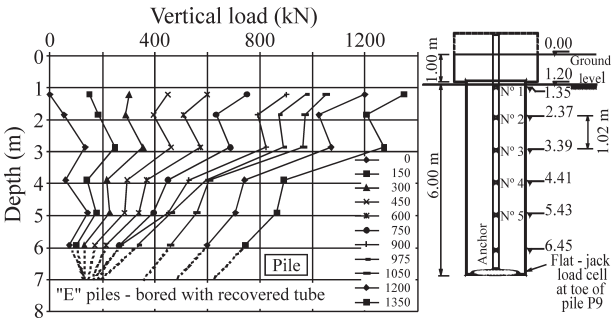

Figure 11 - Load distribution - measured in the 5th cycle of loading.

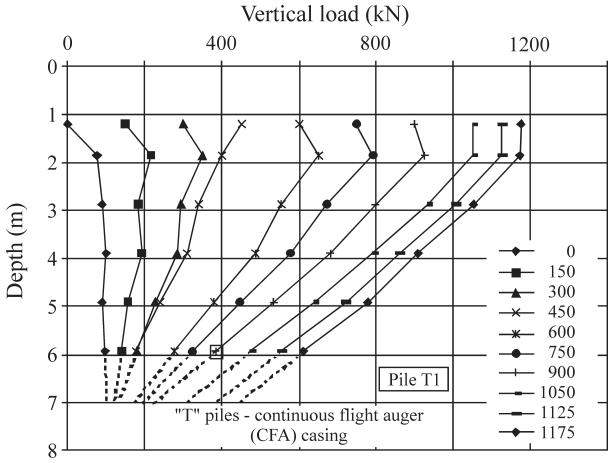

Figure 12 - Load distribution - measured in the 5th cycle of loading.

figure the progressive increase of the base resistance. For the last stages the load increments at the top and at the base are almost equal. It can be concluded that while the ultimate shaft resistance was reached, the base resistance was not fully mobilised. It is also noticeable the presence of residual loads in the beginning of the loading.

Another interesting analysis, as referred above, was the comparative evaluation of the performance of the load cell installed in the bored pile (E9), by taking an area correction or not, and the one deduce from the extensometers. This is relevant as the pile toe of extracted Pile E9 show that, starting at about 0.5 m above the pile toe, the diameter had reduced conically toward the toe to a value of about 525 mm (Fig. 13 includes also a photo of the extracted pile and load cell).

As it is clear from the picture, the correction of the area is essential for the adjustment (mainly at higher loads), taking the values derived from the extensometers to converge to the values of the corrected cell area.

5. Summary of Previous Analysis of the Results of the SPLT

As stated in a previous publication dealing with these results (Fellenius *et al.*, 2007), analysis of pile response to

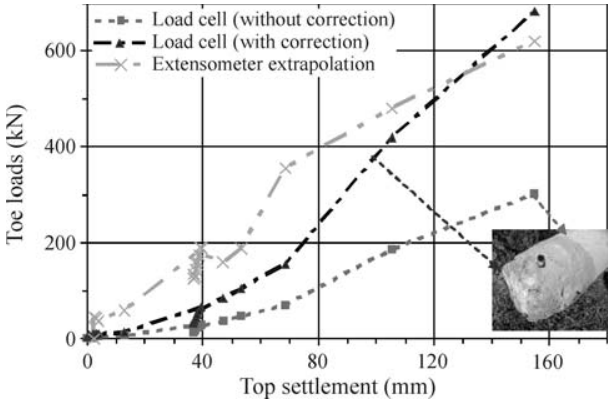

Figure 13 - Comparison of the values of the load transmitted to toe in pile E9, deduced form the load cell without and with area correction and measures from the extensometers.

load may be made from diverse of data input, namely from in situ tests, such as Standard Penetration Test (SPT), Pressuremeter Tests (PMT), Dilatometer Tests (DMT), and Cone Penetrometer Tests (CPT and CPTU). Analysis based on soil parameters determined in laboratory tests rely on simple total stress (alpha) or effective stress (beta) methods, or on more or less sophisticated numerical - finite element - methods. Most of these analyses give unreliable predictions of pile response, as it was proved by the results of ISC'2 International Pile Prediction Event in residual soil from granite (Santos *et al.*, 2005; Viana da Fonseca & Santos, 2007), this may only overcome by through calibrating of these methods from results of full-scale tests in specific geoenvironments.

Fellenius *et al.* (2007) emphasized the inadaptability of an analysis based on alpha method in these granular residual soils, being the beta-method the only adapted to their well-drained conditions. In that paper, preference was given to analysis based on CPTU data, for its continuous and representative scanning of the site spatial variations. The distinction between CPT and CPTU data is that the later includes the area correction of the cone tip resistence, q_c, for the pore pressure, U2. The Dutch method (DeRuiter & Beringen, 1979), the method of Schmertmann (1978), the LCPC method (Bustamante & Gianeselli, 1982) as quoted by the CFEM 1992, the method of Meyerhof (1976), limited to piles in sands, and the method of Tumay & Fakhroo (1981), limited to piles in clay, require input of soil type, but differentiating two soil types, "clays" and "sands". The Eslami-Fellenius method - "E-F CPTU method" - (Eslami 1996, Eslami & Fellenius 1997) differentiates in more diverse types the soil geomechanical behaviour (as calibrated by the authors), from the CPT/CPTU results, generating six soil main classes, with some intermediate materials (CFEM, 1992).

Fellenius *et al.* (2007) simulated the evolution of the load distribution in the static load test obtained in the bored pile (E9), by assuming that the base resistance would be equal to the value measured at the load cell placed at the pile toe, corrected by the ratio of areas of the cell and the 525 mm diameter pile toe as measured after excavation and extraction. It is possible, however, that the stress in the donut-shaped concrete zone outside the load-cell area may experience a stress concentration that is different from the pressure monitored by the load cell. Therefore, the "net" pile toe load derived from the load-cell pressure could be under- or overestimated by unknown degree. Moreover, the area to be used may be different during the test, from the very early stages to "ultimate" load.

From some of the previous analysis of this study, reported in Santos *et al.* (2005) and Fellenius *et al.* (2007), the following conclusions were extracted:

• extensometer measurements available in Piles E9 and T1 allowed for a very reliable estimation of load distribution ("transfer") indicating values of shaft and toe resistances, for 1,200 kN/100 mm movement, of 1,000 kN and 200 kN, and 800 kN and 400 kN, respectively, however, the piles were expected to have some residual loads, locked-in before the static loading test, as consequence of the installation process, with an unknown magnitude, since it was not determined before (the adopted monitoring system and process was not prepared to register these loads); reasonable trial-and-error analysis of the data (as expressed by Fellenius *et al.*, 2007) indicated the presence of residual loads and estimated their values; however overestimating the shaft resistance by 300 kN and consequent underestimation the toe resistance by the same amount; in fact, effective stress analysis of the data, adjusted to these residual loads correlates to a constant beta-coefficient value of 1.0 and a toe coefficient equal of 16; this toe coefficient is not in balance with the beta-coefficient, being this attributed to disturbance of the soil at the toe during the construction process;

• a back-analysis of the loading test on Pile C1 using the same 0.1 value for beta-coefficient, as that derived from the load (transfer) distribution of Piles E9 and T1, indicates total shaft and toe resistances of 520 kN and 980 kN, respectively; this toe resistance corresponds to a toe coefficient of 70, which is in balance with the beta-coefficient of 1.0;

• the compilation of submitted predictions (Santos *et al.*, 2005; Viana da Fonseca & Santos, 2007) indicates that most predictors overestimated the bored pile capacities, mostly due to an overestimation of the toe resistances, which is also expressed in the presence of residual (locked-in) loads.

6. New Analysis of the SPLT Results

6.1. Mathematical model

A new analysis was carried out with the purpose of having a more fundament evaluation of the residual loads and, consequently, the load distribution in ultimate shaft re-

sistance (A_{lr}) and tip resistance (Q_{pr}), namely for 100 mm top settlement. This was possible by applying a mathematical model that allows a back analysis of the top load-settlement curve.

A model to predict single pile performance under vertical loading was proposed by Massad (1995), which includes many aspects of load transfer phenomena, considered previously by Baguelin & Venon (1972), like pile compressibility and progressive failure. In addtion, it takes into account the eventual presence of residual stresses due to driving or subsequent cycling loadings. The solutions are analytical, in closed form, and were derived using load transfer functions based on Cambefort's Laws, accounting for the current knowledge of the shaft and tip displacements, needed to mobilize the full resistances. They may be applied to bored, jacked or driven piles subjected to a preliminary monotonic loading and/or subsequent loading-unloading cycles. The soil is supposed to be homogeneous with depth, along the entire pile shaft.

A coefficient (*k*) that measures the relative stiffness of the pile-soil (shaft) system was introduced and defined as follows:

$$k = \frac{A_{lr}}{K_r y_1} = 4\left(\frac{h}{D}\right)^2 \frac{BD}{E} \qquad (1\text{-a})$$

with

$$K_r = \frac{ES}{h} \qquad (1\text{-b})$$

where A_{lr} is the ultimate shaft load; y_1, the pile displacement (of a few millimeters), required to mobilize full shaft resistance (see Fig. 14); *D* and *h* are the diameter and height (or embedment in the soil) of the pile; B is a Cambefort parameter (see Fig.14); K_r is the pile stiffness; *E*, the modulus of elasticity of the pile material, and, *S*, its cross sectional area. For homogeneous soils, the coefficient *k* is equal to the term $(\mu h)^2$ of Randolph & Wroth model (1978). The last member of Eq. (1-a) is valid for massive piles (see the list of symbols at the end of the paper).

The model gives a further insight on pile behaviour and led to a new pile classification, with respect to *k* values: "short" or rigid ($k \leq 2$); intermediate ($2 \leq k \leq 8$); and "long" or compressible ($k \geq 8$).

The residual stresses can be dealt with a magnifier factor (μ):

$$\mu = 1 + \frac{P_h}{A_{lr}} \qquad (2)$$

where P_h is the residual toe load, which is in equilibrium with the residual negative shaft resistance, assumed to vary linearly with depth. Note that P_h may be treated as an increment to the shaft load: in fact, from Eq. (2) it follows $\mu.A_{lr} = A_{lr} + P_h$. In other words, A_{lr} is magnified by a factor given by μ. One advantage of using μ is that it allows taking the residual loads as shaft loads in the model.

For a first loading of a "purely" bored pile, $P_h = 0$, then $\mu = 1$. Otherwise, as $P_h \leq A_{lr}$, then $\mu \leq 2$. For floating piles, $\mu < 2$. In general, this factor, that is greater than 1, is upper bounded by the smaller value between 2 and $(1 + Q_{pr}/A_{lr})$, where $Q_{pr} = R_p.S$ is the toe load at failure (see also Fig. 15). Note that the maximum and the residual unit shaft resistances (f_u and f_{res}) are supposed to be constant along the pile. Massad (1992 and 1995) showed that it is possible to obtain μ by applying the model to the rebound curve of a pile load test.

a) General equations

For the simpler case of the toe reacting with $A = 0$, that is, with an elastic-plastic behaviour (Fig. 15), the load (P_o)-settlement (y_o) curve at pile top may be expressed by the following equations (details in Massad, 1995):

$$P_o = \mu\, A_{lr} \frac{\beta'_3}{z} \frac{y_o}{\mu\, y_1} \qquad (3)$$

$$\frac{y_o}{\mu\, y_1} = \left(1 - \frac{\beta'^2}{2}\right) + \frac{k}{2}\left(\frac{P_o}{\mu\, A_{lr}}\right)^2 \qquad (4)$$

$$\frac{P_o - \mu\, A_{lr}}{y_o - \dfrac{\mu\, A_{lr}}{2K_r}} = \frac{1}{\dfrac{1}{RS} + \dfrac{1}{K_r}} \qquad (5)$$

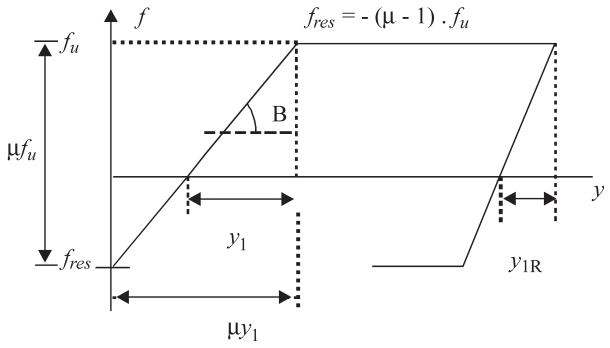

Figure 14 - Modified first Cambefort's Law.

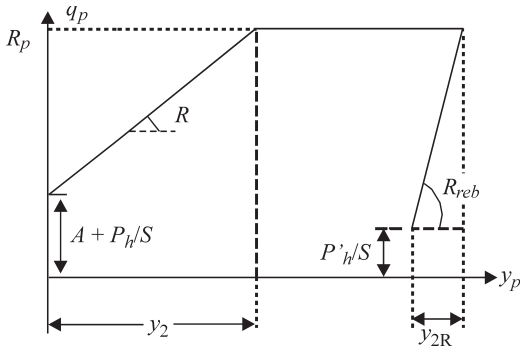

Figure 15 - Modified second Cambefort's Law.

Reporting to Fig. 16, Eqs. (3), (4) and (5) hold true, respectively, between points 0 and 3 (pseudo elastic range); 3 and 4 (progressive mobilization of shaft resistance, from top to bottom); and 4 and 5 (free development of toe resistance). Point 5 is not necessarily associated to the failure load.

The coefficient β' of Eq. (4) depends on the characteristics of the soil-pile system. For compressible piles ("long piles") β' ≅ 1 and the range 3-4 turns parabolic.

For very rigid piles, this range vanishes, that is, points (3) and (4) almost coincide (Fig. 17). The other terms of Eqs. (3), (4) and (5) are defined as:

$$\beta'_3 = \frac{\tanh(z)+\lambda}{1+\lambda\,\tanh(z)},\ \text{with}\ z=\sqrt{k}\ \text{and}\ \lambda=\frac{RS\,/\,K_r}{z} \qquad (6)$$

where λ is the relative stiffness of the pile-soil (shaft and toe) system (Massad, 1995). Using the same notations of Randolph & Wroth (1978), it is possible to rewrite λ as follows:

$$\lambda=\frac{2\,D\,G_l}{(1-\nu)\eta}\,\frac{1}{K_r}\,\frac{1}{\mu\,h} \qquad (7)$$

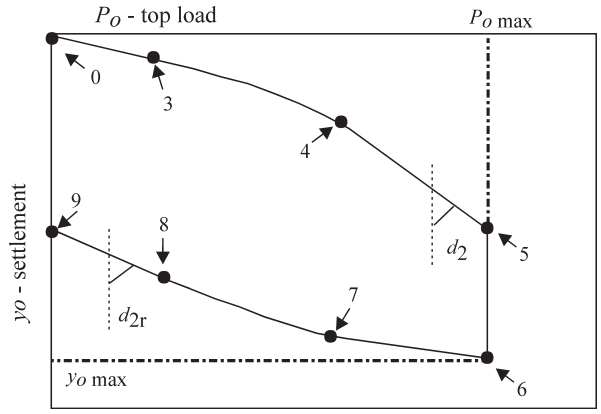

Figure 16 - Theoretical load-settlement curve of pile head for $A = 0$.

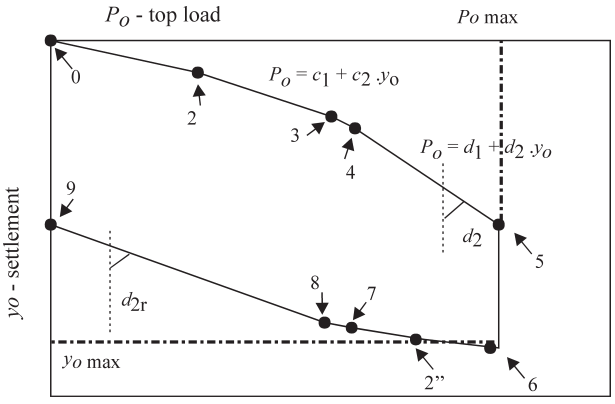

Figure 17 - Theoretical load-settlement curve of pile head for $A \neq 0$ - short piles.

where G_l is the small strain shear modulus of the soil at the pile base level; η is a correction factor to allow for the pile base depth effects and $\mu h = z = \sqrt{k}$. Here, the symbol "μ" has another meaning and must be distinguished from the magnifier factor given by Eq. (2).

Equations (3), (4) and (5) also apply to the unloading ranges 6-7, 7-8, and 8-9 (Figs. 16 or 17): it is sufficient to use the appropriate Cambefort's parameters for rebound, as shown in Figs. 1 and 2; moreover, if the loading stage ends further to point 4 (full mobilization of shaft resistance), μ = 2 at $P_o = P_{omax}$ (see Massad, 1995) and Eqs. (3), (4) and (5) become:

$$P_{o\,\max} - P_o = 2A_{lr}\,\frac{\beta'_3}{z}\,\frac{y_o}{2y_1} \qquad (8)$$

$$\frac{y_{o\,\max}-y_o}{2y_1}=\left(1-\frac{\beta'^2}{2}\right)+\frac{k}{2}\left(\frac{P_o}{2A_{lr}}\right)^2 \qquad (9)$$

$$\frac{P_{o\,\max}-P_o-2A_{lr}}{y_{o\,\max}-y_o-\dfrac{A_{lr}}{K_r}}=\frac{1}{\dfrac{1}{RS}+\dfrac{1}{K_r}} \qquad (10)$$

The practical application of the model includes: the understanding of the factors that control the shape of the P_o - y_o curve; the partition of load in ultimate shaft and toe resistances; the study of the rebound and its influence in the general behaviour, among others.

b) Rigid piles

For rigid or "short" piles ($k < 2$), points 3 and 4 almost coincide and the shape of P_o - y_o curve is reduced to two straight lines. Massad & Lazo (1998) proposed a very simple graphical solution, called "Two Straight Lines Method" (MDR). Later on, this method was modified by Marques & Massad (2004) to include the term $A \neq 0$ (Fig. 15), that is, assuming a rigid-elastic-plastic behaviour for the soil at the base toe of the pile. It will be mentioned here as the "Modified Two Straight Lines Method" (MDRM). The physical meaning of the term $A \neq 0$ may be explained in the following way: for some short piles, as the displacement piles, the toe reacts significantly to small displacements and an elastic bi-linear response would be more adequate than the rigid-elastic one. For simplicity, the MDRM adopted the later response.

Reporting to Fig. 17, the P_o - y_o curve may be represented by a polygonal that starts at point 0 and ends at point 9. The equations of lines 2-3 (pseudo elastic range) and 4-5 (free development of toe resistance) are, respectively:

$$P_o = \mu\,A_{lr}\,\frac{\beta'_3}{z}\,\frac{y_o}{\mu\,y_1} + A\,S\,w_2 \ \text{(range 2-3)} \qquad (11\text{-a})$$

with

$$w_2 = \frac{1}{\cosh(z)+\lambda\,\sinh(z)} \qquad (11\text{-b})$$

and

$$\frac{P_o - (\mu A_{lr} + A S)}{y_o - \frac{\mu A_{lr} + 2A S}{2K_r}} = \frac{1}{\frac{1}{RS} + \frac{1}{K_r}} \text{ (range 4-5)} \quad (12)$$

Based on the load test curve P_o - y_o (see Fig. 17), it is possible to derive the equation:

$$P_o = c_1 + c_2 y_o \quad (13)$$

by carrying out a linear regression for the range 2-3; as a consequence, from Eq. (11-a) the following relations will be obtained:

$$AS = \frac{c_1}{w_2} \quad (14)$$

and

$$\mu y_1 = \frac{\mu A_{lr}}{c_2} \frac{\beta'_3}{z} \quad (15\text{-a})$$

or, taking into account Eq. (1-a):

$$c_2 = K_r \; z \; \beta'_3 \quad (15\text{-b})$$

Similarly, a linear regression for the range 4-5 (Fig. 17) gives rise to the following equation:

$$P_o = d_1 + d_2 y_o \quad (16)$$

From Eq. (12) it follows:

$$\frac{1}{d_2} = \frac{1}{RS} + \frac{1}{K_r} \quad (17)$$

and

$$\mu A_{lr} + AS = \frac{d_1 + AS \frac{d_2}{2K_r}}{1 - \frac{d_2}{2K_r}} \quad (18\text{-a})$$

As the term $AS.d_2/(2K_r)$ is practically negligible, this last equation may be simplified as:

$$\mu A_{lr} + AS \cong \frac{d_1}{1 - \frac{d_2}{2K_r}} \quad (18\text{-b})$$

Equations (14) to (18-b) are the basis of the so-called "Modified Two Straight Lines Method" (MDRM), applicable to rigid piles with $A \neq 0$ and allowing for the estimation of the terms μy_1, μA_{lr}, AS and RS.

6.2. Application to the Static Loading Tests (SPLT)

The analysis started with the bored pile (E9), simpler in its interpretation, followed by the analysis of the CFA pile (T1) and, finally, Pile C1, more complex. For Piles E9 and T1 a comparison was possible between the results of these analyses and of the available extensometer measurements installed along the piles.

Basically, the analysis comprised the following steps:

a) initially, the parameters of Eq. (13), for range 2-3, and (16), for range 4-5, were determined;

b) then, the term RS was computed by means of the Eq. (17); by this, it was also possible to determine λ (one of the terms of Eq. (6); and,

c) finally, z was computed by solving iteratively the Eq. (15-b); then, the values of w_2 (Eq. (11-b)), $A.S$ (Eq. (14)), μA_{lr} (Eq. (18-b) and μy_1 (Eq. (1)) were calculated.

Table 1 shows the values obtained for K_r in the different types of the analyzed piles.

6.2.1. Bored pile (E9)

The modeling of the bored pile (E9) was done by initially assuming that $A = 0$. Consequently, the straight line of range 2-3 (Eq. (13)) passes through the origin. The following linear regression, considering the non-accumulated settlements of all cycles of loadings, was obtained:

$$P_o = 477 \, y_o \quad (19)$$

The linear regression of range 4-5, Eq. (16), was also estimated, resulting in:

$$P_o = 694 + 4.84 y_o \quad (20)$$

This was derived using the non-accumulated settlements of the 4th cycle of loading, together with the points of the 5th cycle, since slope of the range 4-5 ("free development of toe resistance"), defined by parameter R of Cambefort model, is considered unique.

Figure 18 shows how these equations fit the points of the 4th and 5th cycles of loading.

As it is expressed in the fizgure, $d_2 = 4.84$ kN/mm and $d_1 = 694$ kN. Applying the Eqs. (17) and (18-b) to the 4th cycle of loading, it follows $R.S$ = 4.86 kPa/mm, then $R = 17$ kN/mm and $\mu A_{lr} + AS = 696$ kN. Disregarding the influence of the 3 first cycles of loading and taking into account that E9 is a bored pile, it may be assumed $\mu = 1$ at the beginning of the 4th cycle. Therefore, A_{lr} = 696 kN and f_u = 61 kPa. An iterative calculation using Eq. (15-b), with c_2 = 477 kN, led to y_1 = 1.62 mm.

Table 1 - Pile characteristics.

Pile	Type	Diameter or width (mm)	h (m)	E (Gpa)	K_r (kN/mm)
E9	Bored pile	605	6	20	958
T1	Continuous Flight Auger Pile (CFA)	611	6	40	1,955
C1	Driven precast concrete pile	350	6	35.6	727

The linear regression for the range 4-5 of the 5th cycle of loading, considering the non-cumulative settlements, assumed the following equation:

$$P_o = 872 + 4.84 y_o \quad (21)$$

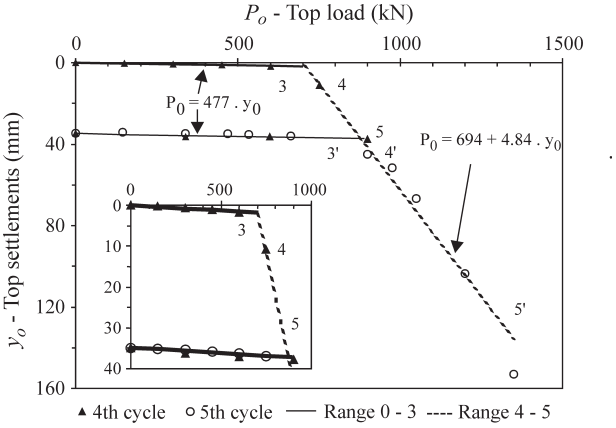

Figure 18 - Ranges 2-3 and 4-5 of 4th and 5th cycles of loadings - E9 Pile.

Observing that the slope d_2 had the same value and, with the new value for d_1, the following relation was obtained: $\mu.A_{lr}+AS = 872$ kN. Since $A_{lr} = 696$ kN and $A = 0$, then: $P_h = 872\text{-}696 = 176$ kN. Finally, the application of Eq. (2) resulted in: $\mu = 1+176/696 = 1.25$.

Note also that:

a) $k = 696/(958 \times 1.62) = 0.45 < 2$, confirming that E9 behaved as a rigid pile (Massad, 1992, 1995) (a better classification would be "very rigid");

b) $\lambda = 0.008$ (almost zero), which means that the toe contribution in terms of rigidity is very small, and,

c) in the same context, $d_2 \cong RS = 4.86$ kN/mm, since K_r value is very high (Eq. (17)).

These results are summarized in Tables 2 to 4, which include also the results of the analysis of the other two types of piles.

Figure 19 presents the measured load-settlement curves compared with the ones obtained by the application of the MDRM model, expressed by Eqs. (11) and (12).

Figure 20 is the same as Fig. 13, with the addition of the theoretical (MDRM modeled) curve, computed using $R.S = 4.86$ kPa/mm. The agreement with the toe values ex-

Table 2 - Linear regressions of ranges 2-3 and 4-5 - Static loading tests.

Pile	Range 2-3		Range 4-5	
	Linear regressions	Cycle of loading	Linear regressions	Cycle of loading
E9	$P_o = 477 y_o$	All	$P_o = 694 + 4.84 y_o$	4th and 5th
			$P_o = 872 + 4.84 y_o$	5th
T1	$P_o = 141 + 354 y_o$	2nd to 5th	$P_o = 990 + 2.13 y_o$	5th
C1	$P_o = 232 + 251 y_o$	All	$P_o = 1296 + 5.24 y_o$	5th

Table 3 - Summary of analysis results.

Pile	RS (kN/mm)	$\mu.A_{lr} + AS$ (kN)	k	AS (kN)	$\mu.A_{lr}$ (kN)	μy_1 (mm)	μ	P_h (kN)	$10^3.\lambda$
E9	4.85	696(*)	0.22	0	696(*)	1.62(*)	1.00(*)	0(*)	6.0
		872(**)			872(**)	2.03(**)	1.25(**)	176(**)	
T1	2.13	990	0.19	155	835	2.23	1.19	132	2.5
C1	5.28	1301	0.38	280	1021	1.85 to 3.64	2 to 1	509 to 0	11.7

Notes: (*) - 4th cycle of loading (**) - 5th cycle of loading.

Table 4 - Cambefort's parameters.

Pile	Shaft resistance				Toe reaction			
	B (kPa/mm)	f_{res} (kPa)	f_u (kPa)	y_1 (mm)	P_h/S (kPa)	A (kPa)	R (kPa/mm)	R_p (kPa)
E9	37.6	-16	61	1.62	0(*) 613(**)	0	17	2276
T1	32.5	-11	61	1.88	450	529	7	> 1610
C1	33.2	-61 to 0	61 to 122	1.85 to 3.64	4164 to 0	2286	43	8200 to 4033

Notes: (*) - 4th cycle of loading (**) - 5th cycle of loading.

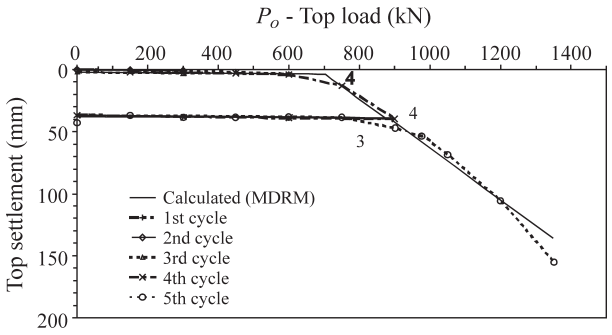

Figure 19 - Load-settlements curves from the static load test on Pile E9, with theoretical curves for the 4th and 5th cycles of loading.

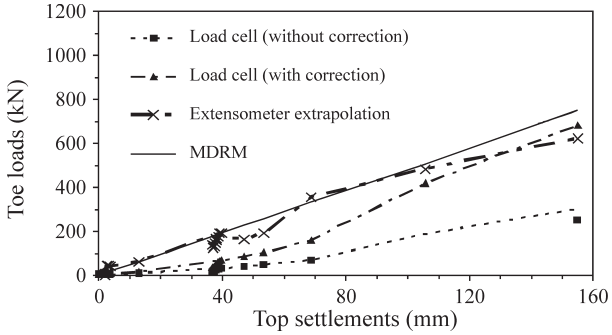

Figure 20 - Measured and computed toe loads.

trapolated from the extensometers measurements is very good.

Figure 21 presents values of the shaft load, obtained by subtracting the toe component from de top load. The toe loads were computed based on the MDRM model. The dashed line corresponds to the average value of A_{lr} = 696 kN.

6.2.2. Pile CFA (T1)

The modeling of the curve of the CFA pile (T1) was done considering the non-accumulated values of the settlements of all cycles of loadings, except for the 1st. The following relation was obtained for the linear regression of range 2-3:

$$P_o = 141 + 354 y_o \quad (22)$$

The linear regression for the 4-5 range of the 5th cycle of loading, considering again the non-accumulated settlements, was:

$$P_o = 990 + 2.13 y_o \quad (23)$$

Figure 22 shows how these equations fit the points of the 5th cycle of loading.

As it is expressed in the graph, the range 4-5 is defined by: d_2 = 2.13 kN/mm and d_1 = 990 kN. Using Eqs. (17) and (18-b), the term *R.S* assumed the value 2.13 kPa/mm, thus *R* = 7 kN/mm and $\mu A_{lr} + AS$ = 990 kN (valid for the 5th

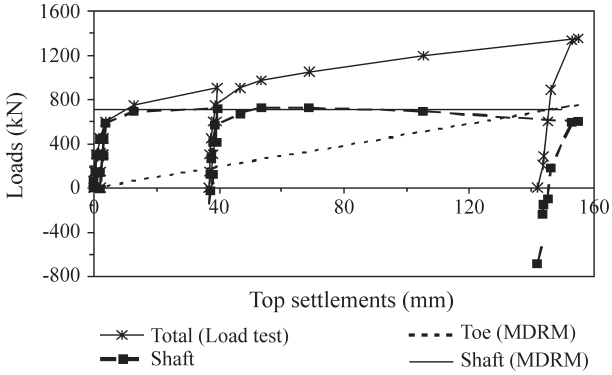

Figure 21 - Computed shaft and toe loads - E9 pile.

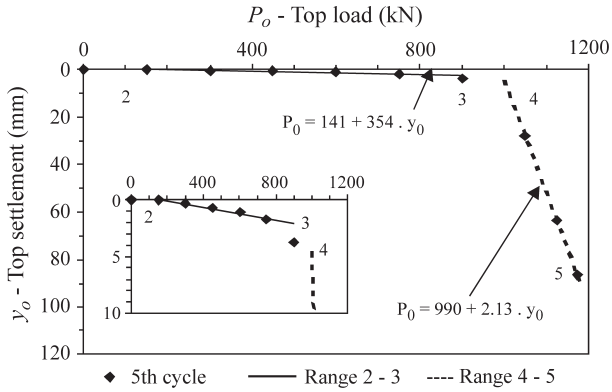

Figure 22 - Ranges 2-3 and 4-5 of the 5th cycles of loading - T1 Pile.

cycle of loading). Admitting the same ultimate unit shaft resistance, derived for E9 Pile, that is, f_u = 61 kPa, it resulted in: A_{lr} = 703 kN.

From Eqs. (6) and (15-b), with c_2 = 354 kN/mm, it was possible to compute, iteratively, z = 0.44 and y_1 = 1.88 mm. Applying Eq. (14), with c_1 = 141 kN, it followed *AS* = 155 kN and therefore: μA_{lr} = 835 kN. Hence $P_h = \mu A_{lr} - A_{lr}$ = 835-703 = 132 kN and, from Eq. (2), μ = 1 + 132/703 = 1.19.

Similarly of what has been deduced from the analysis of the bored pile (E9), the following conclusions were obtained for the CFA pile (T1):

a) k = 703/(1955 x 1.88) = 0.19 < 2, confirming that the pile is very rigid

b) λ = 0.0025, almost zero, meaning that there is a very small toe contribution in terms of stress-strain behaviour; and,

c) in this same context, $d_2 \cong$ RS = 2.13 kN/mm, because K_r is very large (see Eq. (17)).

These results are, as fore mentioned, summarized in Tables 2 to 4.

Figure 23 shows the top measured load-settlement curves, compared with the computed ones, as obtained by the application of Eqs. (11) and (12).

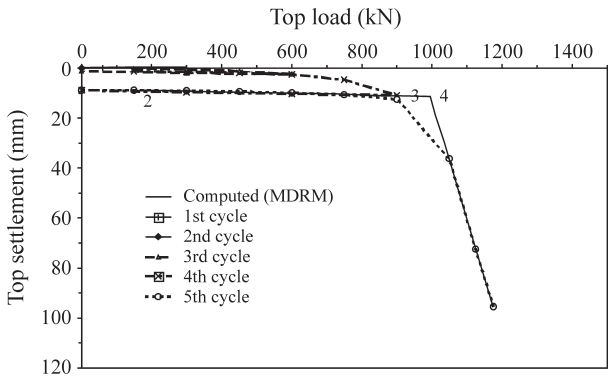

Figure 23 - Load-settlements curves from the static loading test on Pile T1, with modelled (by MDRM) curves for the 5th cycle of loading.

Figure 24 presents values of the shaft and toe loads, measured in the field. For comparison, the computed values by the MDRM are also included.

6.2.3. Precast Pile (C1)

Similarly to what had been done for the other piles, modeling of the precast pile (C1) behaviour was implemented by considering the non-accumulated values of the settlements considering together all cycles of loading. This resulted in the following relation:

$$P_o = 232 + 251 y_o \quad (24)$$

which is really the linear regression of all points in the range 2-3.

Following the same sequence described above, the linear regression for the range 4-5 in the 5th cycle of loading was derived, taking the non-accumulated values of settlements. The results were expressed by:

$$P_o = 1296 + 5.24 y_o \quad (25)$$

Figure 25 illustrates very clearly how these equations fit well the experimental measured points of the 5th cycle of the loading test.

With the deduced constants for the last range, d_2 = 5.24 kN/mm and d_1 = 1296 kN, it was possible to derive, from Eq. (17), $R.S$ = 5.28 kPa/mm. Therefore, the slope of the modified second Cambefort's law (Fig. 15) was obtained, R = 43 kN/mm, and consequently $\mu A_{lr} + AS$ = 1301 kN (Eq. (18-b)), valid for the 5th cycle of loading.

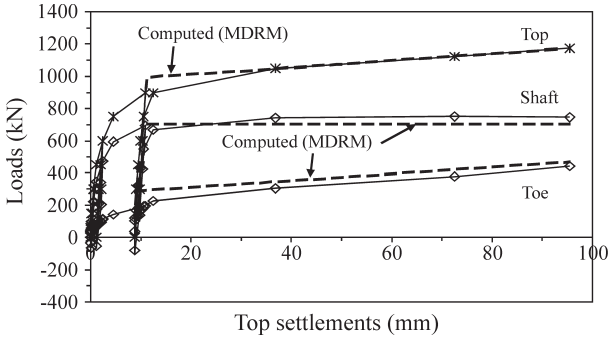

Figure 24 - Measured and computed (by MDRM) loads - T1 Pile (5th cycle).

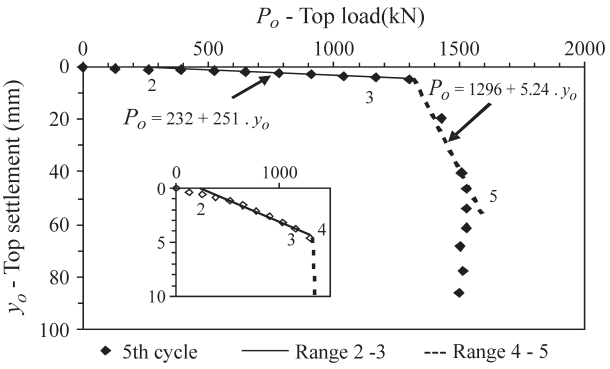

Figure 25 - Ranges 2-3 and 4-5 of the 5th cycle of loading - C1 Pile.

In the same sequence as previously described, Eq. (15-b) was solved iteratively, taking c_2 = 251 kN/mm, resulting in z = 0.62. With c_1 = 232 kN and applying Eq. (14), AS was calculated as 280 kN, resulting finally in μA_{lr} = (1301-AS) = 1021 kN and μy_1 = 3.65 mm.

The determination of μ would require more information about the load test, for example, the rebound curve, as mentioned before. Due to this fact, two extreme hypotheses had to be assumed for this pile:

a) the unit shaft resistance considered to be the same as for E9 Pile, that is: f_u = 61 kPa; consequently, A_{lr} = 512 kN, $P_h = \mu A_{lr} - A_{lr}$ = 1021-512 = 509 kN and μ ≅ 2; or,

b) being C1 a driven pile, it was reasonable to admit f_u > 61 kPa, with an upper bound given by 1021/(0,35 x 0,35 x 6) ≅122 kPa, for which $P_h = \mu A_{lr} - A_{lr}$ = 0 and μ=1.

In the same way as for bored (E9) and CFA (T1) piles, it may be concluded:

a) k = 512/(726 x 1,84) = 0.38 < 2, for μ = 2 or k = 1020/(726 x 3,65) = 0.38 < 2, for μ = 1, confirming that the driven pile (C1) is also very rigid;

b) λ = 0.012, meaning that there is a very small toe contribution in terms of rigidity; and,

c) $d_2 \cong$ RS = 5.28 kN/mm, since the pile is very rigid.

These results are summarized, as referred above, in Tables 2 to 4.

Figure 26 shows the results of this analysis. The computed curve, obtained by the application of the MDRM model, expressed in Eqs. (11) and (12), fits remarkably well with the observed experimental values.

6.2.4. Final comments

With these results, it was possible to evaluate the load distribution for ultimate shaft resistance (A_{lr}) and tip (toe)

Table 5 - Load distribution for 100 mm pile head settlement.

Pile	This paper			Fellenius *et al.* (2007)		
	A_{lr} (kN)	Q_p (kN)	Total load (kN)	A_{lr} (kN)	Q_p (kN)	Total load (kN)
E9 (Bored)	696	481	1177	700	500	1200
T1 (CFA)	703	499	1202	700	500	1200
C1 (Precast)	511 to 1021	1004 to 494	1515	520	980	1500

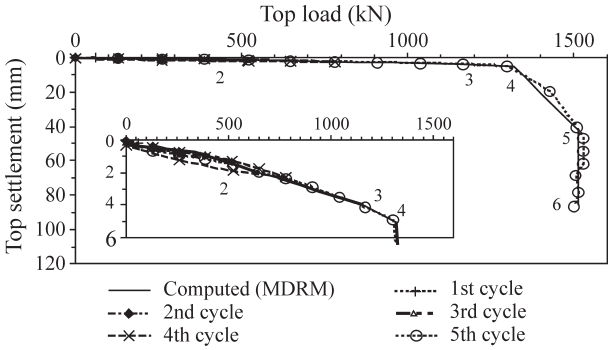

Figure 26 - Theoretical result, as modelled by MDRM, as compared with the experimental results for the 5th Cycle of Loading - Pile C1.

resistance (Q_p) levels, for a reference 100 mm top settlement, as shown in Table 5.

Derived values are in close agreement with those presented in a previous analysis, reported in Fellenius *et al.* (2007). The differences in the evaluations refer to the estimation of the residual loads. While in this paper, values derived for the bored (E9) and CFA (T1) piles were around 150 kN, Fellenius *et al.* (2007) estimated them in 300 kN. The value of 150 kN for the toe residual load is very much consistent with the measured ones indicated in Figs. 11 and 12, for E9 and T1 piles, respectively. Besides that, as far as C1 driven pile is concerned, the model that was described in this paper defined an upper bound value for residual load of 500 kN.

Assuming the validity of the hypotheses mentioned before, the ultimate unit shaft resistance for bored (E9) and CFA (T1) piles will be of 60 kPa. For the driven (C1) pile, this value may be assumed as a lower limit.

7. Conclusions

The analysis of the pile head load-settlement curves of the static load tests of E9 and T1 Piles, using the Modified Two Straight Lines Method (MDRM), led to consistent results with those inferred from the extensometer measurements.

The theoretical relationships between shaft and toe resistances and displacement, derived from the MDRM model, agreed very well with the measured values. For bored (E9) and CFA (T1) piles, the ultimate unit shaft resistance was estimated as 60 kPa. Moreover, the ultimate shaft loads and the toe loads for a 100 mm top settlement were estimated in around 700 kN and 500 kN, respectively, for both E9 and T1 piles, which are in close agreement with the values from a distinct analysis reported by Fellenius *et al.* (2007).

As far as the toe's residual loads are concerned, the estimated values of about 150 kN for the E9 and T1 piles are very much consistent with the measured values (inferred from the tests results), but very much distinct from the "best guess" values reported by Fellenius *et al.* (2007).

For the driven pile (C1), the application of MDRM model assuming two extreme hypothesis, necessary, due to the absence of experimental data to estimate μ, an upper bound value of 500 kN was obtained for the residual load and a lower bound of 500 kN and 60 kPa were derived for the total ultimate and ultimate unit shaft resistances, respectively.

Acknowledgements

The authors are grateful to the Sponsors: Mota-Engil, S.A., Sopecate, S.A.; Tecnasol-FGE, S.A., and Teixeira Duarte, S.A.. This work was developed under the research activities of CEC from the FEUP and ICIST of IST, supported by funding from FCT (Portuguese Science and Technology Foundation). The authors are also indebted to the Polytechnic School of the University of São Paulo, Brazil, for the incentives towards this research.

References

Baguelin, F. & Venon, V.P. (1972) Influence de la compressibilité des pieux sur la mobilizations des éfforts resistant. Bulletin des Liaison Lab. des Ponts et Chaussées. Num. Especial pour les Journées Nationales sur le thème "Le Comportmenet des Sols Avant la Rupture", pp. 308-322.

CFEM (1992). Canadian Foundation Engineering Manual. 3rd ed. Canadian Geotechnical Society, BiTech Publishers, Vancouver, 512 p.

Costa Esteves, E.F.M. (2005) Testing and Analysis of Axially Loaded Piles in a Residual Soil of Granite. M.Sc. Thesis, Faculty of Engineering of the University of Porto, Porto (in Portuguese), 322 p.

Fellenius, B.H. (2001) From strain measurements to load in an instrumented pile. Geotechnical News Magazine, v. 19:1, pp. 35-38.

Fellenius, B.H. (1989) Tangent modulus of piles determined from strain data. Kulhawy, F.H. (ed), The American Society of Civil Engineers, Geotechnical Engineering Division, the 1989 Foundation Congress, v. 1, pp. 500-510.

Fellenius, B.H. (2002a) Basics of Foundation Design. Electronic edition, www.Geoforum.com, 250 p.

Fellenius, B.H. (2002b) Determining the true distribution of load in piles. Proc. International Deep Foundation Congress, An International Perspective on Theory, Design, Construction, and Performance, Orlando, v. 2, pp. 1455-1470.

Fellenius, B.H.; Santos, J.A. & Viana da Fonseca, A. (2007) Analysis of piles in a residual soil - The ISC'2 prediction. Canadian Geotechnical Journal, accepted for publication in v. 1 (January).

Fioravante, V.; Ghionna, V.N.; Jamiolkowski, M. & Pedroni, S. (1995) Load carrying capacity of large diameter bored piles in sand and gravel. Proc. Tenth Asian Regional Conference on Soil Mechanics and Foundation Engineering, pp. 1-13.

Massad, F. (1992) On the interpretation of pile load tests, considering the residual point load and the reversion of the lateral resistance (in Portuguese). Technical Bulletin, Department of Structures and Foundation Engineering, EPUSP, N. BT-PEF 9202. Republished in Solos e Rochas, v. 15:2, pp. 103-115.

Massad, F. (1995) Pile analysis taking into account soil rigidity and residual stresses. Proc. Xth Panamerican Congress on Soil Mechanics and Foundation Engineering, Guadalahara, v. 2, pp. 1199-1210.

Lazo, G. (1996) Prediction of the Behaviour of Precast Piles in S. Paulo Large Region, Brazil, by Means of Mathematical Models. MSc Thesis, EPUSP, University of São Paulo, São Paulo, 222 p.

Massad, F. & Lazo, G. (1998) Graphical method for the interpretation of the load-settlement curve from vertical load tests on rigid and short piles. Proc. XI Brazilian Congress on Soil Mechanics and Geotechnical Engineering, Brasília, v. 3, pp. 1407-1414.

Marques, J.A.F. & Massad, F. (2004) Load tests on instrumented bored piles with bulbs, executed at a seafront in Maceió, Alagoas. Solos e Rochas, v. 27:3, pp. 243-260 (in Portuguese).

Santos, J.S.; Viana da Fonseca, A. & Costa Esteves, E. (2006) ISC'2 experimental site - Prediction & performance of instrumented axially loaded piles. Geotecnia, n. 107, pp. 79-90 (in Portuguese).

Santos, J.A.; Leal Duarte, R.; Viana da Fonseca, A.; Costa Esteves, E. (2005) ISC'2 experimental site - Prediction & performance of instrumented axially loaded piles. Proc. 16th ICSMFE, Osaka, v. 4, pp. 2171-2174.

Viana da Fonseca, A. (2003) Characterizing and deriving engineering properties of a saprolitic soil from granite, in Porto. Tan *et al.*, (eds) Characterization and Engineering Properties of Natural Soils. Swets & Zeitlinger, Lisse, pp. 1341-1378.

Viana da Fonseca, A. & Almeida e Sousa, J. (2001) At rest coefficient of earth pressure in saprolitic soils from granite. Proc. XIV ICSMFE, Istambul, v. 1, pp. 397-400.

Viana da Fonseca, A. & Ferreira, C. (2000) Management of sampling quality on residual soils and soft clayey soils. Comparative analysis of in situ and laboratory seismic waves velocities. Proc. Workshop Sampling Techniques for Soils and Soft Rocks & Quality Control, FEUP, Porto, pp. 3-75 (in Portuguese).

Viana da Fonseca, A. & Ferreira, C. (2002) The application of the Bender Elements technique on the evaluation of sampling quality of residual soils. Proc. XII COBRAMSEG, ABMS, São Paulo, v. 1, pp. 187-199 (in Portuguese).

Viana da Fonseca, A.; Carvalho, J.; Ferreira, C.; Tuna, C.; Costa, E. & Santos, J. (2004) Geotechnical characterization of a residual soil profile: the ISC'2 experimental site, Porto. Viana da Fonseca, A. & Mayne, P.W. (eds) Geotechnical & Geophysical Site Characterizaton. Millpress, Rotterdam, pp. 1361-1370.

Viana da Fonseca, A.; Carvalho, J.; Ferreira, C.; Santos, J.A.; Almeida, F. & Hermosilha, H. (2005) Combining geophysical and mechanical testing techniques for the investigation and characterization of ISC'2 residual soil profile. Proc. 16th ICSMGE, Osaka, v. 2, pp. 765-768.

Viana da Fonseca, A.; Carvalho, J.; Ferreira, C.; Santos, J.A.; Almeida, F.; Pereira, E.; Feliciano, J.; Grade, J. & Oliveira, A. (2006) Characterization of a profile of residual soil from granite combining geological, geophysical, and mechanical testing techniques. Int. J. Geotechnical and Geological Engineering, v. 24:5, pp. 1307-1348.

Viana da Fonseca, A. & Santos, J. (2006) International Prediction Event on the Behaviour of Bored, CFA and Driven Piles in CEFEUP/ISC'2 Experimental Site - 2003. Final Report. Ed. FEUP, Porto (in press).

List of symbols

A: Cambefort parameter (see Fig. 15)
A_{lr}: ultimate shaft resistance
B: Cambefort parameter (see Fig. 14)
c': effective cohesion
CFA: Continuous Flight Auger (pile)
CH: Cross-Hole test
CPTu: Static Cone Penetrometer Test (u for piezocone)
D: diameter or width of the pile
DMT: Marchetti Flat Dilatometer Test
E: deformability (Young's) modulus
E: modulus of elasticity of the pile material
E_M (E_{pm}): Ménard pressuremeter modulus
E_0: small strain (maximum) deformability (Young's) modulus

f_s: CPT shaft resistance;
f_u: ultimate unit shaft resistance
f_{res}: residual negative shaft resistance
$G_0 = G_{max}$: small strain (maximum) shear modulus
G_l: small strain shear modulus at pile base level
h: height of the pile
k: relative stiffness of the pile-soil (shaft) system
K_r: pile stiffness
K_0: coefficient of earth pressure at rest
N_{SPT}: number of blows in SPT tests
N_{60}: NSPT values for a reference energy ratio of 60%
P_h: residual toe load
p_{LM}: Ménard's net limit pressure
P_o: Pile top load
PMT Pre-bored Ménard Pressuremeter Test
q_c: cone resistance in CPT tests
Q_p: Tip load or resistance
Q_{pr}: ultimate tip load or resistance
Q_{rupt}: ultimate total pile load
R: Cambefort parameter (see Fig. 15)
R_{reb}: Cambefort parameter (see Fig. 15)
R_p: Toe unit resistance
s: settlement
S: pile cross section area
SPT: Standard Penetration Test
SPLT: Static Pile Load Test
V_s: shear wave's velocity
y_o: pile top settlement
y_1: Cambefort parameter (see Fig. 14)
y_{1R}: Cambefort parameter (see Fig. 14)
z: square root of k; depth (from the ground surface)
γ: unit weight
η: correction factor to allow for the pile base depth effects
λ: relative stiffness of the pile-soil (shaft and toe) system
μh: Randolph and Wroth's parameter that has the same meaning as k
ϕ': angle of shearing resistance ("friction angle")
μ: shaft friction magnifier factor due to residual load
ν: Poisson's ratio

Book Review

RALPH B. PECK, Educator and Engineer: The Essence of the Man
John Dunnicliff, Nancy Peck Young, editors
ISBN 0-921095-63-5
BiTech Publishers Ltd.
Vancouver, B.C. Canada, September 2006

John Dunnicliff and Nancy Peck Young recall that the idea of writing a biography of Ralph B. Peck arose in 2004, after a conference in honor of Prof. Skempton, in which his daughter, Judith, made a presentation of her biography of her father (*A Particle of Clay*. The Biography of Alec Skempton, Civil Engineer, by Judith Niechcial, Whittles Publishing, Scotland, UK, 2002, 208 pp.). John and Nancy have acted as project managers, as well as editors, in the process of compiling and organizing this most interesting book.

The book is divided into six parts, with something for everyone, from the young geotechnical student, to the professor, to the experienced practitioner.

Self Portrait is a 109 page account of Ralph B. Peck's life, in his own words (dictated, recorded and transcribed by the editors). Among many other reminiscences, he treats the readers to many candid, most revealing stories of engineers and professors, like himself, that we have learned to admire and respect (Terzaghi, Casagrande, Skempton, Bjerrum, to name just a few). Both classroom stories and case histories abound, although they are just a relatively small sample of his over one thousand consulting projects in five continents and twenty-eight countries, with special emphasis on the USA and Canada ("the land of my birth").

Words of Wisdom were selected by Elmo DiBiagio and Kaare Flaate from some of Peck's papers, and first published in the NGI Publication n. 207. These thoughts summarize the essence of Ralph B. Peck as an engineer, consultant, educator, researcher, and communicator.

Selected Publications and Lectures includes about 30 of Peck's over 250 publications, each of them preceded by introductory notes - and in many cases by questions and answers - that help put the text in the proper historical perspective. Here the reader will find the history of the geotechnical profession, ISSMGE and its conferences, written by one of its protagonists, as well as Peck's "philosophical" publications (his "sermons") and some of his most significant contributions on themes related to his long-term interests, such as embankment dams, observations and instrumentation. The "inside story" of the conception of the "Newmark analysis" of the seismic stability of dams is a gem.

Vignettes is a testimonial collection of contributions from colleagues, family, and friends who have known Ralph Peck or worked with him over the years. Some of them are touching, all are entertaining in that they expose the many facets of his unique personality.

Selected Awards and *List of Publications* close the book. Most chapters are illustrated by many photographs.

There is so much interesting information in the book that this review cannot hope to give but a pale idea of what awaits the reader. Reading it will undoubtedly be a most rewarding experience.

Waldemar Hachich
Professor of Geotechnical Engineering
University of São Paulo, Brazil

SOILS & ROCKS
International Geotechnical and Geoenvironmental Journal

Publication of
ABMS - Brazilian Society of Soil Mechanics and Geotechnical Engineering
ABGE - Brazilian Society of Engineering Geology
SPG - Portuguese Geotechnical Society

Volume 30, N. 1, January-April 2007

Author index

Esteves, Elisabete Costa 63
Fonseca, António Viana da 63
Frank, Roger 39
Hachich, Waldemar 81
Massad, Faiçal 63
Penmam, Arthur D.M. 33
Rocha Filho, Pedricto 33
Rowe, R. Kerry 3
Saboya Jr., Fernando 33
Santos, Jaime Alberto dos 63
Vilar, Orencio Monje 51

Instructions to Authors

Category of the Papers

Soils and Rocks is the scientific journal edited by the Brazilian Society of Soil Mechanics and Geotechnical Engineering (ABMS) and by the Brazilian Society of Engineering and Environmental Geology (ABGE). The journal is intended to the divulgation of original research works from all geotechnical branches.

The accepted papers are classified either as an Article paper, a Technical Note, a Case Study, or a Discussion according to its content. An article paper is an extensive and conclusive dissertation about a geotechnical topic. A paper is considered as a technical note if it gives a short description of ongoing studies, comprising partial results and/or particular aspects of the investigation. A case study is a report of unusual problems found during the design, construction or the performance of geotechnical projects. A case study is also considered as the report of an unusual solution given to an ordinary problem. The discussions about published papers, case studies and technical notes are made in the Discussions Section.

When submitting a manuscript for review, the authors should indicate the category of the manuscript, and is also understood that they:

a) assume full responsibility for the contents and accuracy of the information in the paper;

b) assure that the paper has not been previously published, and is not being submitted to any other periodical for publication.

Manuscript Instructions

Manuscripts must be written either in Portuguese, Spanish or English. The text is to be typed in a word processor (MS Word or equivalent), using ISO A4 page size, left, right, top, and bottom margins of 25 mm, Times New Roman 12 font, and line spacing of 1.5. All lines and pages should be numbered. The text should be written in the third person.

The fist page of the manuscript is to include the title of the paper in Portuguese, English and Spanish, followed by the names of the authors with the abbreviation of the most relevant academic title. The affiliation, address and e-mail is to be indicated below each author's name. An abstract of 200 words is to be written in the language of the paper after the author's names. Translations of the abstract in the other languages are to follow the abstract. A list with up to six keywords at the end of the abstract and each translation is required.

Although alteration of the sequence and the title of each section may be required, it is suggested that the text contains the following sections: Introduction, Material and Methods, Results, Discussions, Conclusion, Acknowledgements, References and List of Symbols. A brief description of each section is given next.

Introduction: This section should indicate the state of the art of the problem under evaluation, a description of the problem and the methods undertaken. The objective of the work is to be clearly presented at the end of the section.

Materials and Methods: This section should include all information needed to the reproduction of the presented work by other researchers.

Results: In this section the data of the investigation should be presented in a clear and concise way. Figures and tables should not repeat the same information.

Discussion: The analyses of the results should be described in this section. **Conclusions**: The text of this section should be based on the presented data and in the discussions.

Acknowledgenments: If necessary, concise acknowledgements should be written in this section.

References: References to other published sources are to be made in the text by the last name(s) of the author(s), followed by the year of publication, similarly to one of the two possibilities below:

"while Silva & Pereira (1987) observed that resistance depended on soil density" or "*It was observed that resistance depended on soil density (Silva & Pereira, 1987)*."

In the case of three or more authors, the reduced format must be used, *e.g.*: Silva *et al.* (1982) or (Silva *et al.*, 1982). Two or more citations belonging to the same author(s) and published in the same year are to be distinguished with small letters, *e.g.*: (Silva, 1975a, b, c.). Standards must be cited in the text by the initials of the entity and the year of publication, *e.g.*: ABNT (1996), ASTM (2003).

Full references shall be listed alphabetically at the end of the text by the first author's last name. Several references belonging to the same author shall be cited chronologically. Some examples are listed next:

Papers: Bishop, A.W. & Blight, G.E. (1963) Some aspects of effective stress in saturated and unsaturated soils. Géotechnique, v. 13:2, p. 177-197.

Books: Lambe, T.W & Whitman, R.V. (1979) Soil Mechanics, SI Version, 2nd ed. John Wiley & Sons, New York, p. 553.

Book with editors: Sharma, H.D.; Dukes, M.T. & Olsen, D.M. (1990) Field measurements of dynamic moduli and Poisson's ratios of refuse and underlying soils at a landfill site. Landva A. & Knowles, G.D. (eds) Geotechnics of Waste Fills - Theory and Practice, American Society for Testing and Materials - STP 1070, Philadelphia, p. 57-70.

Proceedings (printed matter or CD-ROM): Jamiolkowski, M.; Ladd, C.C.; Germaine, J.T & Lancellotta, R. (1985) New developments in field and laboratory testing of soils. Proc. 11th Int. Conf. on Soil Mech. and Found. Engn., ISSMFE, San Francisco, v. 1, pp. 57-153.(specify if CD – ROM)

Thesis and dissertations: Lee, K.L. (1965) Triaxial Compressive Strength of Saturated Sands Under Seismic Loading Conditions. PhD Dissertation, Department of Civil Engineering, University of California, Berkeley, 521 p.

Standards: ASTM (2003) Standard Test Method for Particle Size Analysis of Soils - D 422-63. ASTM International, West Conshohocken, Pennsylvania, USA, 8 p.

Internet references: Soils & Rocks available at http://www.abms.com.br.

On line first publications must also bring the digital object identifier (DOI) at the end.

Figures shall be either computer generated or drawn with India ink on tracing paper. Computer generated figures must be accompanied by the corresponding digital file (.tif, .jpg, .pcx, etc.). All figures (graphs, line drawings, photographs, etc.) shall be numbered consecutively and have a caption consisting of the figure number and a brief title or description of the figure. This number should be used when referring to the figure in text. Photographs should be black and white, sharp, high contrasted and printed on glossy paper.

Tables shall be numbered consecutively in Arabic and have a caption consisting of the table number and a brief title. This number should be used when referring to the table in text. Units should be indicated in the first line of the table, below the title of each column. Abbreviations should be avoided. Column headings should not be abbreviated. When applicable, the units should come right below the corresponding column heading. Any necessary explanation can be placed as footnotes.

Equations shall appear isolated in a single line of the text. Numbers identifying equations must be flush with the right margin. International

System (SI) units are to be used. The symbols used in the equations shall be listed in the List of Symbols. It is recommended that the used symbols be in accordance with Lexicon in 8 Languages, ISSMFE (1981) and the ISRM List of Symbols.

The text of the submitted manuscript (including figures, tables and references) intended to be published as an article paper or a case history should not contain more than 30 pages formatted according to the instructions mentioned above. Technical notes and discussions should have no more than 15 and 8 pages, respectively. Longer manuscripts may be exceptionally accepted if the authors provide proper explanation for the need of the required extra space in the cover letter.

Discussion

Discussions should be written in the original language of the paper. The first page of a discussion paper should contain:

• The title of the paper under discussion in the language chosen for publication;

• Name of the author(s) of the discussion, followed by the position, affiliation, address and e-mail. The discusser(s) should refer himself (herself, themselves) as "the discusser(s)" and to the author(s) of the paper as "the author(s)".

Figures, tables and equations should be numbered following the same sequence of the original paper. All instructions previously mentioned for the preparation of article papers, case studies and technical notes also apply to the preparation of discussions.

Editorial Review

Each paper will be evaluated by reviewers selected by the editors according to the subject of the paper. The authors will be informed about the results of the review process. If the paper is accepted, the authors will be required to submit a version of the revised manuscript with the suggested modifications. If the manuscript is refused for publication, the authors will be informed about the reasons for rejection. In any situation comprising modification of the original text, classification of the manuscript in a category different from that proposed by the authors, or refusal for publication, the authors can reply presenting their reasons for disagreeing with the reviewers' comments

Submission

The author(s) must submit for review:

1. A hard copy of the manuscript to Editores - Revista Solos e Rochas, Av. Prof. Almeida Prado, 532 – IPT, Prédio 54 – DEC/ABMS, 05508-901 - São Paulo, SP, Brazil. The first page of the manuscript should contain the identification of the author(s).

2. The digital file of the manuscript, omitting the authors' name and any information that eventually could identify them, should be sent to **abms@ipt.br**. The following must be written in the subject of the e-mail message: "*Paper submitted to Soils and Rocks"*. The authors' names, academic degrees and affiliations should be mentioned in the e-mail message. The e-mail address from which the digital file of the paper was sent will be the only one used by the editors for communication with the corresponding author.

Follow Up

The ABMS Secretariat will provide a password to the corresponding author, which will enable him/her to follow the reviewing process of the submitted manuscript at the ABMS website, clicking in the item menu "Fluxo de Trabalhos."

Volume 30, N. 1, January-April 2007

Table of Contents

EDITORIAL
From Solos e Rochas to Soils and Rocks...
Alberto Sayão, Maria Heloísa Frascá, António G. Correia, Ennio Palmeira and Ricardo Oliveira i

XXIII MANUEL ROCHA LECTURE
Advances and Remaining Challenges for Geosynthetics in Geoenvironmental Engineering Applications
R. Kerry Rowe 3

ARTICLE
Deflections of Upstream Membrane of Rockfill Dams During Reservoir Filling
Fernando Saboya Jr., Pedricto Rocha Filho, Arthur D.M. Penmam 33

Basic Principles of Eurocode 7 on 'Geotechnical Design'
Roger Frank 39

An Expedite Method to Predict the Shear Strength of Unsaturated Soils
Orencio Monje Vilar 51

Analysis of Piles in Residual Soil from Granite Considering Residual Loads
António Viana da Fonseca, Jaime Alberto dos Santos, Elisabete Costa Esteves, Faiçal Massad 63

BOOK REVIEW
RALPH B. PECK, Educator and Engineer: The Essence of the Man,
John Dunnicliff and Nancy Peck Young
By Waldemar Hachich 81